Vol. 68 • No. 4
April 2025

Microwave Journal

horizon house
Founded in 1958
mwjournal.com

MILLER MMIC

Advancing RF MMIC Design Through Human-AI collaboration and competition

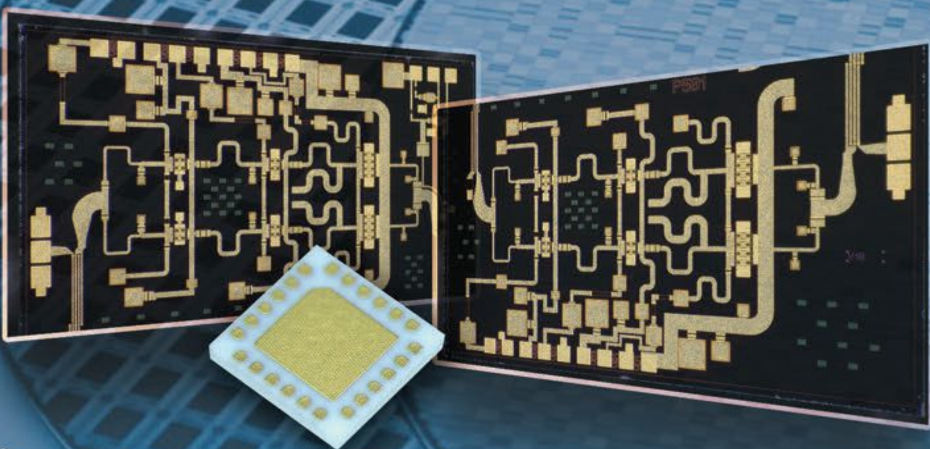

Miller MMIC is a global provider of RF semiconductor solutions with expertise in GaAs and GaN processes. We offer a diverse range of products tailored to various wireless applications. Our product lineup encompasses a wide array of offerings, including Low Noise Amplifiers, Distributed Amplifiers, Power Amplifiers, Driver Amplifiers, RF Switches, RF PIN Diode Switches, and numerous other voltage- and digitally-controllable RF components.

RapidRF MILLER MMIC RapidRF AI Platform for RF MMIC Design

RF Distributed Low Noise Amplifiers

PN	Freq Low (GHz)	Freq High (GHz)	Gain (dB)	NF(dB)	P1dB (dBm)	Voltage (VDC)	Current (mA)	Package
MMW001T	DC	20.0	17~19	1~3.5	23 @ 10GHz	8.0	145	die
MMW4FP	DC	50.00	16.00	4.00	24.00	10	200	die
MMW507	0.20	22.0	14.0	4 - 6	28.0	10.0	350	die
MMW508	DC	30.0	14.0	2.5dB @ 15GHz	24.5	10.0	200	die
MMW509	30KHz	45.0	15.0		20.0	6.0	190	die
MMW510	DC	45.0	11.0	4.5	15.5	6.0	100	die
MMW510F	DC	30.00	20.00	2.50	22.00			die
MMW511	0.04	65.0	10.0	9.0	18.0	8.0	250	die
MMW512	DC	65.0	10.0	5.0	14.5	4.5	85	die
MMW5FN	DC	67.00	14.00	2.00	19.00	4.5	81	die
MMW5FP	DC	67.00	14.00	4.00	21.00	8	140	die
MMW011	DC	12.0	14.0		30.5	12.0	350	die

Low Noise Amplifiers

PN	Freq Low (GHz)	Freq High (GHz)	Gain (dB)	NF(dB)	P1dB (dBm)	Voltage (VDC)	Current (mA)	Package
MML040	6.0	18.0	24.0	1.5	14.0	5.0	35	die
MML058	1.0	18.0	15.0	1.7	17.0	5.0	35	die
MML063	18.0	40.0	11.0	2.9	15.0	5.0	52	die
MML080	0.8	18.0	16.5/15.5	1.9/1.7	18/17.5	5.0	65/40	die
MML081	2.0	18.0	25/23	1.0/1.0	16/9.5	5.0	37/24	die
MML083	0.1	20.0	23.0	1.6	11.0	5.0	58	die

RF Driver Amplifier

PN	Freq Low (GHz)	Freq High (GHz)	Gain (dB)	NF(dB)	P1dB (dBm)	Voltage (VDC)	Current (mA)	Package
MM3006	2.0	20.0	19.5	2.5	22.0	7.0	130	die
MM3014	6.0	20.0	15.0	-	19.5	5.0	107	die
MM3017T	17.0	43.0	25.0		22.0	5.0	140	die
MM3031T	20.0	43.0	20.0		24.0	5.0	480	die
MM3051	17.0	24.0	25.0	-	25.0	5.0	220	die
MM3058	18.0	40.0	20/19.5	2.5/2.3	16/14	5/4	69/52	die
MM3059	18.0	40.0	16/16	2.5/2.3	16/15	5/4	67/50	die

GaAs Medium Power Amplifier

PN	Freq Low (GHz)	Freq High (GHz)	Gain (dB)	P1dB (dBm)	Psat (dBm)	Voltage (VDC)	Current (mA)	Package
MMP107	17.0	21.0	19.0	30.0	30.0	6.0	400	die
MMP108	18.0	28.0	14.0	31.5	31.0	6.0	650	die
MMP111	26.0	34.0	25.5	33.5	33.5	6.0	1300	die
MMP112	2.0	6.0	20.0	31.5	32.0	8.0	365	die
MMP501	20.0	44.0	15.0	27 -- 32	29 - 34	5.0	1200	die
MMP502	18.0	47.0	14.0	28.0	30.0	5.0	1500	die

PN: MMW5FP

RF GaAs MMIC DC-67GHz

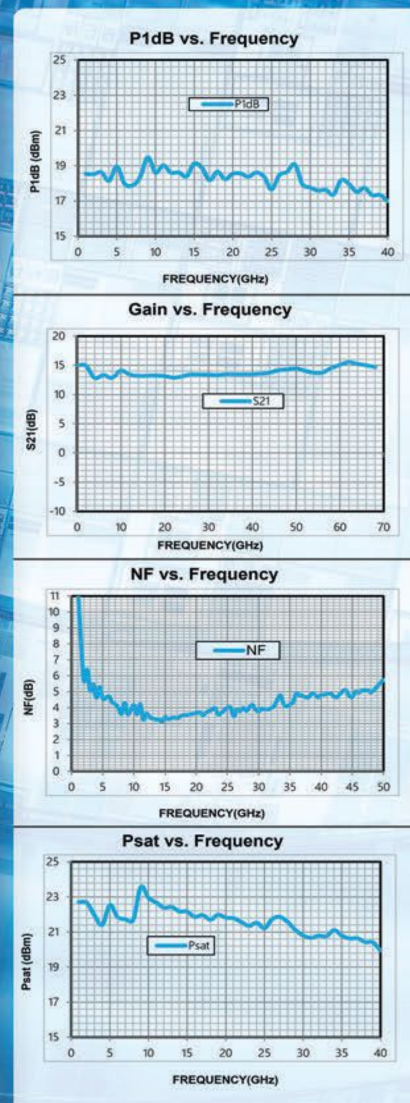

CALL US 1-833-2MILLER(264-5537)
WWW.MILLERMMIC.COM

RapidRF
sales@millermmic.com
support@millermmic.com

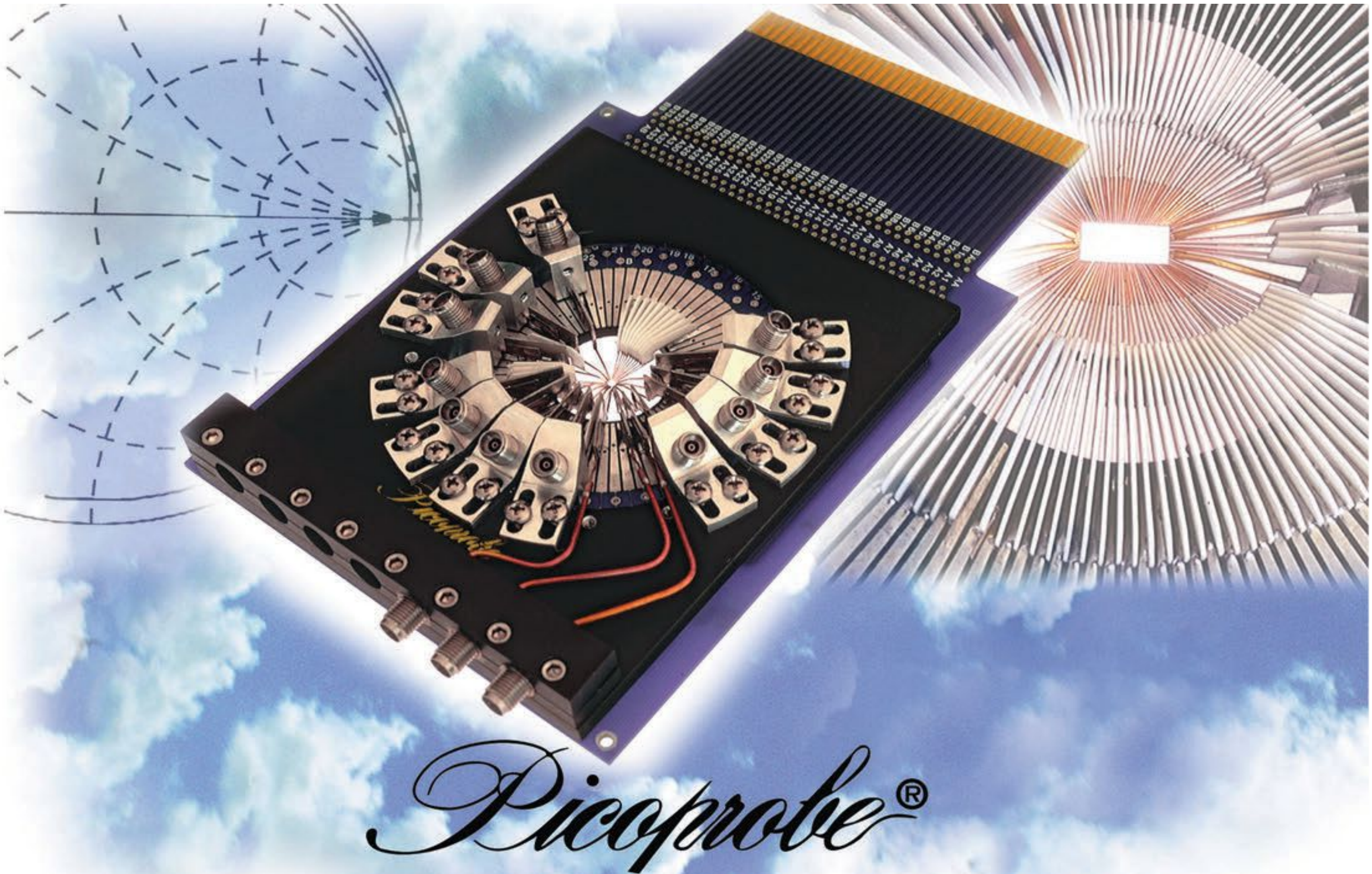

Picoprobe elevates probe cards to a higher level…

(…110 GHz to be exact.)

Since 1981, GGB Industries, Inc., has blazed the on-chip measurement trail with innovative designs, quality craftsmanship, and highly reliable products. Our line of custom microwave probe cards continues our tradition of manufacturing exceptional testing instruments.

Through unique modular design techniques, hundreds of low frequency probe needles and a variety of microwave probes with operating frequencies from DC to 40, 67, or even 110 GHz can be custom configured to your layout.

Our patented probe structures provide the precision and ruggedness you require for both production and characterization testing. And only Picoprobe® offers the lowest loss, best match, low inductance power supplies, and current sources on a single probe card.

Our proven probe card design technology allows full visibility with inking capability and ensures reliable contacts, even when probing non-planar structures.

Not only do you get all the attractive features mentioned, but you get personal, professional service, rapid response, and continuous product support--all at an affordable price so your project can be completed on time and within budget.

Typical Specs	10GHz	20GHz	40GHz
Insertion Loss	0.6 dB	0.8 dB	1.3 dB
Return Loss	22 dB	18 dB	15 dB

For technical assistance, custom product designs, or off-the-shelf delivery,call GGB Industries, Inc., at (239) 643-4400.

GGB INDUSTRIES, INC. • 4196 CORPORATE SQUARE • NAPLES, FL 34104

Telephone (239) 643-4400 • E-mail email@ggb.com • www.picoprobe.com

Benchtop & Rack Mount Test Systems

Software-controlled building blocks for RF test automation from R&D labs to production

LEARN MORE

- Improve test efficiency and throughput without breaking the bank
- Expand and reconfigure as your needs change
- Wide variety of components in stock from DC to 100+ GHz
- The industry's fastest turnaround times

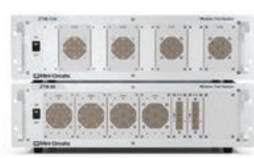

CUSTOMIZABLE & RECONFIGURABLE

Modular Test Systems

Switching, Attenuation & More

DC TO 50 GHz

Mechanical Switching Systems

Long Life & High Reliability

DC TO 67 GHz

Solid-State Switching Systems

Fast Switching & High-Isolation

DC TO 50 GHz

Attenuation Systems

Simulate Loss, Signal Fading & Handover

3 TO N PORTS

Mesh Network Test Systems

Simulate Real-World Mesh Conditions in the Lab

DC TO 100+ GHz

Amplifier Systems

Custom integration with gain control, filtering, switching & more

FLEXIBLE, RELIABLE, AFFORDABLE & FAST

DC TO 50 GHz

N x M Switch Matrices

Blocking, Non-Blocking & Full Fan-Out

9 kHz TO 40 GHz

Power Sensors

Turn Your PC into a High-Performance, Smart Power Meter

1 MHz TO 44 GHz

Signal Generators

Portable Frequency Sources for Your Test Bench

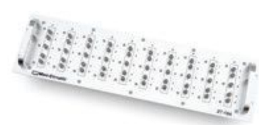

DC TO 65 GHz

Panel Mounted Structures

Adapters, Fixed Attenuators, Splitters & More

DC TO 6 GHz

High Power Test Systems

HTOL, Burn-In, Reliability Testing & More

DC TO 65 GHz

Signal Distribution Systems

Splitter/Combiner & Coupler Arrays for Multi-Channel Setups

FAST TURNAROUND

Custom Systems

Tailored to Your Needs from Definition to Delivery

Mini-Circuits®

INTRODUCING ALTUM RF'S FAMILY OF LOW-NOISE / DRIVER AMPLIFIERS

These compact devices support a range of applications, including telecom, point-to-point radio, ISM, VSAT, SATCOM, aerospace and defense, and test and measurement.

- **ARF1200Q2:** Ka-band, 22 dB linear gain, 1.6 dB NF, ideal for phased array applications
- **ARF1205Q2:** low current consumption, single positive bias operation
- **ARF1211Q3:** ultra-low current consumption, for use in SATCOM, A&D radio systems, test and measurement
- **ARF1218Q2:** for 24 GHz applications, battery-operated applications, single positive bias

Part	Freq. Range (GHz)	Gain (dB)	NF (dB)	P1dB (dBm)	Bias Voltage (V)	Bias Current (mA)	Package
ARF1200Q2	22–31.5	22	1.6	8	3.3	15	2.5 × 2.5 QFN
ARF1201Q2	22–31.5	24	2.4	15	3.3	40	2.5 × 2.5 QFN
ARF1202Q2	37–43.5	21.5	2.5	7	3.3	15	2.5 × 2.5 QFN
ARF1203Q2	37–43.5	21	2.7	12.5	3.3	40	2.5 × 2.5 QFN
ARF1205Q2	13–25	23	1.9	16	4	65	2.5 × 2.5 QFN
ARF1211Q3	6–14	25	1.7	20	5	60	3 × 3 QFN
ARF1218Q2	22–26	29	2.6	9	3.3	6	2.5 × 2.5 QFN

LEARN MORE AT ALTUMRF.COM

INFO@ALTUMRF.COM | +31 (0) 40 2390 888 | TWINNING CENTER, DE ZAALE 11, 5612 AJ EINDHOVEN, THE NETHERLANDS
©2025 ALTUM RF. ALL RIGHTS RESERVED.

800.348.5580 / 630.208.2200 RELLPOWER@RELL.COM RELLPOWER.COM

Richardson Electronics
POWER & MICROWAVE TECHNOLOGIES

Samples of Altum RF's low-noise / driver amplifiers are available now from Richardson Electronics, Ltd.

40W267 Keslinger Road / P.O. Box 393
LaFox, IL 60147-0393

INNOVATIVE SURFACE-MOUNT AND SIP-READY DEVICES

High Performance RF Miniaturization

High Q Lumped Element Filters

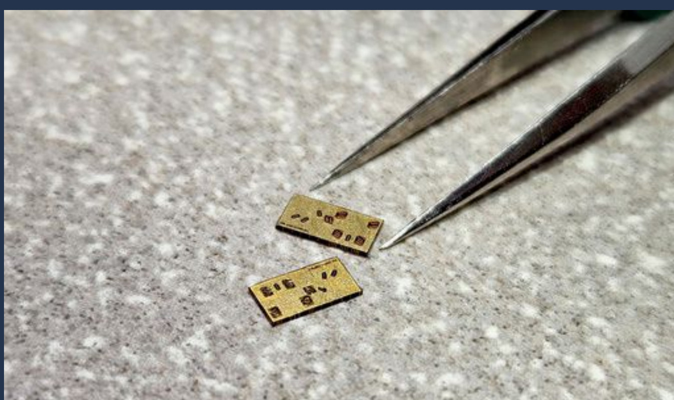

- Product family covers frequency bands between 500 MHz to 10 GHz
- High selectivity with low insertion loss
- Smaller footprint and higher in-band and out-of-band rejection than other surface-mount filters
- Lowpass, highpass, bandpass, notch and diplexer applications including RF SOCs, RF front ends, and phased-array antennas
- Custom derivatives available including multiplexers and switched filter banks
- SiP- and PCB-ready packaging

SAW and High Power SAW Filters

- Product family covers frequency ranges from 20 MHz up to 1.5 GHz with narrow, wide, and fractional bandwidths
- High input power options up to +35 dBm CW
- Shape factors below 1.10:1
- Backside planar etching for improved spurious rejection
- Ultra-flat group delay
- Small footprint with variety of SMT packages
- Semi-standard and custom solutions

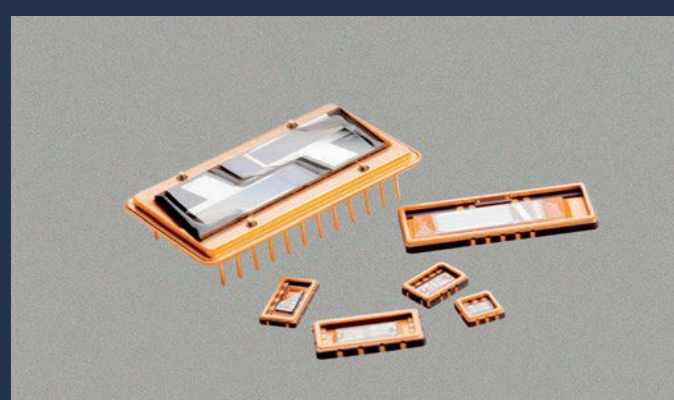

To learn more or to connect with our team visit **spectrumcontrol.com/rf-filters**

SPECTRUM CONTROL™

spectrumcontrol.com © 2025 Spectrum Control, Inc. All rights reserved

All Test and Measurement Components are In-Stock

Pasternack RF test and measurement equipment, calibration kits, cable assembly and other precision interconnects cover a broad range of uses and applications across the radio frequency spectrum to provide phase stability with many cycles of repeatability over a wide temperature range.

In-Stock & Shipped Same-Day

pasternack.com
+1 (800) 715-4396

PE PASTERNACK®
an INFINITE brand


RF-LAMBDA
THE LEADER OF RF BROADBAND SOLUTIONS
BROADBAND SSPA / EMC BENCHTOP
SOLID STATE POWER AMPLIFIER
0.1-22GHZ
ULTRA BROADBAND SSPA
RFLUPA01M22GA
4W 0.1-22GHZ
RFLUPA0218GB
20W 1-19GHZ
300W 6-18GHZ SOLID STATE BROADBAND
400W 8-11GHZ
SOLID STATE BROADBAND
0.1-6GHZ VHZ,
UHF, L, S, C BAND
RFLUPA02G06GC
100W 2-6GHZ
RFLUPA0706GD
30W 0.7-6GHZ
MADE IN USA
6-18GHZ C, X, KU BAND
RFLUPA08G11GA
50W 8-11GHZ
RFLUPA0618GD
60W 6-18GHZ
RFLUPA06G12GB
25W 6-12GHZ
18-50GHZ K, KA, V BAND
RFLUPA18G47GC
2W 18-47GHZ
RFLUPA27G34GB
15W 27-34GHZ
RFLUPA47G53GA2
10W 47-53GHZ
RFLUPA27G34GB
30W 18-40GHZ
BENCHTOP RF MICROWAVE SYSTEM POWER AMPLIFIER
RAMP00G06GA- 30W 0.01-6GHZ
RAMP39G48GA- 4W 39-48GHZ
RAMP01G22GA- 8W 1-22GHZ
RAMP27G34GA- 8W 27-34GHZ
www.rflambda.com
sales@rflambda.com
1-888-976-8880
1-972-767-5998
San Diego, CA, US
Carrollton, TX, US
Ottawa, ONT, Canada
Frankfurt, Germany

Microwave Journal
April 2025
Vol. 68 • No. 4
Amplifiers & Oscillators
mwjournal.com

CONTENTS

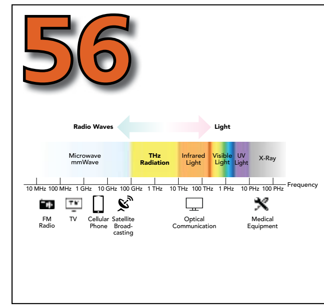

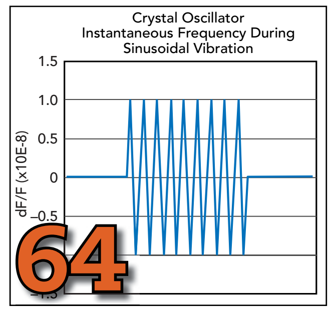

Cover Feature

Special Reports

Tutorial

SCAN ME!
SUBSCRIBE & RENEW NOW

ACCESS NOW!
digital.microwavejournal.com

eXclusive Digital Content ›››

68 YEARS OF PUBLISHING EXCELLENCE

Has Amplifier Performance or Delivery Stalled Your Program?

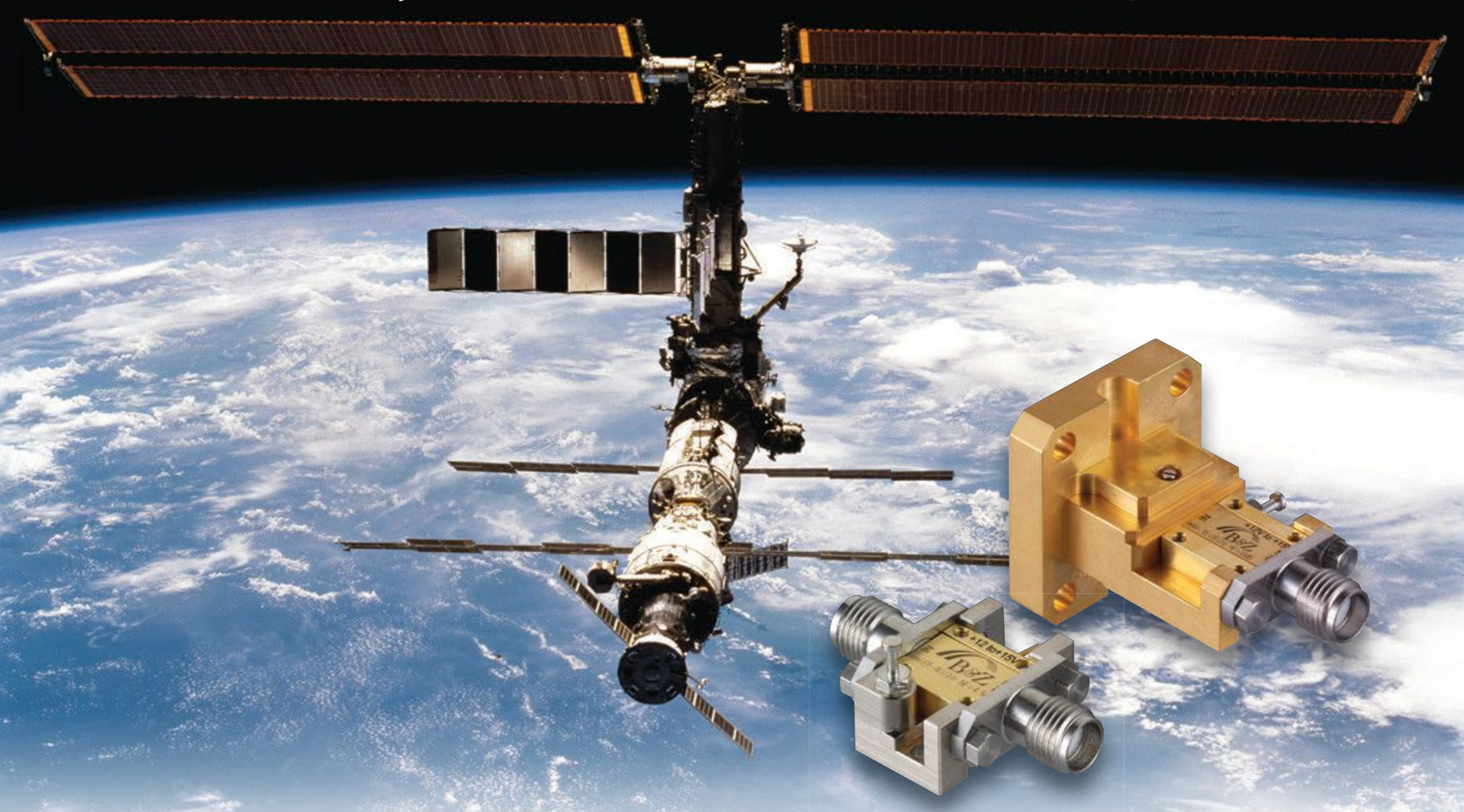

Noise Figure In Select Frequency Bands

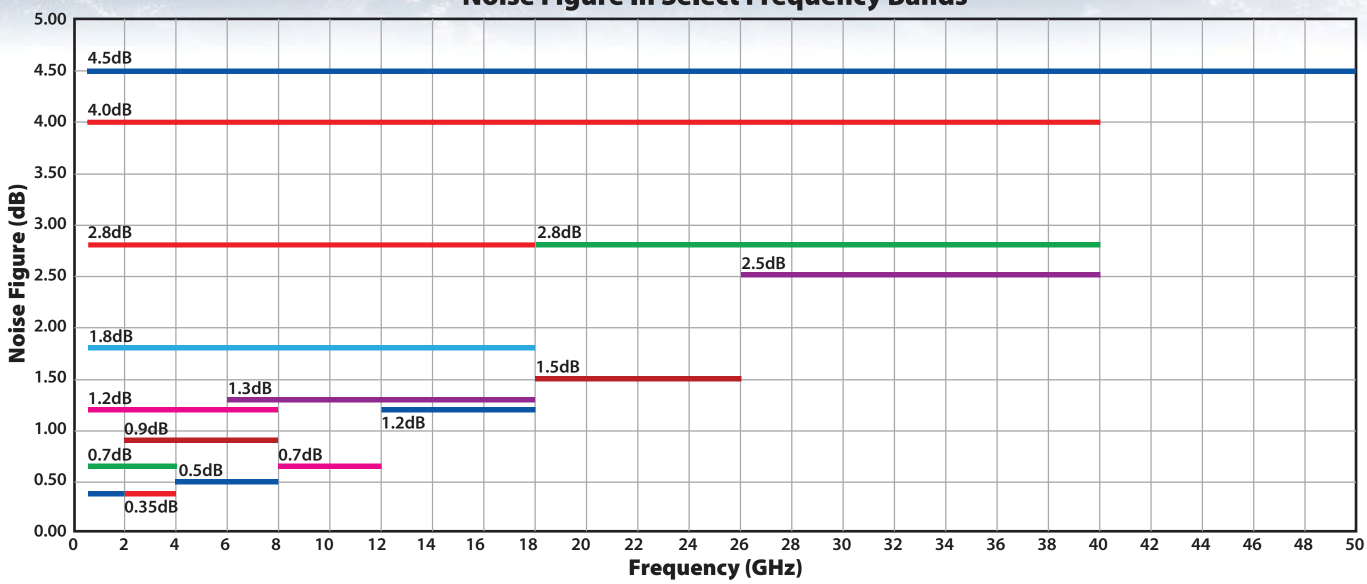

B&Z TECHNOLOGIES

Innovating to Excel

www.bnztech.com

Microwave Journal

CONTENTS

mwjournal.com

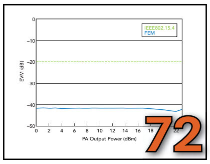

Product Feature

Tech Briefs

Departments

Microwave Journal (USPS 396-250) (ISSN 0192-6225) is published monthly by Horizon House Publications Inc., 685 Canton St., Norwood, MA 02062. Periodicals postage paid at Norwood, MA 02062 and additional mailing offices.

Photocopy Rights: Permission to photocopy for internal or personal use, or the internal or personal use of specific clients, is granted by Microwave Journal for users through Copyright Clearance Center provided that the base fee of $5.00 per copy of the article, plus $1.00 per page, is paid directly to the Copyright Clearance Center, 222 Rosewood Drive, Danvers, MA 01923 USA (978) 750-8400. For government and/or educational classroom use, the Copyright Clearance Center should be contacted. The rate for this use is 0.03 cents per page. Please specify ISSN 0192-6225 Microwave Journal International. Microwave Journal can also be purchased on 35 mm film from University Microfilms, Periodic Entry Department, 300 N. Zeeb Rd., Ann Arbor, MI 48106 (313) 761-4700. Reprints: For PDF reprints, contact Barbara Walsh at (781) 769-9750.

POSTMASTER: Send address corrections to Microwave Journal, PO Box 1028, Lowell, MA 01853 or e-mail mwj@e-circ.net.com. Subscription information: (978) 671-0446. This journal is issued without charge upon written request to qualified persons working in the RF & microwave industry. Other subscriptions are: domestic, $130.00 per year, two-year subscriptions, $200.00; foreign, $225.00 per year, two-year subscriptions, $400.00; back issues (if available) and single copies, $20.00 domestic and $30.00 foreign. Claims for missing issues must be filed within 90 days of date of issue for complimentary replacement.

©2025 by Horizon House Publications Inc.
Posted under Canadian international publications mail agreement #PM40612608

STAFF

Group Director: Carl Sheffres
Associate Publisher: Michael Hallman
Media Director: Patrick Hindle
Brand & Content Director: Jennifer DiMarco
Technical Editor: Eric Higham
Associate Technical Editor: Cliff Drubin
Editorial & Media Specialist: Kelley Roche
Associate Editor: Kaitlyn Joyner
Multimedia Staff Editor: Barbara Walsh
Electronic Marketing Manager: Chris Stanfa
Senior Digital Content Specialist: Lauren Tully
Digital Content Specialist: Vincent Carrabino
Director of Production & Distribution: Edward Kiessling
Art Director: Janice Levenson
Graphic Designer: Ann Pierce

EUROPE

Office Manager: Nina Plesu

CORPORATE STAFF

CEO: William M. Bazzy
President: Ivar Bazzy
Vice President: Jared Bazzy

EDITORIAL REVIEW BOARD

A. Chenakin
R. Dahle
T. K.Das
B. Derat
K. Galitskaya
R. Hershtig
D. Jorgesen
W. Lohmeyer
M. Ozalas
A. Poddar
C. Puente
B. Rautio
M. Roberg
U. Rohde
F. Schindler
R. Smith
D. Vye

EXECUTIVE EDITORIAL OFFICE

685 Canton Street, Norwood, MA 02062
Tel: (781) 769-9750
FAX: (781) 769-5037
e-mail: mwj@mwjournal.com

EUROPEAN EDITORIAL OFFICE

16 Sussex Street, London SW1V 4RW, England
Tel: Editorial: +44 207 596 8730 Sales: +44 207 596 8740
FAX: +44 207 596 8749

SUBSCRIPTION SERVICES

Send subscription inquiries and address changes to:
Tel: (978) 671-0446
e-mail: mwj@e-circ.net

www.mwjournal.com

Printed in the USA

PERFORMANCE THAT SEEMS

INTRODUCING

Marki Microwave's New Broadband LNA Family

Marki Microwave's new LNA family (AMM-9852PSM to AMM-9862PSM) offers industry-leading performance from DC to 40 GHz across ten variants. Covering 20 GHz, 30 GHz, and 40 GHz, each range includes high/low-power models with internal/external biasing. Designed for flat gain, IP3, and noise figure, they achieve noise figures as low as 1.5 dB (20 GHz), 2.25 dB (30 GHz), and 3 dB (40 GHz) in a compact 3mm QFN.

APPLICATIONS

- **RF Front Ends**
- **Test and Measurement Systems**
- **Electronic Warfare**
- **Satellite Communications**

RFMW®

Global Distribution Partner

Contact: sales@rfmw.com

Marki® microwave

The Trusted Leader When Performance Matters

www.markimicrowave.com

Microwave Journal ONLINE .COM

E-LEARNING CENTER

Access webinars on-demand from the archived webinars and events page at www.mwjournal.com/events

WHITE PAPERS

Coilcraft
Using Baluns and RF Components for Impedance Matching

COPPER MOUNTAIN TECHNOLOGIES
Eliminating Fixture Effects from Embedded Measurements

Mini-Circuits
Characteristics & Measurement of Pulsed RF Waveforms

Executive Interview

David Quinn, President of Electronic Components & Assemblies (ECA) Business Unit at Infinite Electronics, discusses his background, the Infinite Electronics brand and how it has evolved, along with his vision for how the company is positioning for the future.

Join Us Online

Follow us @Pathindle @MWJEric @MWJEditor

Join us at the RF and Microwave Community

Become a fan at facebook.com/ microwavejournal

Catch *Frequency Matters*, the industry update from *Microwave Journal*, microwavejournal.com/FrequencyMatters

Revolutionizing Cellphone and Wi-Fi RF Front-Ends with GaN-on-Si

From RF to Terahertz: Advances in On-wafer S-parameter Measurement Technologies

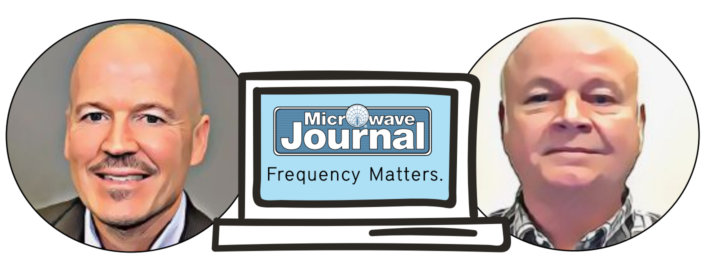

Enabling Applications with High-Power Semiconductor Terahertz Sources

Quartz Crystals in Vibratory Environments

Visit us @ mwjournal.com

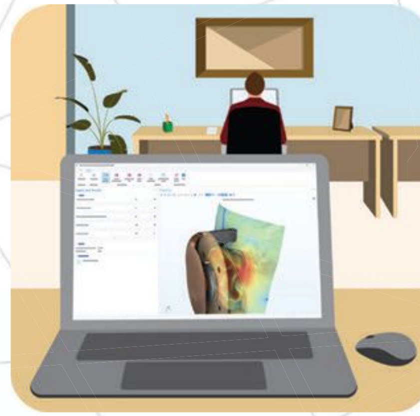

Fast Track Development

with Simulation Apps

Modeling and simulation accelerates design iteration, understanding, and project planning, but requires specific expertise that is not easy to access from the field, factory, or lab where in-the-moment decisions are made. Extend the benefits of simulation to those who need it, when they need it with your own custom apps.

» ***comsol.com/feature/apps***

Effective Collaboration

When simulation experts build custom user interfaces around their models and distribute them as apps, colleagues and customers can use simulation to guide decisions in real time.

Full Control

Building, editing, and distributing your own apps is easy with COMSOL Multiphysics®. Compile them and distribute as standalone apps worldwide with COMSOL Compiler™. Control and manage access to the apps with your own COMSOL Server™ environment.
The choice is yours.

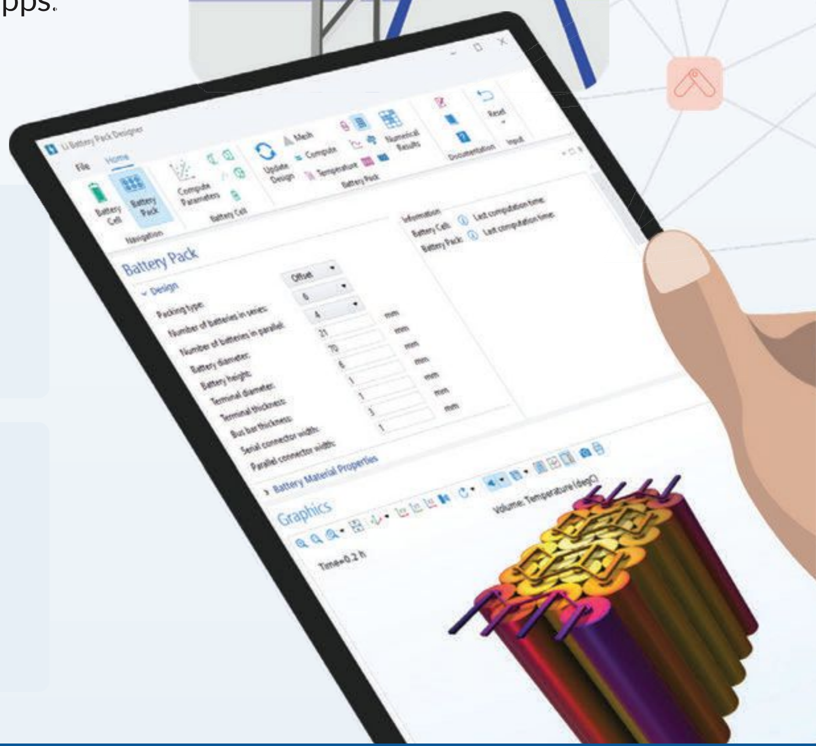

COMSOL

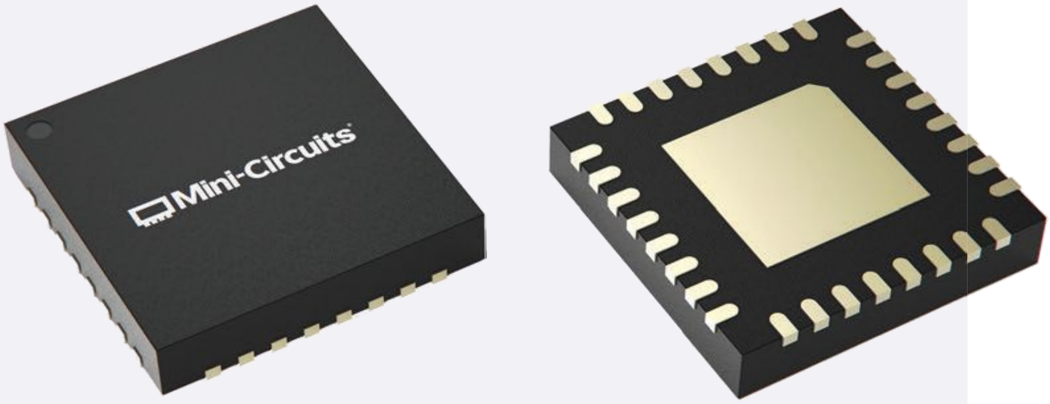

0.01 TO 10 GHz

MMIC PA's up to 2W

Wide Bandwidth & High Linearity

1W and 2W GaAs MMIC amplifiers achieve high dynamic range from 0.01 to 10 GHz

PMA5-63-2W+
- 0.01 - 6 GHz
- Low NF, 2.7 dB
- P1dB, +31.2 dB
- P_{SAT} +33.8 dBm
- OIP3, +44.5 dBm

PMA5-83-2W+
- 0.01 - 10 GHz
- Low NF, 3.9 dB
- P1dB, 31 dBm
- P_{SAT} +33 dBm
- OIP3, +40.9 dBm

P5-83-LV+
- 0.01 - 10 GHz
- Low NF, 2.6 dB
- P1dB, +28.7 dBm
- P_{SAT} +31.2 dBm
- OIP3, +40.8 dBm

LEARN MORE

Mini-Circuits®

MARK YOUR CALENDAR

STAY CONNECTED TO COMING EVENTS

APRIL

14-15
WAMICON
Cocoa Beach, Fla.
www.ieeewamicon.org

16-18
MilSatCom USA
Arlington, Va.
www.smgconferences.com/defence/northamerica/conference/MilSatCom-USA

24-26
The 59th Annual Microwave Power Symposium (IMPI 59)
Edmonton, Alberta, Canada
https://impi.org/events/symposium/

JUNE

2-4
Space Tech Expo USA
Long Beach, Calif.
www.spacetechexpo.com

15-17
RFIC 2025
San Francisco, Calif.
https://rfic-ieee.org

15-20
IMS2025
San Francisco, Calif.
https://ims-ieee.org

20
ARFTG
San Francisco, Calif.
http://arftg.org/105-conference

JULY

13-18
IEEE AP-S/URSI
Ottawa, Canada
https://2025.apsursi.org/

AUGUST

18-22
IEEE EMC + SIPI
Raleigh, N.C.
https://emc2025.org/

SEPTEMBER

21-26
EuMW 2025
Utrecht, The Netherlands
www.eumw.eu

ONLINE PANEL SERIES

5/8
Metamaterials

Call for Papers Deadlines

5/5 AMTA

5/9 BCICTS

FOR DETAILS VISIT MWJOURNAL.COM/EVENTS

Revolutionizing Cellphone and Wi-Fi RF Front-Ends with GaN-on-Si

Hal Emmer, Michael Guyonnet and Vincent Johnson
Finwave Semiconductor, Waltham, Mass.

The last 30 years have seen a dramatic increase in data traffic across all wireless networks. This increase has been fueled by video streaming, social networks, online gaming and soon, generative AI with its multitude of expected new applications. Smartphones, infrastructure networks, including small cells, Wi-Fi and fixed wireless access (FWA) all must innovate to stay ahead of the curve.

After three years of decline, smartphone sales are rebounding[1] with projected year-over-year growth supported by the deployment of 5G SA and 5G Advanced. 6G is anticipated around 2030, leveraging new frequency bands, known as FR3, between 6 and 15 GHz. Meanwhile, Wi-Fi is entering its seventh generation with the addition of the 6 GHz band and other innovations supporting higher data rates. A planned eighth generation will include an extension to mmWave bands. Forecasters say that Wi-Fi 7 is on track to surpass Wi-Fi 6 by 2027.[2]

FWA is poised to replace some cable/fiber-optic deployments.[3] At the end of 2024, FWA data traffic represented 25 percent of the global mobile network data traffic and this is poised to quadruple by 2030. Unlike mobile wireless, where the user's location must be tracked geographically, FWA uses fixed consumer premises equipment (CPE) to deliver broadband internet to a home or business. When a line-of-sight link between the base station and the CPE can be established, the complex propagation challenges of the FR2 frequency band at 28 to 39 GHz can be overcome by using high gain antennas and higher power amplifiers (PAs). This FR2 frequency range has the bandwidth to enable FWA to provide a genuine alternative to cable and fiber-optic networks.

While these wireless access technologies have varying needs and specifications, they share a common element: the radio frequency front-end (RFFE). The RFFE, located between the RF transceiver and the antenna, is a critical component responsible for transmitting and receiving wireless signals. The RFFE comprises several key components, including the PA on the transmit path and a low noise amplifier (LNA) and switches on the receive path. These components must work together seamlessly to ensure efficient signal transmission and reception while minimizing power consumption and maintaining signal integrity. For these applications, the average output power of the RFFE is in the range of 0.25 to 4 W, with peak power up to 10 W. This range of output power compensates for the losses of the filters and switches with the actual value depending on the signal bandwidth, QAM modulation, frequency, interference and other factors.

While GaAs was the dominant technology used for the PA, switch and LNA for the first 20 years of mobile cellphone and Wi-Fi applications, it has been progressively displaced by silicon-on-insulator (SOI) technology. This shift to SOI has primarily occurred in the switch and LNA functions, leaving the PA function to GaAs HBT technology for high-power, sub-6 GHz applications and GaAs pHEMT technology for low-power applications in the 6 to 40 GHz frequency range. However, with the progressive shift to higher frequencies, as evidenced by applications in the FR3 band and Wi-Fi 7 with similar or higher transmit power demands, GaAs HBT technology is falling short in power efficiency and this poses a clear challenge to the industry.

5 V GAN-ON-SI E-MODE: A POWERFUL SOLUTION

Enhancement-mode (E-mode) GaN-on-Si offers a compelling alternative to GaAs in 5 V applications due to its unique properties. Produced in a state-of-the-art 8-in. silicon foundry, Finwave Semiconductor's GaN-on-Si leverages a cost-effective supply chain to deliver cutting-edge technology. From a performance and process control perspective, 8-in tools offer advantages over 6-in. tools in addition to the cost reduction realized by fabricating more devices per wafer.

Unlike mainstream depletion-mode (D-mode) GaN, which requires biasing and sequencing of the negative gate voltage with the drain voltage, E-mode GaN is "normally off." This means the device

The only
QPL Certified
MECHANICAL
SWITCH
House!
Quick Turn
RF FILTER
Prototypes
are in our DNA!
Huge Library
of PASSIVES
with Best in Show
HIGH POWER
COUPLER
offering!
RLC ELECTRONICS
L-4241A
S/N 2206001
RUGGED & RELIABLE
AGILE & ADAPTIVE
HIGH POWER & VARIETY
RLC
RF MECHANICAL SWITCHES,
RF FILTERS & RF PASSIVES
AS9100 CERTIFIED, MADE IN USA
High Performance Precision Microwave Components
Serving the world-wide aerospace & defense community since 1959
Robust Catalog Portfolio - no hassle, quick turn, custom solutions our specialty
RLC Electronics | 83 Radio Circle, Mt. Kisco, NY 10549 | 914-241-1334 | sales@rlcelectronics.com | www.rlcelectronics.com

requires a positive gate voltage to turn on and, therefore, does not need to be sequenced with the drain voltage. This eliminates the need for a bias controller, which significantly simplifies the application, reduces the die size and lowers cost.

GAN-ON-SI ADVANTAGES OVER GAAS HBT

As Finwave has developed the E-mode GaN-on-Si process, several advantages have become apparent:

- **Higher breakdown voltage:** GaN can withstand higher voltages than GaAs, making it more robust and reliable. This is important for handling signal fluctuations and preventing device damage.
- **Better gain and efficiency at higher frequencies:** GaN maintains good power efficiency up to 40 GHz. This is crucial for supporting all frequency bands in use and proposed for mobile and FWA (FR1 to FR2 and FR3), Wi-Fi 7 and Wi-Fi 8 (2.4, 5 and 6 GHz, along with mmWave bands).
- **Lower cost**: GaN-on-Si is becoming increasingly cost-competitive with GaAs, thanks to advancements in manufacturing. This makes it a more affordable option for cellphone manufacturers.
- **Integration:** Going to higher frequencies necessitates integrating the switch, LNA and amplifier on the same die for optimal performance. GaN HEMTs generally exhibit good noise figure characteristics due to their high electron mobility and low parasitic capacitances, which contribute to the lower noise generation required for LNAs. Additionally, GaN HEMTs offer very fast switching speeds and low insertion loss in an SPDT configuration.

Finwave's E-mode RF transistor technology has fully realized the advantages of GaN-on-Si, demonstrating the capability of the technology to meet these evolving market demands. Fabricated with a CMOS-compatible process on 200 mm GaN-on-Si wafers, this technology is currently in the process of being transferred to GlobalFoundries for mass production, leveraging their facility in Burlington, Vt. Finwave's proprietary approach has several innovations that result in record performance and excellent manufacturability, including regrown N++ ohmic contacts with a structure to improve source resistance further, as well as an etch-stop epitaxy structure allowing for highly repeatable fabrication processes with high uniformity.

Excellent Contact and Source Resistance

Finwave's RF devices employ regrown, heavily doped contacts to achieve excellent contact resistance. ***Figure 1a*** shows a wafer map of transfer length method (TLM) measurements for contact resistance on a 200 mm GaN-on-Si wafer. A median contact resistance of 0.126 Ohm-mm was achieved with a cross-wafer standard deviation of 10 percent. ***Figure 1b*** shows TLM measurements of sheet resistance on the 200 mm GaN-on-Si wafer.

In addition to the low contact resistance, a proprietary method is used to further reduce the source resistance by about 50 percent compared to a standard GaN device structure. The source resistance is a key device parameter that drives performance in RF transistors used in all parts of the RFFE. Aside from simply contributing to on-resistance ($R_{ds\text{-}on}$), the source resistance acts as a feedback resistor when the transistor is used as an amplifier. The result is that in the linear region, the effective transconductance (g_m) is reduced by the factor shown in ***Equation 1***:

$$g_{me} = g_{mi}/(1 + Rs * g_{mi}) \qquad (1)$$

Where:

g_{me} is the effective g_m

g_{mi} is the intrinsic device transconductance (a theoretical maximum value for g_m if the source resistance is reduced to 0)

Figure 2 shows a comparison of transconductance, g_m, versus V_{gs} for the Finwave device with reduced source resistance and a standard device. As shown, the device with reduced source resistance shows a g_m peak of 760 mS/mm, while a standard device structure with higher source resistance has a g_m peak of 620 mS/mm. Small-signal RF measurements show that the devices with reduced source resistance and higher transconductance have an RF gain that is approximately 0.5 dB higher between 5 and 8.5 GHz and more than 1 dB higher between 8.5 and 24 GHz.

When configured as a switch, the low contact and source/drain resistances directly contribute to the figure of merit, R_{on}*C_{off}. While not presented here in detail, initial switch designs with Finwave's process yielded a figure of merit of 140 femtoseconds, better than typical values for GaAs and approaching those achieved with SOI.[4] GaN has the additional advantage of higher intrinsic breakdown voltage and, thus, improved power handling than either incumbent technology. Finally, this RF switch was fabricated

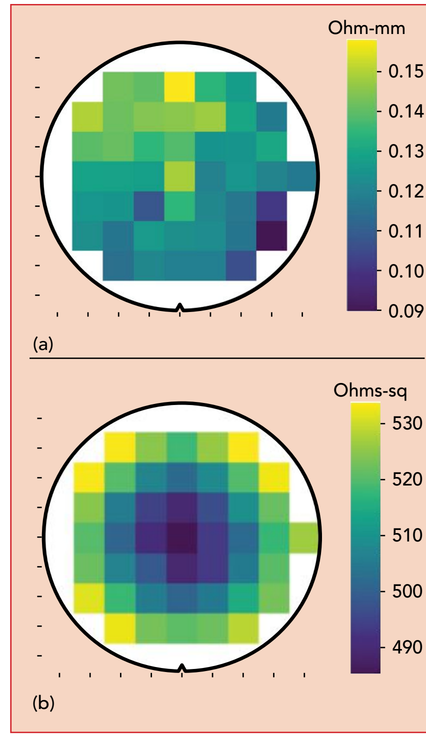

Fig. 1 Wafer map of contact resistance, Rc (a) and sheet resistance, Rsh (b).

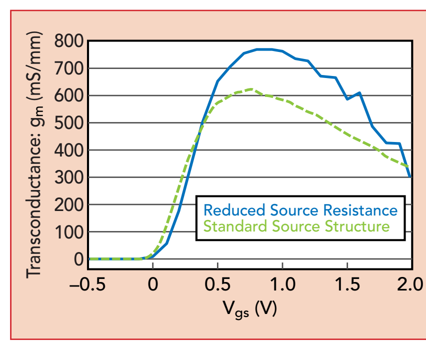

Fig. 2 Transconductance versus V_{gs}.

MILLER MMIC

AI Powered RFIC Design Platform

RapidRF

Revolutionizing RFIC Design with AI-Driven Innovation.
Our AI driven design platform is redefining the future of the RFIC design industry. We automate the design of RFICs for the next generation of wireless communication, accelerating innovation for a smarter future.

AI-Driven Design Automation – Multiplying Engineers Productivity

- Technology Independent: GaAs, GaN, and Silicon proven
- Fast and reliable: more than 100x faster than an experienced design engineer
- AI-Driven Layout Optimization: cutting down costs, maximizing performance

Reference Design Done by Experienced Engineer

≈10 Days/Design

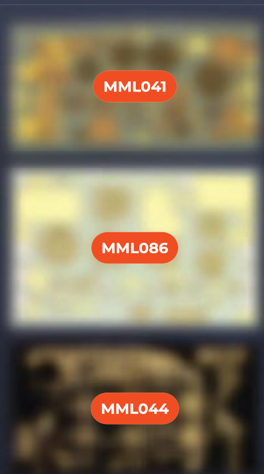

AI MMIC Design Process

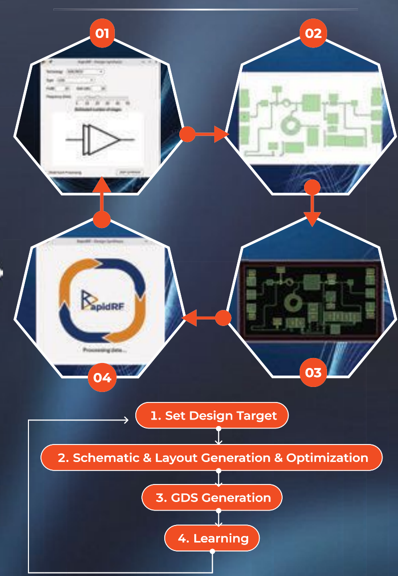

Design Done by RapidRF AI Platform

≈5 Hours/Design

Performance Comparisons: RapidRF AI vs Human Engineer Designs

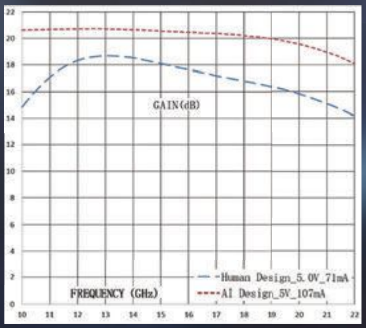

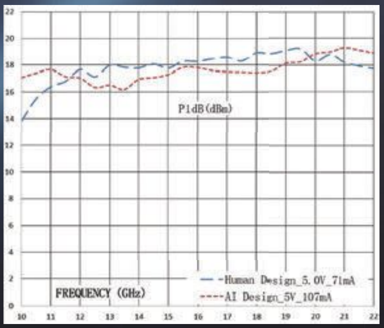

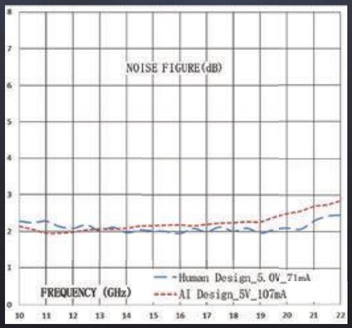

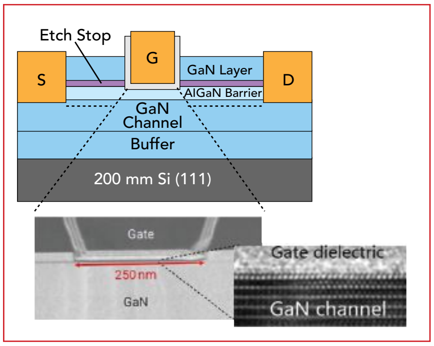

Fig. 3 Transistor structure and TEM of gate dielectric interface.

using a process optimized for amplifier transistors, with the possibility of use in a fully integrated RFFE. This figure of merit could likely be improved in a process optimized for RF switches.

Etch-Stop Technology

Figure 3 shows a TEM image of the 250 nm L_g and gate dielectric interface, along with the transistor structure. Finwave's GaN-on-Si epitaxial wafers contain an etch-stop layer, which facilitates the formation of an E-mode channel and ohmic contacts in a highly reproducible way. Instead of relying on a tightly controlled etch rate and time to etch a specific depth into the AlGaN barrier layer to achieve the target transistor properties, the channel etch can land on the etch-stop layer in a controllable way. By using an etch process selective to our etch-stop layer to remove the GaN cap layer over the gate region, we can achieve a low-damage gate recess and a high-mobility channel. This comes with the additional benefit of excellent across-wafer uniformity, including a standard deviation in the on-resistance of 3 percent and threshold voltage less than 100 mV, both with room to improve as we scale toward full production.

Device Reliability

Reliability is a challenge for GaN-on-Si MISHEMT devices. One of the key issues is the gate dielectric reliability and its effect on the bias temperature instability (BTI). Defects within the gate dielectric bulk material and at the semiconductor-dielectric interface are both able to trap charges, causing V_{th}, R_{on} and other device parameter shifts.[5] Finwave's device achieves excellent gate reliability through the optimization of device design and process conditions. High-temperature gate bias (HTGB) stress tests conducted at 150°C with V_g = 1 V, V_d = 0 V for 10,000 seconds show minimal shifts in all device parameters, with a V_{th} change of less than 50 mV and R_{on} change less than 0.2 percent. This state-of-the-art reliability performance is achieved by minimizing the effect of the deep traps in the gate region with a high-quality dielectric and low-defect interface. This is critical to enable our technology to operate stably for various RF applications over their lifetime.

DEVICE RESULTS

Figure 4a shows DC measurements at 600 ns pulsed IV. ***Figure 4b*** shows the same FET with subthreshold I_d-V_{gs} measurement at V_{ds} = 50 mA and 5 V and transconductance measured at V_{ds} = 5 V. ***Figure 4c*** shows breakdown voltage measurements of the FET at different V_{gs} bias voltages. Destructive breakdown occurs at around 30 V. All these devices are 2-finger RF transistors with a source-to-drain distance (L_{sd}) of 700 nm, gate length (L_g) of 250 nm and width (W_g) of 50 µm per finger. These were fabricated using standard CMOS-compatible processes and materials, including the passivation and gate dielectrics, as well as the gate, ohmic and interconnect metal layers.

The E-mode FET has a knee voltage, V_{knee}, around 1 V, on-resistance, R_{on}, of 0.8 to 0.9 Ohm-mm, peak transconductance, g_m, of 760 mS/mm and a threshold voltage, V_{th}, around 0.15 V. Pulsed-IV measurements reveal excellent dynamic behavior and minimal trapping, with current collapse less than 10 percent around the V_{knee} voltage. The device has a subthreshold swing of 80 mV/dec and a negligible DIBL of 40 mV/V, demonstrating an MIS interface with very low interface state density.

The DC breakdown voltage was measured at V_{gs} = -1, -2 and -3 V on the same device. Drain-to-source punch-through was observed for V_{gs} = -1 and -2 V, resulting in non-destructive soft breakdown behavior. Destructive breakdown occurs at V_{ds} = 30 V and V_{gs} = -3 V and it is caused by gate dielectric reverse

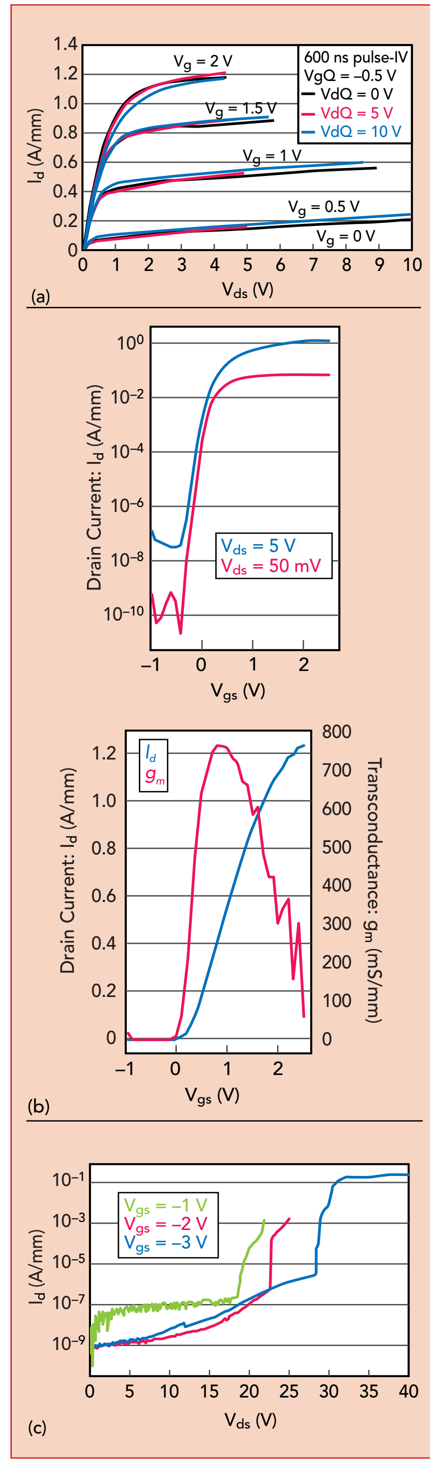

Fig. 4 DC measurements of the 2 x 50 µm L_g = 0.25 µm FET.

breakdown, resulting in a permanent increase of gate leakage. The off-state leakage of the transistor is typically less than 1 uA/mm, orders of magnitude lower than the conventional Schottky-gate D-mode GaN FETs.[6]

RF Characteristics

Figure 5a shows F_t and F_{max} as a

3H Communication Systems
AS9100 & ISO9001:2015 CERTIFIED

Offering RF/microwave filter solutions that are innovative, high quality, cost-effective, DC to 50 GHz, with a 5-year warranty.

THE PROOF IS IN THE PERFORMANCE

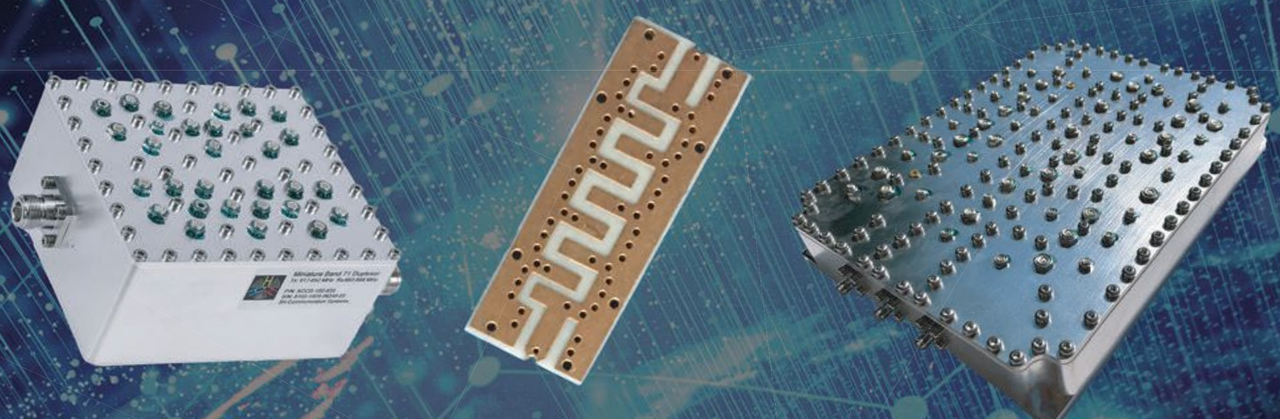

LC • CERAMIC • CAVITY • PRINTED • MULTIPLEXERS • SWITCHED FILTER BANKS • MULTI-FUNCTION ASSEMBLIES

949.529.1583 | sales@3hcomm.com
3HCommunicationSystems.com

function of I_d. ***Figure 5b*** shows RF gain versus frequency at I_d = 300 mA/mm and V_{ds} = 5 V. These small-signal measurements were made on the same 2 × 50 µm, L_g = 0.25 µm FET used for the DC measurements. The results show that extracted F_t is typically between 60 to 65 GHz and F_{max} is between 100 and 110 GHz. F_{max} is limited by the relatively high gate resistance of the thin Al gate metal which can be improved with standard CMOS back-end processing like copper-based interconnects.

Large-signal load-pull measurements were conducted on the 2 × 50 µm, L_g = 0.25 µm FET at 8, 13 and 26 GHz, covering the proposed usage range of the FR3 band. ***Figure 6a*** shows transducer gain and PAE versus P_{out} at 8, 13 and 26 GHz with V_{dd} = 5 V. ***Figure 6b*** shows load-pull with V_{dd} of 1 to 5 V at 8 GHz and ***Figure 6c*** shows 8 GHz AM-PM within 1.5 degrees for AM-AM within 3.5 dB and V_{dd} from 2 to 5 V.

The source and load impedances at the fundamental frequency were tuned for maximum PAE, while the impedances at the second and third harmonics were both set to 50 Ohms. The FET demonstrated 16 dB and 14 dB transducer gain with PAE of 62 percent and 56 percent at 8 GHz and 13 GHz, respectively. At 26 GHz, the device gain and PAE are reduced to 9 dB and 45 percent due to the limitation of the relatively large L_g and gate resistance. By reducing L_g and W_g to 220 nm and 2 × 20 µm, respectively, the high frequency performance improves to a gain of 12 dB and 51 percent PAE at 26 GHz.

With the device's low R_{on} and V_{knee}, operation is possible at low V_{dd}, which is important in envelope-tracking applications. Load-pull measurements were performed with V_{dd} stepped from 1 to 5 V, with a constant impedance determined to be optimal at a V_{dd} of 5 V. Device gain and PAE remained high, above 13 dB and 50 percent, respectively, when V_{dd} was reduced to 2 V. The device also demonstrated good linearity in this range of operation, with AM-PM within 1.5 degrees for AM-AM compression up to 3.5 dB at V_{dd} of 2 to 5 V.

With a DC breakdown voltage greater than 20 V, the GaN FET is capable of operating at a V_{dd} higher than 5 V. For example, measurements at V_{dd} = 8 V showed a gain of 17 dB and PAE of 60 percent at 8 GHz with a P_{out} of 21 dBm. The resulting power density of more than 1.25 W/mm demonstrates the advantage of GaN over GaAs for higher V_{dd} and power density.

The high DC breakdown voltage and soft breakdown characteristics result in excellent device robustness to sub-optimal RF conditions. A stress test was performed with a VSWR of 10:1 with V_{dd} = 5 V. The device was exposed to loads of $|\Gamma|$ = 0.9 moved around the Smith chart for 30 minutes. Following a cooldown period, large-signal measurements showed no shifts in device performance.

LINEARITY OF BROADBAND MODULATED SIGNAL

Of the many specifications a PA must meet, linearity is the most critical to ensure compliance with 3GPP

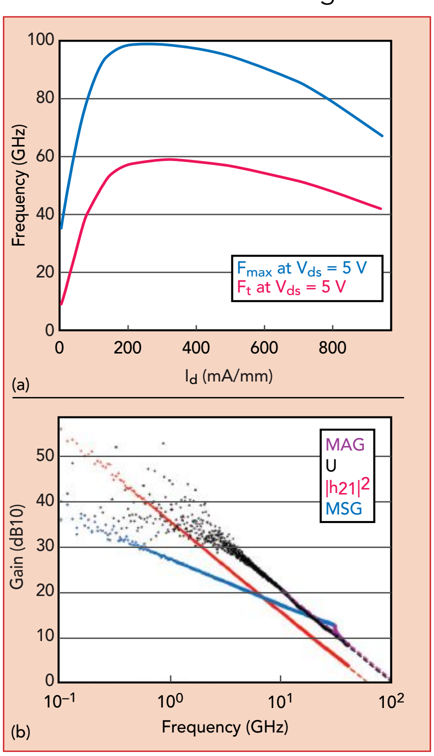

Fig. 5 **Small-signal FET measurements.**

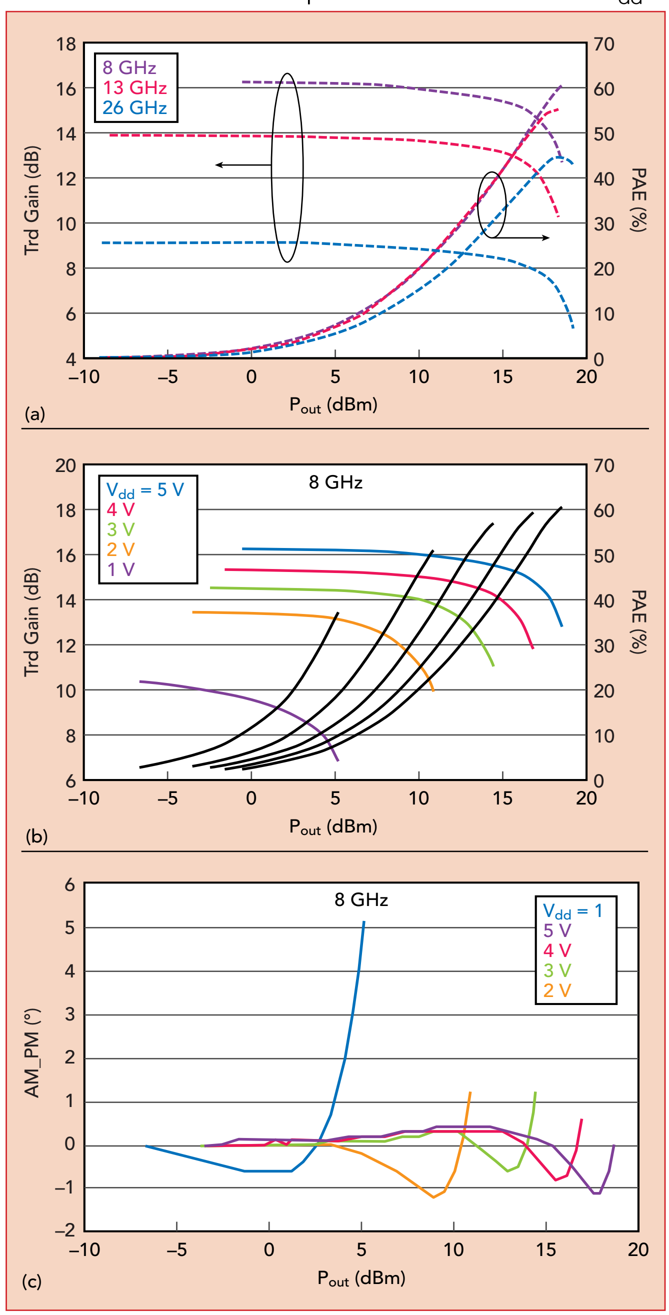

Fig. 6 **Large-signal FET measurements.**

26.5-40GHz 500W

Solid State Power Amplifier

Features

- Ultra Wide Band: 26.5-40GHz
- Gain: 57dB Min •
- Output Power: 57.5dBm Min
- High-efficiency GaN technology
- Low power consumption
- Low spurious signal
- Forward/reverse power monitoring
- Over voltage, over temperature, over current protection
- Optional overdrive protection

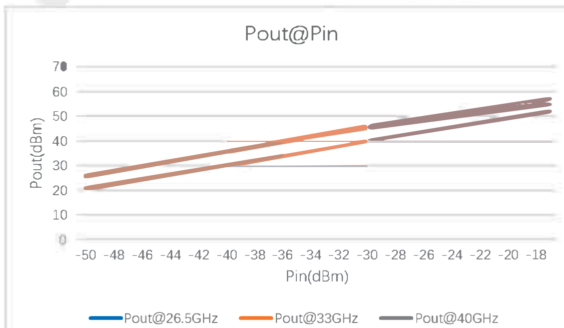

DC solid state power amplifier Modules

Fast Delivery!

- 26.5-40GHz Output Psat： 47dBm
- Model： TLPA26.5G40G-47-47

- 2-18GHz Output Psat： 45dBm
- Model： TLPA2G18G-45-45

AC Type Benchtop Power Amplifier up to 10KW

Three Years Warranty

- 0.5-6GHz 500W Solid State Power Amplifier
- 6-18GHz 250W Solid State Power Amplifier
- 2-18GHz 100W Solid State Power Amplifier
- 26-40GHz 500W Solid State Power Amplifier
- 40-60GHz 100W Solid State Power Amplifier
- 75-100GHz 10W Solid State Power Amplifier
- 8-18GHz 2000W Pulse Solid State Power Amplifier

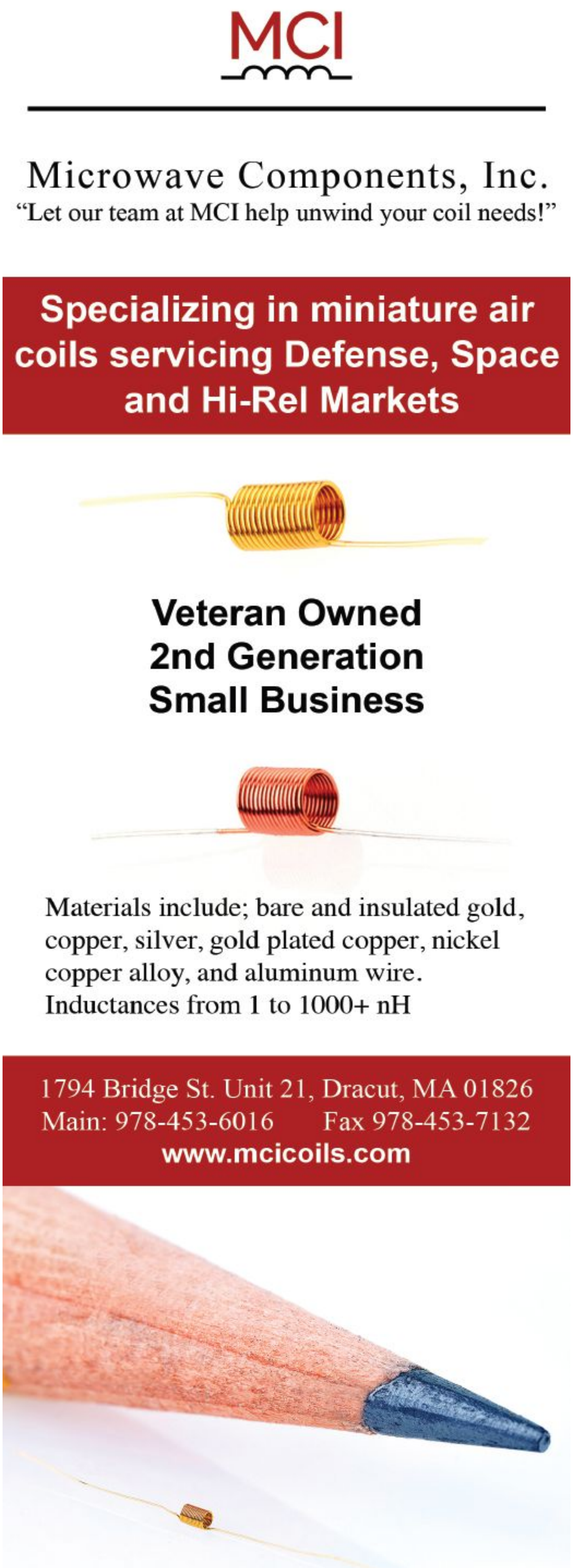

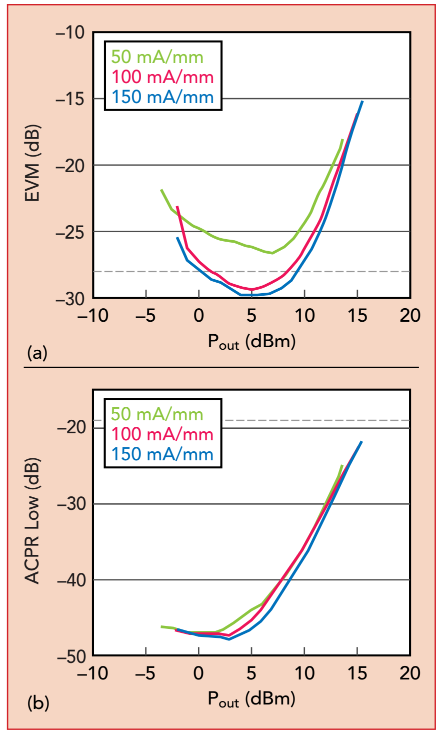

Fig. 7 **EVM (a) and ACPR (b) at three different I_{dq} bias currents.**

standards.[7] Using a mixed-signal active load-pull system, the fundamental and baseband impedances of the source and load were matched for optimum linearity and efficiency. ***Figure 7a*** shows the measured error vector magnitude (EVM) and ***Figure 7b*** shows the adjacent channel leakage ratio (ACLR). Both measurements were made using a 5G 64-QAM modulated signal with 100 MHz bandwidth and 7.5 dB PAPR. 3GPP specification target values are shown with a dotted line in the graphs. These measurements demonstrate that the Finwave MISHEMT GaN-on-Si E-mode device can exceed the linearity specifications for I_{dq} values between 50 and 150 mA/mm. Further improvements are expected in devices that are optimized for baseband decoupling.

CONCLUSION

As the wireless communications market continues to demand higher frequency and higher power devices to meet a growing list of high bandwidth applications, new technology is required to deliver the right balance of high performance and low cost to meet these demands. Finwave's CMOS-compatible E-mode 200 mm GaN-on-Si process meets these challenges. By using existing silicon foundries, this technology can quickly scale to meet the fast production cycle and high volumes required by the handset market. Finally, Finwave's versatile technology can produce different components needed for the RFFE. It can, therefore, be used to create highly-integrated, high performance, compact and cost-effective RFFE modules. ■

References

1. "Ericsson Mobility Report," Ericsson, 2024.
2. P. S. C. C. G. L. Claus Hetting, Interviewee, *Evolution of Wi-Fi 7 Devices: Market Outlook*, Innovations in XR, & more. [Interview]. 11 March 2024.
3. "Fixed Wireless Access Handbook 2025," Ericsson, 2025.
4. B. Baxter, "Why SOI? Marki Enters the Silicon World," *Marki Microwave*, 2022.
5. G. Meneghesso, M. Meneghini, I. Rossetto, D. Bisi, S. Stoffels, M. Van Hove, S. Descoutere and E. Zanoni, "Reliability and Parasitic Issues in GaN-based Power HEMTs: A Review," *Semiconductor Science and Technology*, 2016.
6. V. Johnson, Z. Pogrebin, M. Dipsey, H. S. Emmer, Z. Yuxuan, D. Pei and B. Lu, "200-mm Enhancement-mode Low-knee-voltage GaN-on-Si MISFETs for High-frequency Handset Applications," *CS Mantech*, 2024.
7. 3GPP, "Technical Specification on User Equipment Radio Transmission and Reception TS 38.101-1 V19.0.0," 2024.

RF-LAMBDA

MADE IN USA

THE LEADER OF RF BROADBAND SOLUTIONS

EMC Broadband RF Power Amplifier

High Power Solid State

HUNDREDS IN STOCK

FAST SHIPPING

FREQUENCY UP TO 90GHZ

POWER UP TO 2KW CW

REMC06G18GG

6-18GHZ 300W

- AUTOMATIC BUILT IN SELF CALIBRATION AND BIAS ADJUSTMENT.
- OVER TEMPERATURE, CURRENT, INPUT POWER PROTECTION.
- VSWR MEASUREMENT AND OPEN CIRCUIT PROTECTION.
- USER FRIENDLY CONTROL INTERFACE.
- REMOTE ETHERNET CONTROL AND FIRMWARE UPDATE.
- HIGH POWER EFFICIENCY AND LIGHTWEIGHT.

RAMP42G47GA 42-47GHZ 8W

REMC02G06GE 2-6GHZ 500W

RAMP18G40GB-U 18-40G 20W

RAMP05M80GC 0.5-80GHZ

REMC08G11GE 8-11GHZ 400W

RF Amplifiers and Sub-Assemblies for Every Application

Delivery from Stock to 2 Weeks ARO from the catalog or built to your specifications!

- Competitive Pricing & Fast Delivery
- Military Reliability & Qualification
- Various Options: Temperature Compensation, Input Limiter Protection, Detectors/TTL & More
- Unconditionally Stable (100% tested)

ISO 9001:2000 and AS9100B CERTIFIED

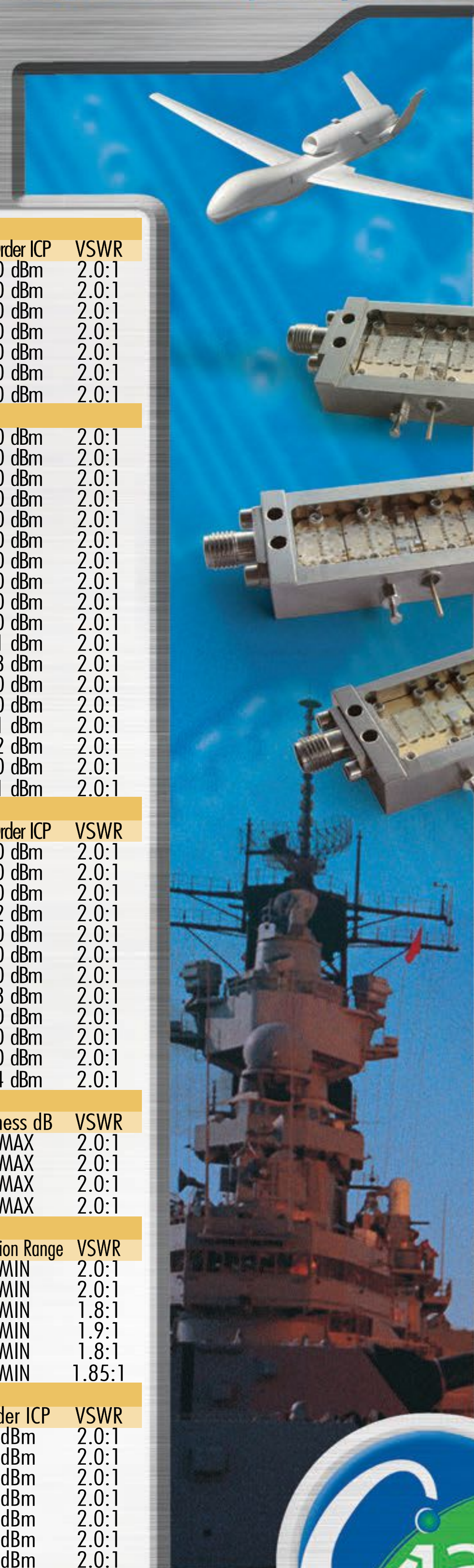

OCTAVE BAND LOW NOISE AMPLIFIERS

Model No.	Freq (GHz)	Gain (dB) MIN	Noise Figure (dB)	Power-out @ P1-dB	3rd Order ICP	VSWR
CA01-2110	0.5-1.0	28	1.0 MAX, 0.7 TYP	+10 MIN	+20 dBm	2.0:1
CA12-2110	1.0-2.0	30	1.0 MAX, 0.7 TYP	+10 MIN	+20 dBm	2.0:1
CA24-2111	2.0-4.0	29	1.1 MAX, 0.95 TYP	+10 MIN	+20 dBm	2.0:1
CA48-2111	4.0-8.0	29	1.3 MAX, 1.0 TYP	+10 MIN	+20 dBm	2.0:1
CA812-3111	8.0-12.0	27	1.6 MAX, 1.4 TYP	+10 MIN	+20 dBm	2.0:1
CA1218-4111	12.0-18.0	25	1.9 MAX, 1.7 TYP	+10 MIN	+20 dBm	2.0:1
CA1826-2110	18.0-26.5	32	3.0 MAX, 2.5 TYP	+10 MIN	+20 dBm	2.0:1

NARROW BAND LOW NOISE AND MEDIUM POWER AMPLIFIERS

Model No.	Freq (GHz)	Gain (dB) MIN	Noise Figure (dB)	Power-out @ P1-dB	3rd Order ICP	VSWR
CA01-2111	0.4 - 0.5	28	0.6 MAX, 0.4 TYP	+10 MIN	+20 dBm	2.0:1
CA01-2113	0.8 - 1.0	28	0.6 MAX, 0.4 TYP	+10 MIN	+20 dBm	2.0:1
CA12-3117	1.2 - 1.6	25	0.6 MAX, 0.4 TYP	+10 MIN	+20 dBm	2.0:1
CA23-3111	2.2 - 2.4	30	0.6 MAX, 0.45 TYP	+10 MIN	+20 dBm	2.0:1
CA23-3116	2.7 - 2.9	29	0.7 MAX, 0.5 TYP	+10 MIN	+20 dBm	2.0:1
CA34-2110	3.7 - 4.2	28	1.0 MAX, 0.5 TYP	+10 MIN	+20 dBm	2.0:1
CA56-3110	5.4 - 5.9	40	1.0 MAX, 0.5 TYP	+10 MIN	+20 dBm	2.0:1
CA78-4110	7.25 - 7.75	32	1.2 MAX, 1.0 TYP	+10 MIN	+20 dBm	2.0:1
CA910-3110	9.0 - 10.6	25	1.4 MAX, 1.2 TYP	+10 MIN	+20 dBm	2.0:1
CA1315-3110	13.75 - 15.4	25	1.6 MAX, 1.4 TYP	+10 MIN	+20 dBm	2.0:1
CA12-3114	1.35 - 1.85	30	4.0 MAX, 3.0 TYP	+33 MIN	+41 dBm	2.0:1
CA34-6116	3.1 - 3.5	40	4.5 MAX, 3.5 TYP	+35 MIN	+43 dBm	2.0:1
CA56-5114	5.9 - 6.4	30	5.0 MAX, 4.0 TYP	+30 MIN	+40 dBm	2.0:1
CA812-6115	8.0 - 12.0	30	4.5 MAX, 3.5 TYP	+30 MIN	+40 dBm	2.0:1
CA812-6116	8.0 - 12.0	30	5.0 MAX, 4.0 TYP	+33 MIN	+41 dBm	2.0:1
CA1213-7110	12.2 - 13.25	28	6.0 MAX, 5.5 TYP	+33 MIN	+42 dBm	2.0:1
CA1415-7110	14.0 - 15.0	30	5.0 MAX, 4.0 TYP	+30 MIN	+40 dBm	2.0:1
CA1722-4110	17.0 - 22.0	25	3.5 MAX, 2.8 TYP	+21 MIN	+31 dBm	2.0:1

ULTRA-BROADBAND & MULTI-OCTAVE BAND AMPLIFIERS

Model No.	Freq (GHz)	Gain (dB) MIN	Noise Figure (dB)	Power-out @ P1-dB	3rd Order ICP	VSWR
CA0102-3111	0.1-2.0	28	1.6 Max, 1.2 TYP	+10 MIN	+20 dBm	2.0:1
CA0106-3111	0.1-6.0	28	1.9 Max, 1.5 TYP	+10 MIN	+20 dBm	2.0:1
CA0108-3110	0.1-8.0	26	2.2 Max, 1.8 TYP	+10 MIN	+20 dBm	2.0:1
CA0108-4112	0.1-8.0	32	3.0 MAX, 1.8 TYP	+22 MIN	+32 dBm	2.0:1
CA02-3112	0.5-2.0	36	4.5 MAX, 2.5 TYP	+30 MIN	+40 dBm	2.0:1
CA26-3110	2.0-6.0	26	2.0 MAX, 1.5 TYP	+10 MIN	+20 dBm	2.0:1
CA26-4114	2.0-6.0	22	5.0 MAX, 3.5 TYP	+30 MIN	+40 dBm	2.0:1
CA618-4112	6.0-18.0	25	5.0 MAX, 3.5 TYP	+23 MIN	+33 dBm	2.0:1
CA618-6114	6.0-18.0	35	5.0 MAX, 3.5 TYP	+30 MIN	+40 dBm	2.0:1
CA218-4116	2.0-18.0	30	3.5 MAX, 2.8 TYP	+10 MIN	+20 dBm	2.0:1
CA218-4110	2.0-18.0	30	5.0 MAX, 3.5 TYP	+20 MIN	+30 dBm	2.0:1
CA218-4112	2.0-18.0	29	5.0 MAX, 3.5 TYP	+24 MIN	+34 dBm	2.0:1

LIMITING AMPLIFIERS

Model No.	Freq (GHz)	Input Dynamic Range	Output Power Range Psat	Power Flatness dB	VSWR
CLA24-4001	2.0 - 4.0	-28 to +10 dBm	+7 to +11 dBm	+/- 1.5 MAX	2.0:1
CLA26-8001	2.0 - 6.0	-50 to +20 dBm	+14 to +18 dBm	+/- 1.5 MAX	2.0:1
CLA712-5001	7.0 - 12.4	-21 to +10 dBm	+14 to +19 dBm	+/- 1.5 MAX	2.0:1
CLA618-1201	6.0 - 18.0	-50 to +20 dBm	+14 to +19 dBm	+/- 1.5 MAX	2.0:1

AMPLIFIERS WITH INTEGRATED GAIN ATTENUATION

Model No.	Freq (GHz)	Gain (dB) MIN	Noise Figure (dB)	Power-out @ P1-dB	Gain Attenuation Range	VSWR
CA001-2511A	0.025-0.150	21	5.0 MAX, 3.5 TYP	+12 MIN	30 dB MIN	2.0:1
CA05-3110A	0.5-5.5	23	2.5 MAX, 1.5 TYP	+18 MIN	20 dB MIN	2.0:1
CA56-3110A	5.85-6.425	28	2.5 MAX, 1.5 TYP	+16 MIN	22 dB MIN	1.8:1
CA612-4110A	6.0-12.0	24	2.5 MAX, 1.5 TYP	+12 MIN	15 dB MIN	1.9:1
CA1315-4110A	13.75-15.4	25	2.2 MAX, 1.6 TYP	+16 MIN	20 dB MIN	1.8:1
CA1518-4110A	15.0-18.0	30	3.0 MAX, 2.0 TYP	+18 MIN	20 dB MIN	1.85:1

LOW FREQUENCY AMPLIFIERS

Model No.	Freq (GHz)	Gain (dB) MIN	Noise Figure dB	Power-out @ P1-dB	3rd Order ICP	VSWR
CA001-2110	0.01-0.10	18	4.0 MAX, 2.2 TYP	+10 MIN	+20 dBm	2.0:1
CA001-2211	0.04-0.15	24	3.5 MAX, 2.2 TYP	+13 MIN	+23 dBm	2.0:1
CA001-2215	0.04-0.15	23	4.0 MAX, 2.2 TYP	+23 MIN	+33 dBm	2.0:1
CA001-3113	0.01-1.0	28	4.0 MAX, 2.8 TYP	+17 MIN	+27 dBm	2.0:1
CA002-3114	0.01-2.0	27	4.0 MAX, 2.8 TYP	+20 MIN	+30 dBm	2.0:1
CA003-3116	0.01-3.0	18	4.0 MAX, 2.8 TYP	+25 MIN	+35 dBm	2.0:1
CA004-3112	0.01-4.0	32	4.0 MAX, 2.8 TYP	+15 MIN	+25 dBm	2.0:1

CIAO Wireless can easily modify any of its standard models to meet your "exact" requirements at the Catalog Pricing.

Visit our web site at www.ciaowireless.com for our complete product offering.

Ciao wireless

Ciao Wireless, Inc. 4000 Via Pescador, Camarillo, CA 93012

Tel (805) 389-3224 Fax (805) 389-3629 sales@ciaowireless.com

Cliff Drubin, Associate Technical Editor

RTX's Raytheon Demonstrates First-Ever AI/ML-Powered Radar Warning Receiver for 4th Generation Aircraft

Raytheon, an RTX business, has successfully completed flight testing on the first-ever AI/machine learning (ML)-powered radar warning receiver (RWR) system for a fourth-generation aircraft.

The Cognitive Algorithm Deployment System (CADS) combines the latest embedded graphics processing unit with Deepwave Digital's computing stack, enabling AI models to be integrated into Raytheon's legacy RWR systems for AI/ML processing at the sensor. This integration allows CADS to employ cognitive methods to sense, identify and prioritize threats. With the CADS capability, the enhanced RWR will increase aircrew survivability while facilitating the rapid and cost-effective mass deployment of modern AI/ML capabilities.

CADS (Source: RTX)

Initial CADS hardware and cognitive radar processing capabilities were tested on Raytheon's flight test aircraft. CADS performed successfully during additional flight testing and demonstrations on an F-16 at the Air National Guard's test range near Tucson, Ariz., in December. The flight tests incorporate containerized AI/ML techniques from the Georgia Tech Research Institute, Vadum, Inc. and Raytheon's cognitive electronic warfare team.

CADS is expected to begin being procured across multiple platforms in early 2025.

LM, Nokia and Verizon Advance Defense Capabilities Through 5G.MIL Collaboration

Lockheed Martin (LM) and Verizon recently announced the successful integration of Nokia's industry-leading, military-grade 5G solutions into Lockheed Martin's 5G.MIL® Hybrid Base Station (HBS). The technology advances new capabilities to integrate commercial 5G connections with military communications systems to provide decisive information for national defense. 5G is playing an expanding role in supporting tactical military missions, seamlessly complementing existing battlefield solutions.

In a series of recent demonstrations, Lockheed Martin integrated Nokia's military-grade 5G solutions into the 5G.MIL Unified Network Solutions ecosystem, including interoperability with Verizon's network operations and management solutions. These tests successfully integrated traditional tactical communications solutions with 5G using open systems architecture and commercial standards. Leveraging open standards in this way allows for rapid integration of new, advanced capabilities into HBS configurations, ensuring new products and technology solutions are drop-in ready with no risk of vendor lock.

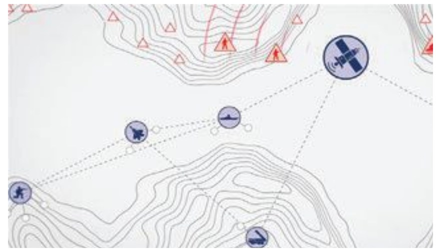

Military 5G Communications (Source: Lockheed Martin Corporation)

Initial integration was completed with equipment from Nokia's leading 5G portfolio at Verizon's Boston Innovation Center and HBS components at Lockheed Martin's Valley Forge laboratory in Pennsylvania. Final systems integration, testing and demonstration were accomplished at Lockheed Martin's facility in Fort Worth, Texas.

The demonstration included HBS connectivity to hybrid user equipment that allows users to switch access links between commercial 5G and tactical low-probability-of-detection (LPx) waveforms while maintaining uninterrupted user application sessions on an Android user device. LPx designates low-probability-of-detection, interception, exploitation, jamming, geolocation and spoofing. By integrating the 5G.MIL HBS with Nokia's 5G solutions, as well as demonstrating interoperability with Verizon's public 5G network and leveraging their network operations management software, Lockheed Martin and its strategic collaborators are well positioned to bring new levels of performance, scalability and reliability to military, national security wireless and ally international defense networks.

5G Network Analysis Detects Unauthorized Drones

The Helmut-Schmidt-University of the Federal Armed Forces Hamburg (HSU/UniBw H) has embarked on a pioneering research collaboration with ipoque, a Rohde & Schwarz company.

This strategic partnership aims to develop cutting-edge technology capable of identifying and mitigating potential threats from unauthorized drones (UAS) by analyzing patterns within vast 5G network data streams.

Leveraging the university's state-of-the-art 5G Campus Network, established by Deutsche Telekom Global Business in conjunction with Ericsson as part of the Digital Sensor-2-Cloud Campus Platform (DS2CCP/dtec.bw) project, the research team will focus on anom-

For More Information

Visit mwjournal.com for more defense news.

Drone (Source: Rohde & Schwarz)

aly detection in 5G Campus Networks and drone detection in mobile networks. This innovative approach is set to bolster the security of critical infrastructure, such as airports and stadiums, against drone-based threats.

The Hamburg-based researchers, known for their development of the FALKE interceptor drone, are at the forefront of European research in this domain. ipoque will contribute its expertise in network analysis software, renowned for enhancing network optimization, management, connectivity and security.

L3Harris and Shield AI Team for Breakthrough in Autonomy

L3Harris Technologies and Shield AI will collaborate on a demonstration to enable an electronic warfare (EW) operation with AI-enabled unmanned systems that will sense, adapt and act while executing physical and electromagnetic movements.

DiSCO (Source: L3Harris Technologies)

At the core of this effort is L3Harris' Distributed Spectrum Collaboration and Operations, or DiSCO™, a software-defined Electromagnetic Battle Management ecosystem that can detect, collect and analyze known and unknown threat signals within minutes. This specific collaboration pairs DiSCO with Shield AI's Hivemind.

"Adversaries' kill webs are complex, restrict access and put assets at risk. Countering them requires shifting to distributed, autonomous kill webs that sense, decide and act in real-time," said Christian Gutierrez, vice president of Hivemind solutions, Shield AI. "Integrating Hivemind autonomy with L3Harris' EW capabilities enables dynamic maneuverability in contested environments."

L3Harris and Shield AI will continue further demonstrations and integrations, leveraging the strengths of both companies to deliver scalable, multi-domain solutions for the U.S. and its allies.

Quantic Wenzel

Ultra Low-noise Frequency Control & Timing Solutions

Unmatched precision, low-g sensitivity and ultra-low phase noise distinguish our engineering expertise, so our customers can execute with full confidence – and without hesitation.

OCXOs
PLOs
Vibration Isolated
IMAs
Space Qualified

Access a complete list of frequency control and timing products, datasheets, and technical resources at quanticwenzel.com.
Or contact us at 512.835.2038 or sales@quanticwenzel.com.

Reactel, Inc

Reacting First to All Your Filter Needs

RF, Microwave & Millimeter Wave Filters, Multiplexers and Multifunction Assemblies Covering DC to 67 GHz.

8031 Cessna Avenue • Gaithersburg, Maryland 20879
(301) 519-3660 • reactel@reactel.com • reactel.com

Fold Page Over Like This

A ▸ Fold This Section Over Left ◂ B Fold Back So A Meets B


Visitors from around the world, ready to call it a great week, gather in San Francisco to see the entire RF & Microwave Industry and Reactel in the Moscone Center. All of the company Booths will be filled with new electronics as over 632 companies demonstrate their capabilities.


Intertek • RoHS • in • Made In MD Since 1979

A ▸ ◂ B

DC TO 86 GHz

Filter Technologies

For Every Application

LEARN MORE

CAVITY

- Passbands to 43.5 GHz
- Stopbands to 57 GHz
- Bandwidths as narrow as 1%
- 100+ dB rejection

CERAMIC RESONATOR

- Fractional bandwidths from 0.5 to 40%
- Excellent power handling, up to 20W
- High Q in miniature SMT package

LUMPED L-C

- Wide catalog selection
- Several package options including aqueous washable
- Variety of filter topologies

LTCC

- Tiny size, as small as 0202
- Industry's widest selection of mmWave LTCC filters
- Proprietary designs with stopband rejection up to 100 dB

MICROSTRIP

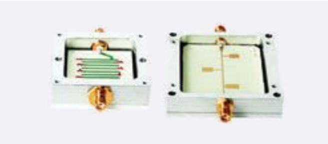

- Connectorized designs with 4 to 40% fractional bandwidth
- Power handling up to 10W
- Flat group delay

MMIC REFLECTIONLESS

- Patented topology absorbs and internally terminates stopband signals
- Perfect for pairing with amplifiers, mixers, multipliers, ADC/DACs & more

RECTANGULAR WAVEGUIDE

- WR-12, WR-15 and WR-28 interfaces
- Passbands up to 87 GHz
- High stopband rejection, 40 dB

SUSPENDED SUBSTRATE

- Ultra-wide passbands up to 26 GHz
- Wide stopbands up to 40 GHz
- High Q

THIN FILM ON ALUMINA

- Passbands from DC to 40 GHz
- High rejection with wide passband
- Miniature SMT package

Mini-Circuits®

Nearly US$1 Billion Dollars Flow into Automotive Radar Startups

According to IDTechEx's report, "Automotive Radar Market 2025-2045: Robotaxis & Autonomous Cars," newly established radar startups worldwide have raised nearly US$1.2 billion over the past 12 years, approximately US$980 million of which is predominantly directed toward the automotive sector. Through more than 40 funding rounds, these companies have driven the implementation and advancement of radar technologies in key areas such as autonomous driving and advanced driver assistance systems (ADAS). The funding peak occurred in 2021 and 2022, propelled by the surge in robotaxis and Level 4/5 autonomous driving. While there has been a modest uptick in 2024, investment levels are unlikely to reach the previous highs.

This influx of capital can be attributed to three key drivers. First, the automotive industry's growing demand for safety and robust environmental perception highlights radar's all-weather, high-reliability detection capabilities. Second, the rise of electric vehicles and robotaxis has opened up broader application scenarios for radar. Finally, emerging technologies such as 4D imaging radar, high-resolution radar and radar-on-chip solutions continue to improve sensing accuracy and data fusion, maintaining long-term investor confidence in the radar market.

During this funding wave, companies like Arbe, Uhnder and Mobileye have taken the lead by launching multiple high performance radar products. These solutions use innovations such as high-resolution sensing and digital beamforming (DBF), leading to notable gains in detection accuracy and processing speed. Concurrently, advancements in semiconductor manufacturing have decreased production costs, enabling OEMs to integrate radar systems into premium models and across a broader range of mass-market vehicles.

IDTechEx's review of automaker brochures over the past 25 years shows that the use of radar in ADAS systems has expanded dramatically in the last two decades. A decade ago, radar-enabled features like adaptive cruise control (ACC) were limited to luxury models. Today, with decreasing sensor costs and tighter safety requirements from organizations such as NCAP, functionalities like automatic emergency braking (AEB) and blind spot detection (BSD) have become increasingly prevalent. In 2023, 71 percent of newly sold vehicles are equipped with AEB — a 16 percentage point increase over 2020 — while ACC adoption reached 55 percent, up from 52 percent in 2022 and 40 percent in 2020. BSD usage has also climbed from 28 percent in 2020 to 40 percent in 2023. These figures reflect consumers' growing focus on safety and efforts by OEMs and suppliers to bring more advanced radar sensing solutions to a broader range of vehicle segments.

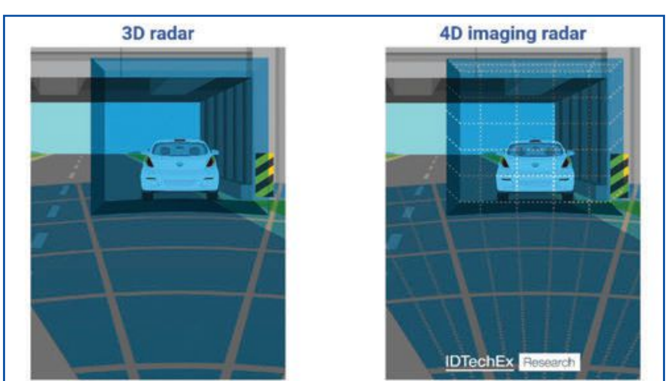

4D Imaging Radar (Source: IDTechEx)

Of particular note is BSD's trajectory toward 360-degree monitoring, which requires multiple short-range radars placed around the vehicle and is complemented by forward radar to enable safety features such as pedestrian automatic emergency braking (PAEB) in more complex scenarios. PAEB uses radar, cameras and intelligent algorithms to detect crossing pedestrians, bicycles or other obstacles when turning or exiting side roads, issuing warnings and applying automatic brakes if necessary. As more Level 3 autonomous models enter the market, radars will move beyond driver assistance to serve as a critical layer in environmental perception and advanced decision-making. IDTechEx anticipates strong growth for radar-driven ADAS and autonomous functions in the coming years, offering substantial opportunities across the automotive value chain.

The IDTechEx report, "Automotive Radar Market 2025-2045: Robotaxis & Autonomous Cars," provides a comprehensive analysis of the global automotive radar landscape, covering radars for autonomous cars and robotaxis, long-range radar, short-range radar, radar cocooning, 4D imaging radar, high-channel-count radars, semiconductor technologies for radar, waveguide antenna and detailed market forecasts. In addition to these technical insights, the report offers assessments of value chain positioning, business models and forward-looking projections — supported by data from primary research and practical economic models.

Global NTN and D2C Market Revenue to Grow as Tech Giants, Satellite Operators and MNOs Transform Global Connectivity

The non-terrestrial network (NTN) and direct-to-cellular (D2C) market is entering a transformative phase in 2025, driven by strategic advancements from Apple, SpaceX, AST SpaceMobile, satellite operators and mobile network operators (MNOs). ABI Research forecasts that the NTN-D2C

For More Information
Visit mwjournal.com for more commercial market news.

"The beginning of a transformative era in global communications."

segment will potentially reach US$25 billion in service revenues by 2035, with over 200 million connections.

Apple's partnership with Globalstar, starting with a US$450 million investment in 2022 and an additional US$1.5 billion in 2024, has established Apple as a leader in consumer satellite services. Key features include Emergency SOS, Roadside Assistance, Messages and Find My App for off-grid sharing. Looking ahead, Apple may introduce tiered satellite messaging and AirTag tracking subscriptions, potentially bundled with Apple One. This partnership aims to extend satcom capabilities to iPads, Apple Watches and MacBooks, expanding satellite technology's reach into outdoor and rugged device markets. This strategic move could also lead to new ruggedized devices designed for extreme environments, aligning with Apple's ecosystem-driven strategy and positioning the company in emerging markets for satellite-enabled consumer devices.

SpaceX has also emerged as a key player in the D2C space. It deployed over 330 D2C satellites in 2024, using eNodeB modems to enable direct LTE connectivity with smartphones. With partnerships across major MNOs, including T-Mobile, KDDI, Optus, Kyivstar and Rogers, SpaceX is leading in satellite-to-phone connectivity globally.

AST SpaceMobile, like SpaceX, has formed partnerships with over 45 MNOs, including AT&T, Vodafone and Telefónica, covering around 2.8 billion users. These alliances boost AST SpaceMobile's global scalability. The growth of the D2C market is further supported by regulatory advancements like the FCC's Supplemental Coverage from Space (SCS), enabling satellite operators to use terrestrial spectrum. Partnerships between satellite operators and MNOs, such as SpaceX, T-Mobile and AST SpaceMobile, will benefit from SCS, allowing seamless satellite-terrestrial network integration and opening new consumer markets and revenue opportunities.

"As we look ahead to 2025 and beyond, the D2C market will continue to evolve," Victor Xu, industry analyst at ABI Research, said. "From emergency services to logistics and adventure tourism, satellite-enabled applications are unlocking new possibilities for industries worldwide. This is just the beginning of a transformative era in global communications."

INNOVATIVE RF SOLUTIONS FOR EVERY APPLICATION

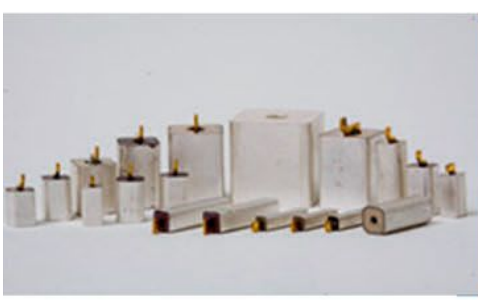

Find the Perfect Resonator & Inductor For Your Needs!

Try the *Trans-Tech WebCOAX Coaxial Resonator Selector*

Trans-Tech
Ceramic Enabled Solutions

Trans-Tech provides advanced RF solutions from 300 MHz to 7 GHz, ensuring high Q and excellent temperature stability. Customize with quarter wave, half wave, or custom lengths in tabbed or non-tabbed variants.

Our durable designs are **made in the USA** and offer quick turnaround times for standard bands.
For frequencies outside the mentioned range, please contact our factory.
Email: sales@trans-techinc.com

ERAVANT

FORMERLY SAGE MILLIMETER

INTEGRATED

SUBASSEMBLIES

UP TO 330 GHz

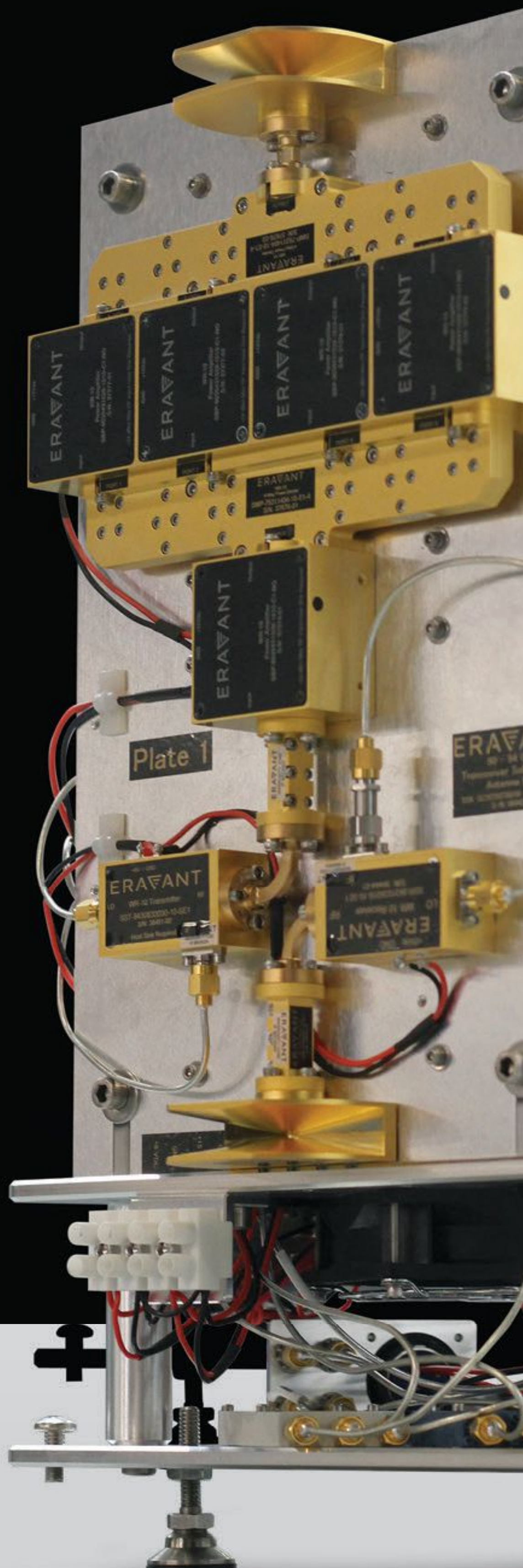

- **Comprehensive Support:** End-to-end assistance from initial concept through production
- **Rapid Prototyping:** Accelerated development cycles to meet tight project timelines
- **Engineered to Your Specifications**

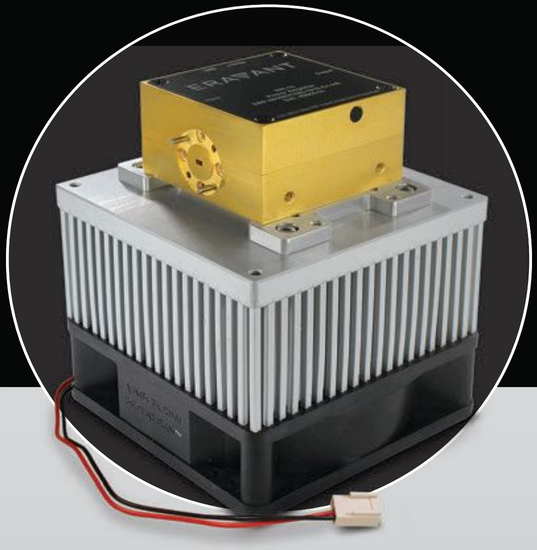

2 Watt High Power Amplifiers available off-the-shelf

WWW.ERAVANT.COM

www.eravant.com 501 Amapola Avenue Torrance, CA 90501
T: 424-757-0168 F: 424-757-0188 support@eravant.com

Adapters • Amplifiers • Antenna Feeds • Antennas • Attenuators • Bias Tees • Cable Assemblies • Corner Reflectors • Couplers • DC Blocks • Detectors • Ferrite Devices • Filters • Frequency Converters • Frequency Multipliers • Limiters • Magic Tees • Mixers • Noise Sources • Oscillators • Phase Shifters • Power Dividers • Radar Sensors • Subassemblies • Switches • Termination Loads • Test Equipment • Test Hardware & Accessories • TX/RX Modules • Uni-Guide™ • Waveguide Sections

Around the **Circuit**

Barbara Walsh, Multimedia Staff Editor

MERGERS & ACQUISITIONS

ETL Systems has acquired **IRT Technologies**, a Canadian innovator in satellite communication products. This strategic move is part of their ongoing commitment to growth and innovation within the global satellite communications market. IRT Technologies is renowned for designing and manufacturing advanced GaN and GaAs powered BUC/SSPB/SSPA, uplink SSPA/SSPB and downlink LNB redundancy solutions which are critical to the real-time delivery of voice, data and multimedia services globally. The Canadian company is also a pioneer in the high and low-power tropo-band solid-state power amplifier market, revolutionizing 'beyond line-of-sight' communication.

COLLABORATIONS

As the ecosystem around 5G evolves, **Verizon** has been actively optimizing its network with 5G advanced technology, high speed fiber, edge computing and intelligent management to efficiently handle the massive data demands of real-time applications, seamless cloud connectivity and data-intensive demands of AI-driven workloads. Verizon and its collaborators **Ericsson** and **Qualcomm Technologies Inc.** just made another large leap forward in advancing that ecosystem. Using a combination of two time-division duplex carrier component aggregation with C-Band spectrum and uplink MIMO technology, the companies achieved a U.S. record-breaking 480 Mbps uplink speed using sub-6 GHz spectrum.

SynaXG, a provider of AI-RAN solutions, in collaboration with **Kyocera** and **NVIDIA**, unveiled the world's first data transmission and reception over mmWave radios utilizing the NVIDIA GH200 Grace Hopper™ Superchip. This industry-first milestone marks a transformative leap toward AI-native wireless communications, enabling operators worldwide to unlock new AI-based monetization opportunities and achieve significant gains in wireless network performance and efficiency with AI.

NEW STARTS

Infineon Technologies AG announced the formation of a new business unit to drive the company's growth in the area of sensors by combining the existing sensor and RF businesses into one dedicated organization. The new business unit, Sensor Units & Radio Frequency (SURF), will be part of the power and sensor systems division and include the former automotive and multi-market sense and control businesses. By combining its sensor and RF expertise, Infineon strengthens its competitiveness and go-to-market approach by leveraging cost and R&D synergies, accelerating innovation and value to customers. This strategic move will capitalize on the vast market po-

CPI EDB's microwave power module (MPM) contains an integrated 100 W, I/J band, super mini helix traveling wave tube. The CPI EDB MPM uses an optimized, high-density, switched-mode power supply suitable for all high-performance electronic countermeasure (ECM) applications.

- Ruggedized for ground mobile, naval or airborne applications
- Compact
- Lightweight
- Efficient

Download datasheet here

Visit us at AOC Europe 2025, 6-8 May Rome, Italy, Stand D41

Contact the MPM experts at CPI EDB:
ElectronDevices@cpi-edb.com

CPI Electron Device Business • 150 Sohier Road, Beverly, MA 01915-5536, USA • www.cpi-edb.com

GOLD STANDARD

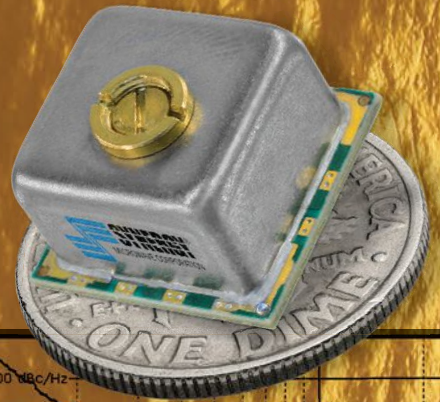

GSDRO series

0.75" x 0.75" x 0.53"

* Typical For 10 GHz RF Output

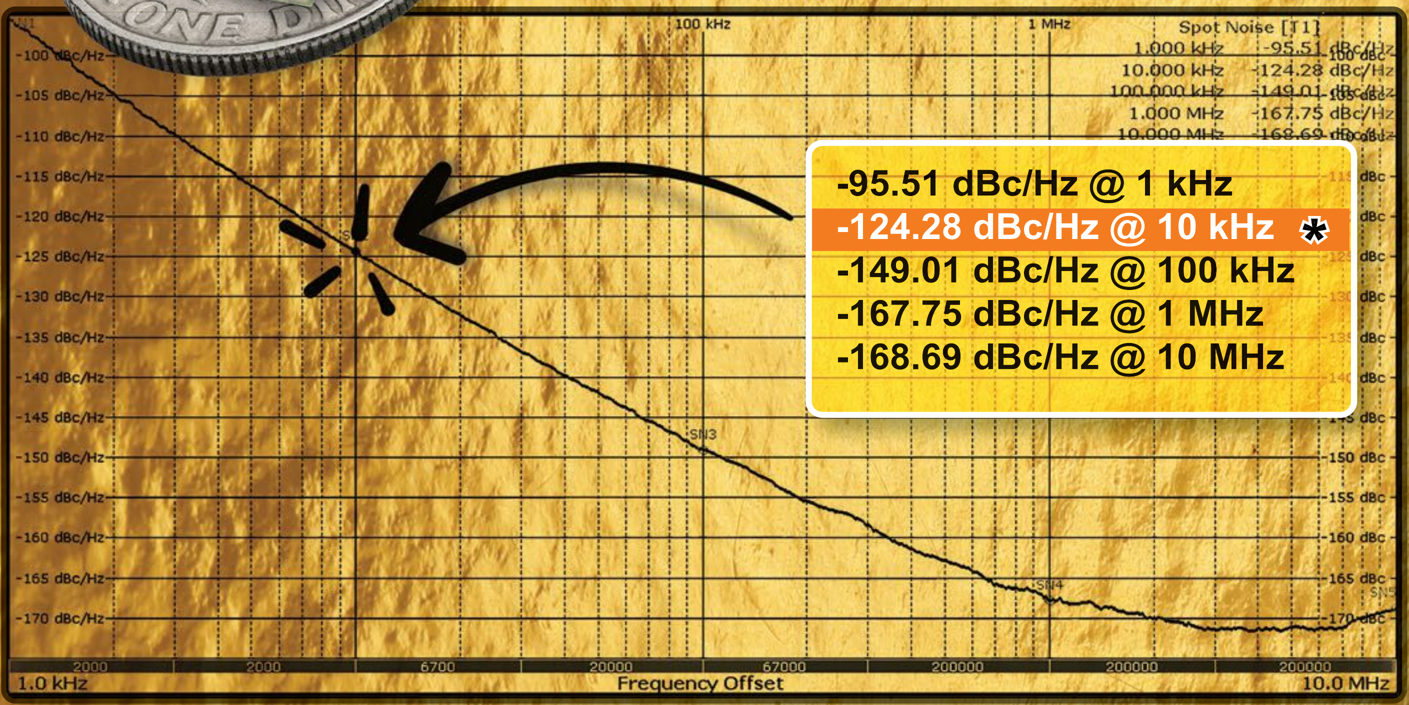

FEATURES:

- *Exceptional Phase Noise*
- *Lead Free RoHS Compliant*
- *Patented Technology*

Applications:
Radar, Test Equipment,
5G, Frequency Synthesizer

Now Up To 22 GHz!

Check out our website for available frequencies.

Talk To Us About Your Custom Requirements.

SYNERGY® MICROWAVE CORPORATION

Phone: (973) 881-8800 | Fax: (973) 881-8361
E-mail: sales@synergymwave.com | Web: www.synergymwave.com
Mail: 201 McLean Boulevard, Paterson, NJ 07504

tential of the sensor and RF markets, projected to exceed 20 billion U.S. dollars by 2027.

Gilat Satellite Networks Ltd. announced the formation of its new defense division, a strategic move designed to target the increasing demand for government and defense satcom solutions. Gilad Landsberg has been appointed president of Gilat's Defense Division, bringing over 20 years of experience in the defense industry. Gilat Defense provides secure, rapid-deployment satcom solutions tailored for military and HLS organizations, government agencies and defense integrators, with a strong focus on supporting the U.S. Department of Defense and allied forces worldwide. By unifying, under one umbrella, the expertise and technologies of Gilat, and the wholly-owned subsidiaries Gilat DataPath and Gilat Wavestream, the division delivers end-to-end solutions with multiple layers of communication redundancy, ensuring maximum operational availability.

ACHIEVEMENTS

NASA's quiet supersonic X-59 research aircraft has cleared electromagnetic testing, confirming its systems will work together safely, without interference across a range of scenarios. Electromagnetic interference occurs when an electric or magnetic field source affects an aircraft's operations, potentially impacting safety. This interference, whether from an external source or the aircraft's own equipment, can disrupt the electronic signals that control critical systems — similar to effects that lead to static or crackling on a radio from a nearby emitting device, like a phone. The tests, conducted at contractor Lockheed Martin Skunk Works' facility in Palmdale, Calif., ensured that the X-59's onboard systems — such as radios, navigation equipment and sensors — did not interfere with one another or cause unexpected problems.

For controlling prosthetics, the body's signals must be detected to move the artificial limb. Currently, implanting electrodes is the most common technique, but this is invasive, and electrodes can deteriorate or move position. A completely different approach is now developed by the multidisciplinary consortium **QHMI** in Stuttgart, Germany, using quantum sensors to detect the incredibly small and fast nerve signals. The ultra-sensitive quantum magnetometers will be carried outside the body, measuring the neural signals through the skin. At this stage, the scientists are using Spectrum Instrumentation's ultrafast digitizers (M5i.3357) and arbitrary waveform generators (M4x.6631) to characterize the signals and to finally design the required application-specific integrated circuits and photonic integrated circuits.

Israel's first quantum computer, which will provide advanced superconducting technology, is now operational and will strengthen its position as a leader in quantum technology. The 20-qubit quantum computer was developed under the leadership of the **Israel Innova-**

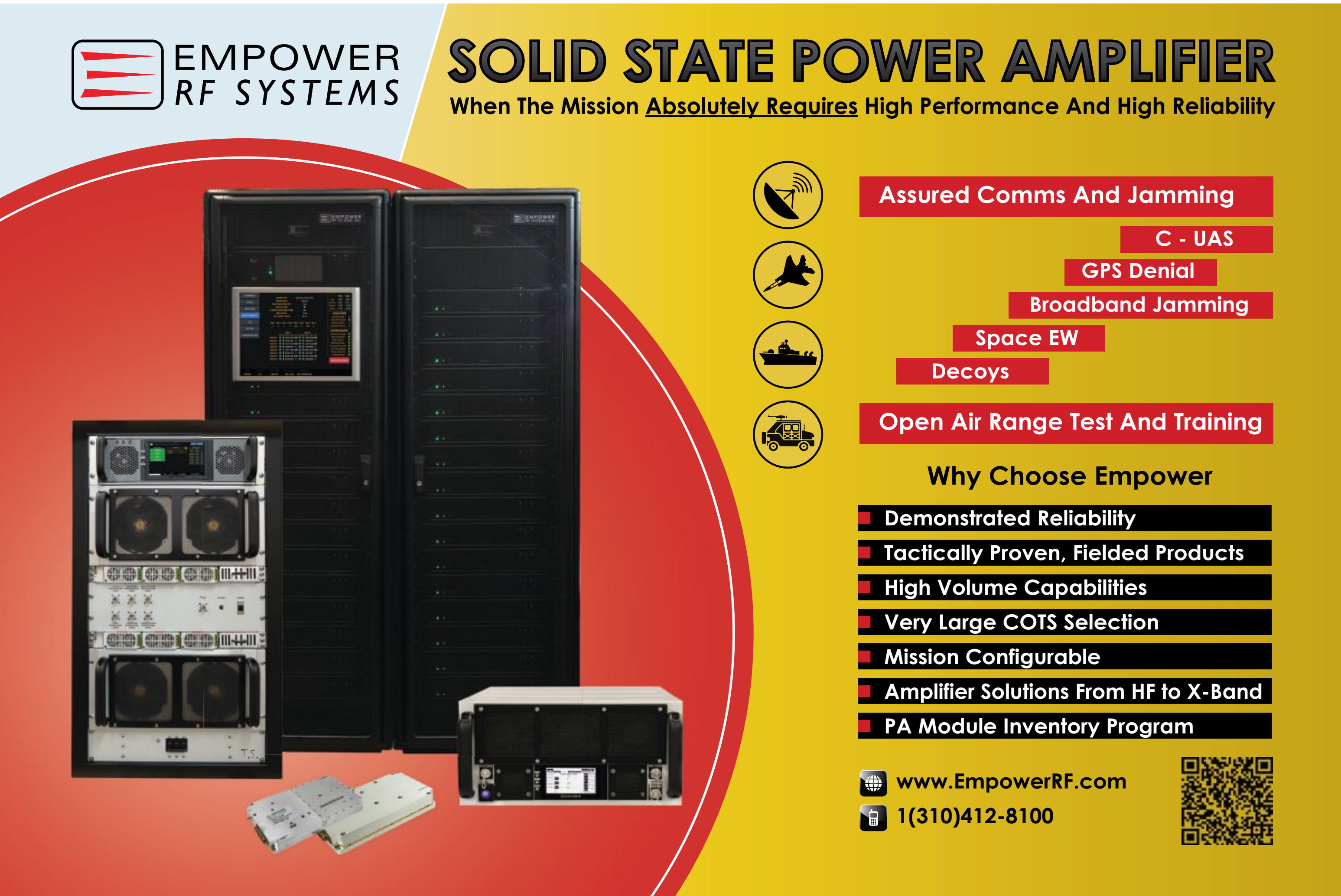

MI-WAVE

Millimeter Wave Products Inc.

HIGH POWER AND LOW NOISE AMPLIFIERS

Engineering Excellence at Millimeter Wave

MI-WAVE (Millimeter Wave Products Inc.) is a trusted leader in designing and manufacturing advanced solutions for RF and millimeter wave applications across a wide spectrum of frequencies.

From high-power amplifiers and precision antennas to waveguide components and custom subsystems, MI-WAVE delivers reliable, high-performance technology trusted by professionals in radar, telecommunications, satellite systems, defense, and scientific research.

What Sets MI-WAVE Apart?

- Broad Frequency Support – Covering key RF and millimeter wave bands
- Proven Performance – High output power, low noise, and high efficiency
- Custom & Standard Solutions – Tailored to your needs or ready to deploy
- Expert Engineering – Decades of hands-on experience in high-frequency design

From concept to production, MI-WAVE provides precision RF solutions built to perform in the world's most advanced systems.

MADE IN THE U.S.A. WITH PRIDE

CERTIFIED ISO 9001-2015 COMPANY

ANNIVERSARY 35 YEARS IN BUSINESS

2007 Gandy Blvd N Suite 1310
St. Petersburg, FL 33702

Tel: (727) 563-0034
Email: sales@miwv.com

tion Authority, **Israel Aerospace Industries**, **Hebrew University of Jerusalem** and the university's technology transfer company, **Yissum**. This collaboration establishes a superconductor-based quantum computer infrastructure alongside a robust development and integration environment. These advancements mark a strategic knowledge foundation for Israel, supporting both defense and civilian applications. The global race for quantum supremacy has accelerated in recent years with groundbreaking discoveries in the field.

Verus® Research has secured a four-and-a-half-year, $5.8 million award for science and technology developments in the Department of Defense Test Resource Management Center's (TRMC) Electronic Warfare Test Technology area. Under this award, Verus Research has proposed Cognitive Information-Theoretic Attack-pod for Dynamic ELectronic-attack engagementS (CITADELS). CITADELS will support the TRMC's need for the development of an airborne, adaptive electronic attack system that utilizes cutting-edge cognitive techniques to increase the effectiveness of electronic attack threat simulators against sophisticated "blue radar" systems during flight test events.

ICEYE will be the consortium lead in an industrial participation program for the **Finnish Ministry of Defense** F-35 program. The consortium will develop advanced space and joint intelligence technologies, along with intelligence, surveillance and reconnaissance (ISR) capabilities for military users such as the Finnish Defense Forces. The consortium, comprised of ICEYE and prominent Finnish industry players Insta, Huld, DA-Group and the Finnish Meteorological Institute as a supplier, will work together with Lockheed Martin on advancing technological development. This will include the progression of disruptive capabilities such as analytics with AI and encompass mobile ISR cell development, advanced analytics and high performance SAR imaging for all weather and light conditions.

PEOPLE

Otava Inc. has appointed **Alastair Upton** as its new chief revenue officer, reporting directly to CEO Victoria Pereira. In this role, Alastair will lead the company's sales and business development initiatives, manage partnership programs and provide his expertise in aerospace and defense and telecommunications. This appointment comes at a strategic time for Otava Inc., as there are significant opportunities for continued growth in the rapidly evolving defense, satcom, and 5G/6G markets. Upton brings more than 40 years of experience in the semiconductor industry, focusing on defense electronics and high volume commercial applications.

▲ *Alastair Upton*


RF & Microwave Amplifiers
10KHz-75GHz
EXODUS
ADVANCED COMMUNICATIONS
Amplifiers
CW & Pulse
dBm to KW
Best in Class RF Amplifier SSPA's
Engineering Excellence,
Ultimate Solutions!
AMP20090
1.0-2.5 GHz, 8KW Pulse
AMP20141
0.4-1.0 GHz, 4KW Pulse
AMP20097
4.0-8.0 GHz, 2KW Pulse
With our in-house engineering capabilities and fully equipped manufacturing facilities, Exodus Advanced Communications is committed to provide the best RF products, leading in quality along with excellent lead times.
EXODUS ADVANCED COMMUNICATIONS
www.exoduscomm.com
sales@exoduscomm.com
3674 E. Sunset Road, Suite 100, Las Vegas, Nevada 89120
Tel: 1-702-534-6564

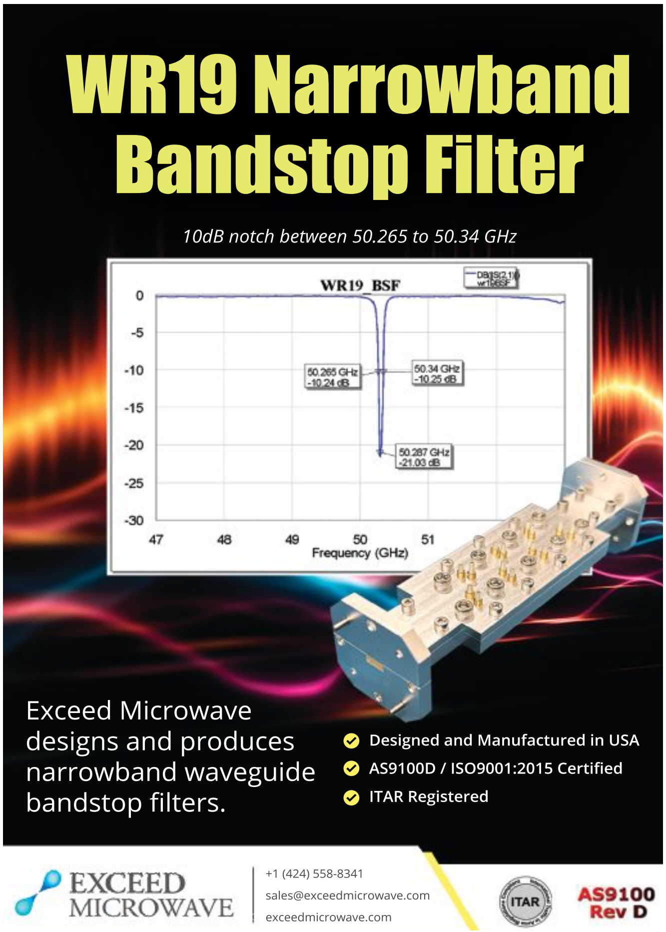

Around the **Circuit**

▲ *Mark J. Lachiw*

TagoreTech announced the appointment of **Mark J. Lachiw** as senior quality and supply chain manager. In this key leadership role, Lachiw will be instrumental in enhancing TagoreTech's commitment to quality assurance, supply chain optimization and continuous improvement across all product lines. Lachiw brings over 30 years of extensive experience in engineering, project management and quality assurance from some of the leading companies in the technology and automotive sectors. His background includes managing complex product launches in cellular, automotive and semiconductor industries, showcasing a proven track record of driving product quality and reliability.

REP APPOINTMENTS

Lane Electronics, a franchised distributor for many of the industry's major electrical, electronic and optical connector manufacturers, has increased their stockholding of **HUBER+SUHNER** products and can now offer many hundreds of parts for fast delivery from their webshop that has over 30,000 parts that customers can order online 24/7. Lane Electronics is actively expanding the range to include cables and components such as attenuators, terminations, DC blocks and additional connectors. Lane Electronics has a long history of selling RF components, and with recently increased technical support, is now in a position to support new customers and new projects.

Insight SiP, the developer of advanced miniature RF modules, has appointed **Ashtec Inc.** as its manufacturer's representative for the Northeastern U.S. Ashtec covers all six New England states, New York state, New Jersey, Eastern Pennsylvania and Florida. As a specialist in RF and microwave, Ashtec is ideally suited to supporting Insight SiP's range of advanced RF modules. With a focus on robotics, medical and industrial OEMs, Ashtec has a close alignment with Insight SiP's typical customer base. They also have excellent relationships with the contract manufacturers.

Samtec Inc., a service leader in the connector industry, has announced that it has signed **TTI Inc.** as an authorized distributor of the full line of Samtec cable and connector products. TTI, Inc. is a specialty distributor of interconnect, passive, electromechanical components and discrete semiconductors. With this new agreement, TTI will provide Samtec PCB interconnects to electronics manufacturers worldwide, simplifying customers' BOM purchases.

For More Information

For up-to-date news briefs, visit mwjournal.com

Nxbeam™

Ka / V / E - Band GaN MMIC Power

Ka

- NPA2001-DE | 26.5-29.5 GHz | 35 W
- NPA2002-DE | 27.0-30.0 GHz | 35 W
- NPA2003-DE | 27.5-31.0 GHz | 35 W
- NPA2004-DE | 25.0-28.5 GHz | 35 W
- NPA2020-DE | 24.0-25.0 GHz | 8 W
- NPA2030-DE | 27.5-31.0 GHz | 20 W
- NPA2040-DE | 27.5-31.0 GHz | 10 W
- NPA2050-SM | 27.5-31.0 GHz | 8 W

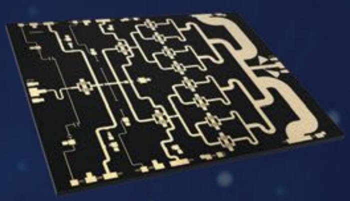

V

- NPA4000-DE | 47.0-52.0 GHz | 1.5 W
- NPA4010-DE | 47.0-52.0 GHz | 3.5 W

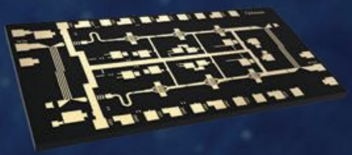

E

- NPA7000-DE | 65.0-76.0 GHz | 1 W

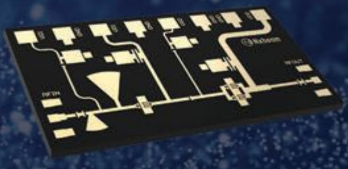

4388 Cerritos Avenue
Los Alamitos, CA 90720

www.nxbeam.com
info@nxbeam.com

Phone: 949-656-2883
info@nxbeam.com

© Copyright 2024 Nxbeam

From RF to Terahertz: Advances in On-wafer S-parameter Measurement Technologies in China and Abroad

Aihua Wu,[*,**] Hai Wang[*] and Chen Liu[**]
[*]*School of Aerospace Science and Technology, Xidian University, Xi'an, China*

[**]*Department of Metrology and Maintenance, The 13th Research Institute of China Electronics Technology Group Corporation, Shijiazhuang, China*

On-wafer S-parameter measurement can be achieved by establishing a signal connection channel between the vector network analyzer (VNA) and the wafer through a probe station. Before 2010, the development of on-wafer S-parameter measurement technologies was relatively slow in China and it had been using existing foreign technologies for a long time. In the past 10 years, China has been catching up in this field and continuously narrowing the gap with the rest of the world. China has been gradually completing the localization of calibration methods, wafer probes and on-wafer calibration standards from RF to terahertz frequencies to develop the metrological capability of on-wafer S-parameter measurement equipment. This article introduces the development of relevant technologies in this field, both domestically and internationally, which provides guidance for subsequent development.

With the development of semiconductor technology, MMICs are constantly evolving toward higher frequency bands and more challenging performance requirements are becoming common. As a result, the measurement accuracy requirements are becoming increasingly strict and new high-precision calibration methods are constantly emerging. Before 2020, all components required for S-parameter measurement were imported to China. In recent years, with the rapid development of the domestic semiconductor industry in China, the gap between on-wafer S-parameter measurement technology and capabilities between China and foreign counterparts has gradually narrowed and breakthroughs have been made in related technologies. Increasingly, key components for on-wafer measurement are being internally developed in China.

TECHNIQUES OUTSIDE CHINA

Typically, the on-wafer S-parameter measurement system consists of a VNA and frequency extender module, a probe station, microwave probes, on-wafer calibration standards and some ancillary components, as shown in ***Figure 1***. On-wafer S-parameter measurement systems need to be calibrated before measurement.

Regarding on-wafer S-parameter calibra-

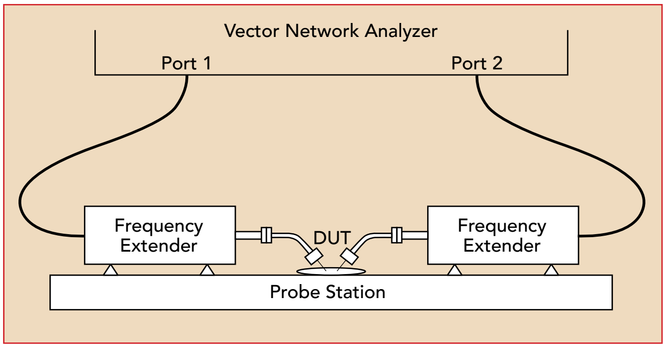

Fig. 1 **On-wafer S-parameter measurement system diagram.**

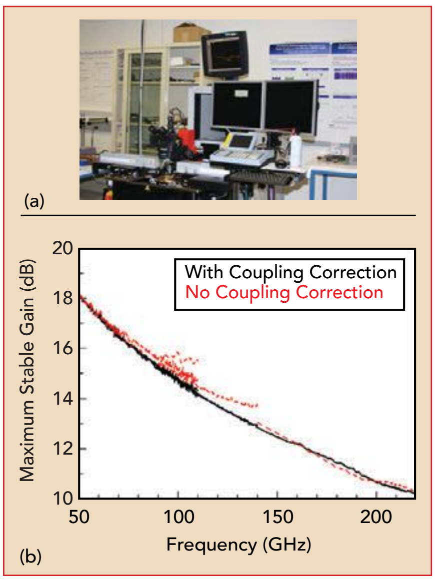

Fig. 2 **(a) NIST on-wafer S-parameter calibration system. (b) Comparison results for maximum stable gain before and after crosstalk correction.**

tion from RF to terahertz, the National Institute of Standards and Technology (NIST) in the U.S. has always been in a leading position. NIST has considered the introduction of new error sources in the on-wafer S-parameter measurement systems in the terahertz frequency band compared to microwave and RF frequencies.[1] Since 2013, research on calibration techniques for on-wafer S-parameters in the RF to terahertz frequency range has not stopped and the calibration frequency band has been raised from the previous limits of 110 GHz and 325 GHz to the current 1.1 THz. With funding from the U.S. Defense Advanced Research Projects Agency (DARPA), NIST proposed optimized multiline TRL[2], a new calibration method for precise on-wafer S-parameters in the terahertz frequency band. They have also developed corresponding on-wafer calibration standards. This calibration method has achieved good results in transistor modeling in the frequency range below 325 GHz and enables continuous measurement for even higher accuracy. ***Figure 2a*** shows a photo of the on-wafer S-parameter measurement system established by NIST and ***Figure 2b*** shows the comparison results before and after coupling correction.

In August 2022, the U.S. government proposed the CHIPS and Science Act, which provides financial support and tax incentives for the domestic semiconductor industry through legislation. Meanwhile, NIST released the Strategic Opportunities for U.S. Semiconductor Manufacturing-Facilitating U.S. Leadership and Competitiveness through Advancements in Measurements and Standards based on the content of the CHIPS and Science Act. This document outlines seven major challenges facing the U.S. semiconductor industry as a priority development direction for the next five years. This includes "modeling and simulation of semiconductor materials, design and components," which involves the importance and challenges of precise modeling of semiconductor chips at terahertz frequencies. In October 2023, NIST restarted its research on terahertz frequency metrology and measurement technology.

EU metrology institutions such as NPL in the U.K. and PTB in Germany closely follow the U.S. The EU supports 12 institutions, including NPL, PTB and MEATS in Switzerland, along with VSL in the Netherlands, to conduct EU-funded "Microwave Measurement of Planar Circuits and Components" project. The EU metrology agency has established an on-wafer S-parameter calibration system covering 110 to approximately 325 GHz and conducted calibration technology research in related fields. In terms of calibration algorithms, considering the existence of new error sources in the on-wafer S-parameter measurement system in the terahertz frequency band, the EU's metrology technical agency recommends 16-term error model calibration[3] to reduce measurement errors in on-wafer S-parameter measurement in the terahertz frequency band and improve the measurement accuracy. From 2019 to 2024, the European Association of National Metrology Institutions conducted traceability and validation work on the on-wafer S-parameters ranging from 100 GHz to 1.1 THz.[4,5] ***Figure 3a*** shows the on-wafer S-parameter calibration system from NPL and ***Figure 3b*** shows the wafer calibration standards based on 16-term error models developed by PTB.

DOMESTIC CALIBRATION METHODS

For frequencies below 67 GHz, on-wafer calibration methods have matured in China and have been widely applied. These include short-open-load-through (SOLT),[6] short-open-load-reciprocal (SOLR),[7] line-reflect-reflect-match (LRRM)[8] and through-reflect-line (TRL).[9] In addition, some specialized on-wafer calibration methods have been developed for specific applications, such as the series resistor calibration method. The multiline TRL calibration method was first proposed by Marks[10] to address the traceability

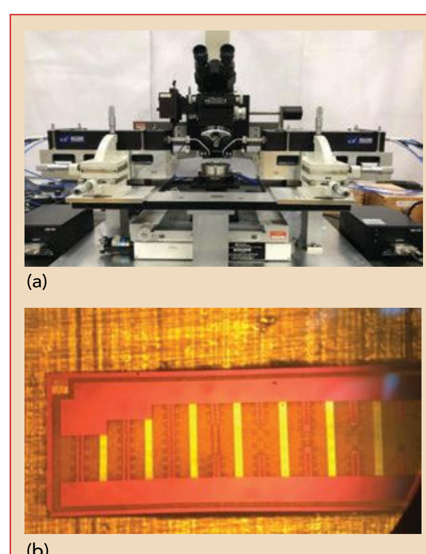

Fig. 3 **(a) On-wafer S-parameter calibration system from NPL. (b) On-wafer calibration standards based on 16-term error models developed by PTB.**

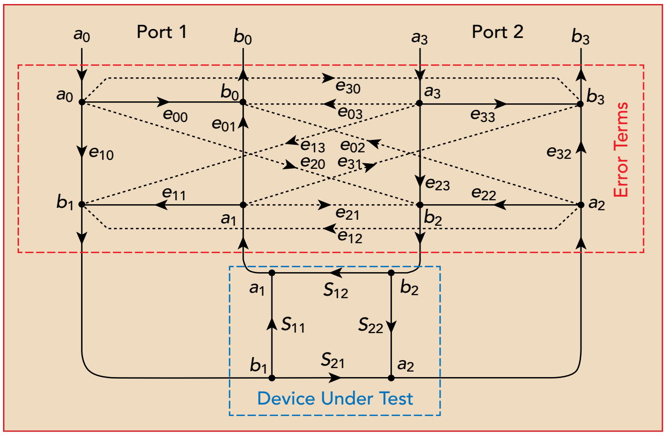

▲ Fig. 4 **16-term error model including crosstalk error.**

of waveguide systems and has now been implemented in on-wafer S-parameters metrology.

However, the accuracy of the traditional calibration methods mentioned previously decreases with increasing frequency. The main reason is that the error model used in the calibration method cannot characterize the leakage between the probe ports, which is known as crosstalk. Crosstalk can occur for several reasons; it may result from the radiation of electromagnetic energy from the device under test (DUT), energy leakage between probe tips and energy leakage between substrates. To solve this problem, one technical approach is to use a 16-term error model calibration method with crosstalk errors, as shown in ***Figure 4*** and other new calibration methods derived from the 16-term error model. Another approach is to use a parallel crosstalk error method with obvious physical significance, combined with the conventional waveguide port calibration and microwave probe extraction two-step calibration method, which has been applied in on-wafer systems.

The enhanced SOLR (eSOLR) calibration method[11] uses an 8-term error model, shown in ***Figure 5*** and includes e_{00}, e_{11}, e_{01}, e_{10}, e_{22}, e_{33}, e_{23} and e_{32}. In the

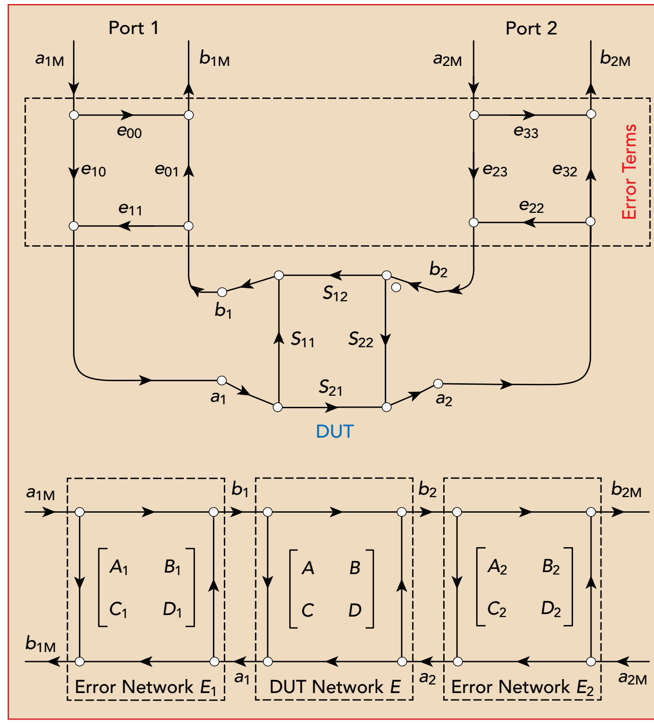

▲ Fig. 5 **8-term error model and its simplified ABCD error network.**

actual calibration process, only seven of the eight systematic error models need to be solved to complete the calibration. There are two processes for solving the eSOLR calibration algorithm. The first step is to solve the 6-term error model and the second is to solve the scale coefficient.

To facilitate the calculation, the eight basic error terms are expressed by the equivalent ABCD transfer matrix. The error network E_1 corresponds to the error network composed of e_{00}, e_{11}, e_{01} and e_{10} and the error network E_2 corresponds to the error network composed of e_{22}, e_{33}, e_{23} and e_{32}. E_1 and E_2 contain

Coilcraft

0201HT Series

Lowest Profile, High Q Chip Inductors

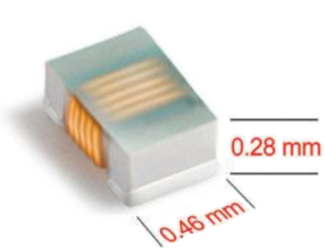

- Measure just 0.58 x 0.46 mm and only 0.28 mm tall
- Exceptionally high Q and lower DCR than thin-film types
- 14 inductance values from 0.5 to 13 nH
- Ideal for high-frequency applications such as cell phones, wearable devices, and LTE/5G IoT networks

Free Samples @ coilcraft.com

Aerospace and Defense Electronics
TeledyneADE.com
TELEDYNE

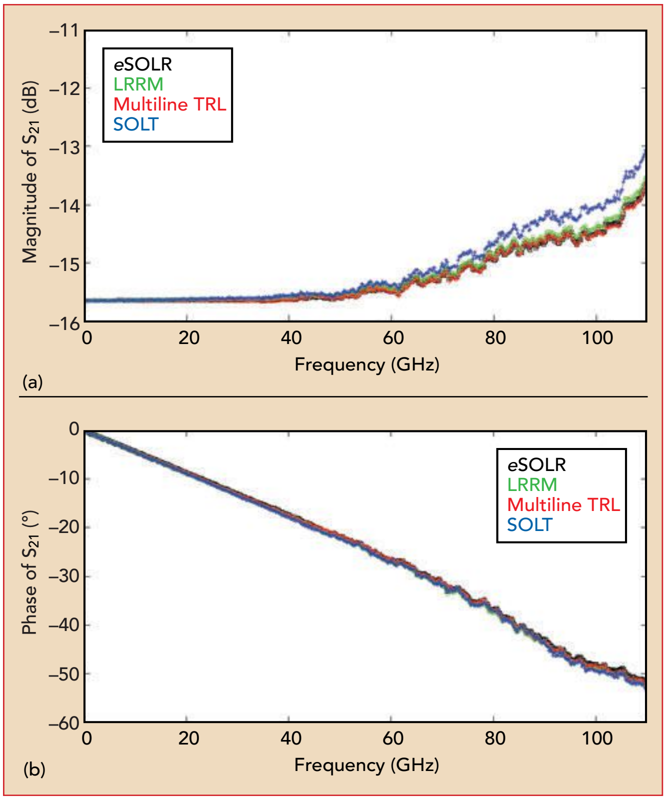

Fig. 6 (a) S_{21} magnitude comparison for different calibration methods. (b) S_{21} phase comparison for different calibration methods.

parasitic parameters of the contact points of the DUT. The eSOLR calibration method provides the foundation for terahertz measurement by combining a straight-through transmission line standard that does not need to be defined, two pairs of reflection standards (open and short standard) and a pair of accurately-defined load standards to enable terahertz wafer calibration.

Mismatch attenuators were tested by using the multiline TRL, SOLT, LRRM and eSOLR calibration methods. Magnitude and phase results for S_{21} are shown in ***Figure 6a*** and ***Figure 6b***, respectively. As can be seen from Figure 6a, the measured S_{21} magnitude results using SOLT, LRRM and eSOLR calibration methods are close but somewhat different from those of the multiline TRL calibration method due to the imperfection of the single-port load model used. In Figure 6b, the results for the phase of S_{21} using the four calibration methods were consistent, with the eSOLR calibration method agreeing better with the multiline TRL calibration method.

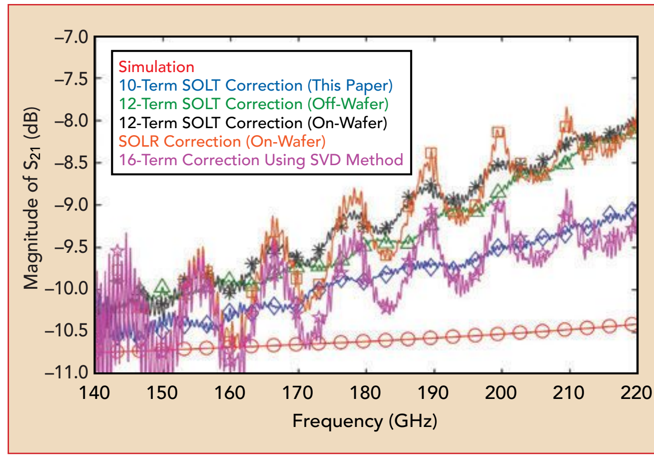

Fig. 7 Measurement results using different calibration methods.

New SOLT Calibration Method Using 10-term Error Model

Based on the 16-term error model, the new SOLT calibration method that uses a 10-term error model[12] deletes the crosstalk errors e_{30} and e_{03} from the VNA receiver and the receiver-to-probe port errors e_{20}, e_{31}, e_{02} and e_{13}. By removing these six crosstalk errors, the error term has been reduced from 16 to 10 so that the calibration can be done using the same calibration standards as the SOLT calibration method, i.e., short, open,

MiCable

SSMP 40GHz Female Right Angle

C25F Series MILLIMETER WAVE CABLE ASSEMBLY

Ideal for connection and jumper requiring extremely limited installation space and high reliability

NEW

3mm Min. Bend Radius

Excellent Phase Stability vs. Temp.

Excellent Mechanical/Temp. Stability

High Freq. Low Loss Low VSWR

Small Size for High Density Arrangement

VSWR

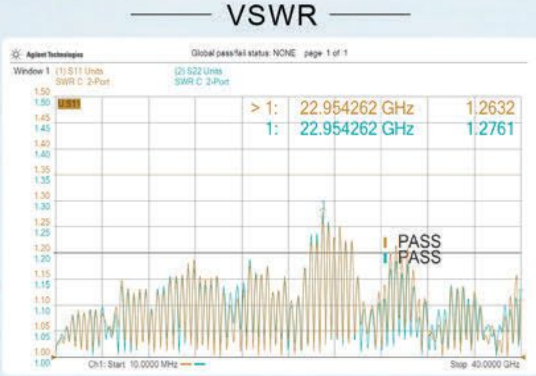

Cable Diameter	1.42mm
Frequency	DC~40GHz
Cable Attenuation	7.69dB/m@40GHz
VSWR	<1.40@40GHz
Shielding Effectiveness	<-90dB
Phase Stability vs. Flex.	<±4°@40GHz
Phase Stability vs. Temp.	<200ppm@-15°C~+35°C <400ppm@-40°C~+70°C
Amplitude Stability vs. Flex.	<±0.1dB/m@40GHz

More Information-
Scan the QR Code

MIcable Inc.

www.micable.cn sales@micable.cn +86-591-87382856

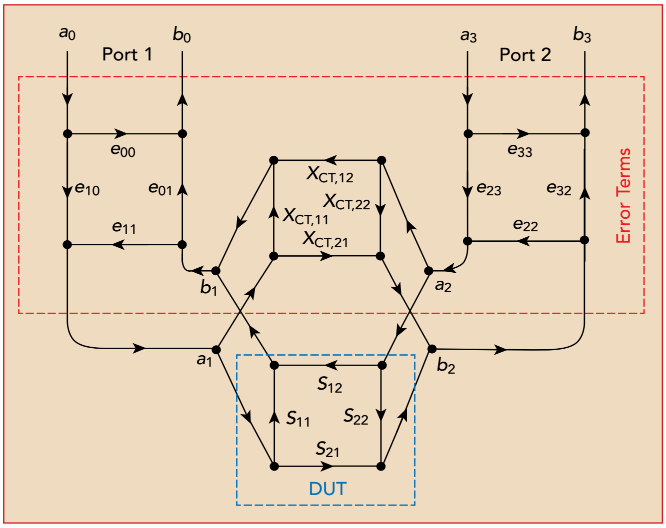

Fig. 8 Error model for the calibration-on-the-fly method.

load and through. ***Figure 7*** shows a comparison of the results measured with a 10 dB attenuator calibrated with different methods. In addition, the simulation results are given as a reference value in Figure 7. The figure shows that the measurement results of the new SOLT calibration method using the 10-term error model are closer to the simulation results and smoother as frequency increases, indicating that the crosstalk correction has achieved the desired result.

Calibration-on-the-Fly Method

The calibration-on-the-fly calibration method[13] is based on the traditional 8-term error model and four crosstalk error terms are extended based on the 8-term error model. Since the crosstalk occurs between two probe heads, the four error terms that are extended can be thought of as a virtual two-port device connected in parallel with the DUT between the two probe heads. This two-port device has distinct S-parameters, so the electromagnetic wave transmission in this virtual two-port device is related to the reflection of its DUT, which is different from the traditional 16-term error model, treating the crosstalk term as a constant. The 12-term error model with a crosstalk term is shown in ***Figure 8***, where the S-parameter of the virtual two-port device is denoted as S_{CT}.

Figure 9 shows the comparison between the calibration-on-the-fly method and the traditional SOLT, 16-term calibration at 10 dB. The measurement results at 180 GHz are not much different. As the frequency increases, the measured value of S_{21} using the calibration-on-the-fly method is significantly lower than that of the SOLT calibration meth-

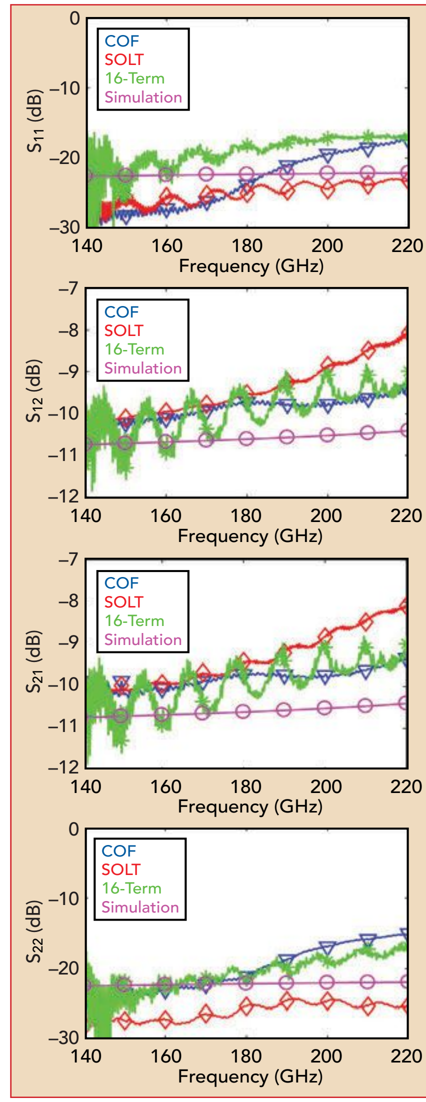

Fig. 9 Comparison of the measurement results with different calibration methods.

High Performance RF & Microwave Oscillators and Modules Accelerating R&D

SHOP NOW AT STORE.ZCOMM.COM

NEW

SFSLX PL Series Phase Locked Oscillator

- Custom Orders in 48 hours!
- 50MHz to 22.5GHz
- Reference input 5MHz–200MHz
- Small 0.6x0.6 inch Footprint

SFS/RFS Fixed Frequency Synthesizers

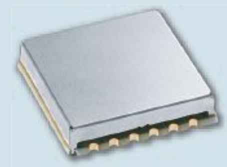

- 2GHz–16GHz
- Optimized for Phase Noise
- Available with Onboard Reference

SMART Synthesizers/ Oscillators

- Unique Bluetooth Control
- Cost effective Lab Solutions
- Compact Connectorized Housings
- Available frequencies from 45MHz–22.6GHz
- Readily Available, in stock

DRO Oscillators

- Superior phase noise, –106dBc/Hz@10kHz CF12GHz
- 7GHz–16GHz
- Low Power Consumption

Amplifiers & RF Switches

- DC to 30GHz Bandwidths
- Low Noise
- Excellent Return Loss
- High Isolation

Voltage Controlled Oscillators

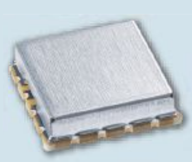

- Low Noise Series, –120dBc/Hz@10kHz CF2.5GHz
- Octave Tuning Series
- Small Size, Low Power Consumption

For your specific requirements, call 858-621-2700 x250 or email applications@zcomm.com

Z~Communications, Inc.

38 Years of Performance, Reliability and Delivery you can Trust

zcomm.com | +1 (858) 621-2700 | sales@zcomm.com

AS9100D ISO9001:2015 CERTIFIED BY NSF-ISR

VISIT Z-COMM AT IMS BOOTH #158

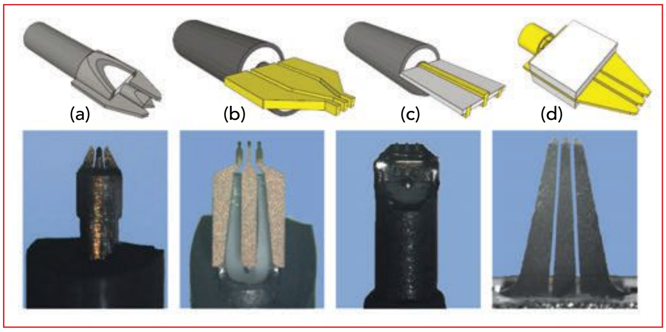

Fig. 10 **Probes using different processes.**

od. The S_{21} measurement results are about one dB lower than those of traditional SOLT measurement results at 220 GHz and are closer to the simulation results. The calibration-on-the-fly calibration method affects the correction of crosstalk progression.

DOMESTIC AND INTERNATIONAL TRENDS FOR PROBES AND CALIBRATION STANDARDS

Before 2020, most of the probes and on-wafer calibration standards came from the U.S., Japan and Taiwan. Probes from FormFactor and GGB in the U.S. reached an upper frequency of 1.1 THz and they had several different form factors. ***Figure 10a*** shows micro-coaxial probes from GGB. ***Figure 10b*** shows air coplanar probes (ACP) from FormFactor. ***Figure 10c*** shows MEMS Z-probes from FormFactor and ***Figure 10d*** shows thin-film Infinity probes from FormFactor.

Since 2022, the Chinese mainland has developed and refined the ACP microwave probe process. Companies such as the 13th Research Institute of China Electronics Technology Group Corporation (CETC-13) have developed a 110 GHz microwave probe based on this process with performance comparable to the best available from other countries. The probe products launched in China reach 110 GHz. As semiconductor chips are required at higher frequencies, microwave probes will also be developed to operate at higher test frequencies and provide a longer service life.

As an example of these development activities, a team at Ohio State University in the U.S. used new non-contact measurement probe technology[14] to achieve 140 to 220 GHz passive mmWave wafer characterization measurement. This non-contact probe measurement method enables fast, repeatable, low-cost and wear-free evaluation of microwave, mmWave and terahertz integrated circuits. This new method accommodates a wide frequency range from mmWave to terahertz (60 GHz to 3 THz). A team from the University of Virginia in the U.S. used a silicon-based insulator process to fabricate a micromechanical process probe[15] that can scale to terahertz frequencies. At present, this kind of micromachined coplanar waveguide probe has been used in the WR-1.0 band (0.75 to 1.1 THz) to realize wafer measurement of coplanar devices. This technology may also be applied to higher test frequencies in the future.

Commercially available on-wafer calibration parts, also known as impedance standard substrates (ISS), are typically made of ceramic substrates. At present, the applicable frequency range of commercial wafer calibration parts outside China reaches 325 GHz. For higher frequency on-wafer measurement requirements, special on-wafer calibration parts need to be made on the tested wafer.[16] At the same time as the launch of microwave probes in China, various commercial on-wafer calibration parts were launched, with a frequency covering 110 GHz. At present, CETC-13 is competitive with the best performance for probe resistance change on its commercial calibration standards.

METROLOGY IN CHINA

Since 2012, CETC-13 has completed a number of research programs addressing topics like MMIC

Elve's Advanced mmWave Amplifiers Enable Gbit Speeds for Next-Gen Wireless and Beyond

Elve

Experience Elve mmWave Amplifiers risk-free with our new two-month free hardware "First Light" product demo program. Elve unlocks access to high power and high efficiency mmWave amplifiers with advanced materials and additive manufacturing processes. Our products enable Gbit speeds for next-gen multi-domain connectivity with large scale production of TWTAs at significantly lower costs in Ka, Q, V, E and W-bands.

Contact us at https://elvespeed.com/ for more information.

iNRCORE

iNRCORE FAMILY OF BRANDS

Maximize Performance. Minimize Size.

Unlock Precision and Reliability **with iNRCORE!**

HIGH-FREQUENCY EXCELLENCE

iNRCORE is your trusted partner in high-performance electronic components, delivering innovative solutions tailored to meet the most demanding technical requirements. Our products are engineered to optimize signal integrity and power management across critical industries, including aerospace, defense, medical, and telecommunications.

Planar Transformers | Ethernet Transformers | Chip Inductors | Broadband Conicals | Transceiver Modules | Military QPL Inductors

EMI/RFI Filters | Capacitors | Resistors | RF Filters | Custom Magnetics

KEY FEATURES

- **Advanced Magnetic Components:** Precision-engineered for flawless performance in extreme environments.
- **High-Speed Signal Transmission:** Designed to handle mission-critical applications with uncompromising reliability.
- **Custom Solutions:** Tailored designs to meet unique specifications and rigorous industry standards.
- **Ruggedized Construction:** Built to withstand shock, vibration, and harsh operating conditions.

IDEAL FOR

- Aerospace systems
- Medical devices
- Defense technology
- RF and microwave communications

Why iNRCORE?

With over 70 years of expertise, iNRCORE products ensure unmatched performance in the most challenging environments. Choose iNRCORE for excellence you can rely on!

For more information **SCAN HERE!**

ISO 9001 CERTIFIED | AS9100 CERTIFIED | ITAR *Registered* International Traffic in Arms Regulations

www.iNRCORE.com +1-215-781-6400

automatic test systems, on-wafer S-parameters, load-pull and noise parameters. They are also responsible for compiling several calibration specifications for on-wafer measurements and probe stations. CETC-13 has established the unique CNAS (China National Accreditation Standard) calibration capability for on-wafer S-parameters, on-wafer load-pull and noise test systems in China.

Organized by the State Administration for Market Regulation in 2022, CETC-13 led the national measurement comparison program of on-wafer S-parameters. According to the measurement comparison, on-wafer S-parameter measurements for the joined laboratory were verified, the accuracy and reliability of the transmission of on-wafer S-parameter measurements were ensured, and more relevantly, the main sources of uncertainty in the measurement of on-wafer S-parameters were unified. At the same time, the measurement comparison program also provides the industry with a comparison platform for the consistency of on-wafer S-parameter measurement.

CONCLUSION

This article has reviewed the current development of on-wafer S-parameter calibration methods from RF to terahertz frequency ranges, microwave probes, on-wafer calibration standards and the construction of on-wafer metrology in China. After years of catching up, China has reached a new level in this area. However, for the terahertz frequency band, there is still a gap between China and the rest of the world in terms of microwave probes, on-wafer calibration standards and metrology technologies. ■

References

1. D. F. Williams, F.J. Schmückle, R. Doerner, et al., "Crosstalk Corrections for Coplanar-waveguide Scattering Parameter Calibrations," *IEEE Transactions on Microwave Theory and Techniques*, Vol. 62, No. 8, 2014, pp. 1748–1761.
2. D. F. Williams, C. M. Wang and U. Arz. "An Optimal Multiline TRL Calibration Algorithm," *IEEE MTT-S International Microwave Symposium Digest*, 2003.
3. J. V. Butler, D. K. Rytting, M. F. Iskander, et al., "16-term Error Model and Calibration Procedure for On-wafer Network Analysis Measurements," *IEEE Transactions on Microwave Theory and Techniques*, Vol. 39, No. 12, 1991, pp. 2211–2217.
4. X. Shang, et al., "Some Recent Advances in Measurements at Millimeter-Wave and Terahertz Frequencies: Advances in High Frequency Measurements," *IEEE Microwave Magazine*, Vol. 25, No. 1, 2024, pp. 58–71.
5. X. Shang, et al., "Interlaboratory Investigation of On-wafer S-parameter Measurements from 110 GHz to 1.1 THz," *53rd European Microwave Conference*, 2023.
6. J. Fitzpatrick, "Error Models for Systems Measurement," *Microwave Journal*, Vol. 21, No. 5, 1978, pp. 63–66.
7. A. Ferraro, "Two-port Network Analyzer Calibration Using an Unknown 'Thru'," *IEEE Microwave and Guided Wave Letters*, Vol. 2, No. 12, 1992, pp. 505–507.
8. A. Davidson, K. Jones and E. Strid, "LRM and LRRM Calibrations with Automatic Determination of Load Inductance," *36th ARFTG Conference Digest*, 1990.
9. G. F. Engen and C. A. Hoer, "Thru-Reflect-line: An Improved Technique For Calibrating The Dual Six-Port Automatic Network Analyzer," *IEEE Transactions on Microwave Theory and Techniques*, Vol. 27, No. 12, 1979, pp. 987–993.
10. B. Marks, "A Multiline Method of Network Analyzer Calibration," *IEEE Transactions on Microwave Theory and Techniques*, Vol. 39, No. 7, 1991, pp. 1205–1215.
11. A. Wu, Y. W. Yehuo, et al., "An Enhanced SOLR Calibration Method," *Acta Metrologica Sinica*, Vol. 43, No. 8, 2022, pp. 973–978.
12. C. Liu, A. Wu, C. Li, et al., "A New SOLT Calibration Method for Leaky On-Wafer Measurements Using a 10-Term Error Model," *IEEE Transactions on Microwave Theory and Techniques*, Vol. 66, No. 8, pp. 3894–3900.
13. A. Wu, et al., "Calibration on the Fly—A Novel Two-Port S-Parameter Measurement Method for On-Wafer Leaky Systems," *IEEE Transactions on Microwave Theory and Techniques*, Vol. 68, 8, 2020, pp. 3558–3564.
14. K. Sertel, "Automated Performance of On-Wafer Calibration and Characterization Using Non-Contact Probes," *92nd ARFTG Microwave Measurement Conference*, 2019.
15. M. F. Bauwens, N. Alijabbari, A. W. Lichtenberger, et al., "A 1.1 THz Micromachined On-wafer Probe," *IEEE MTT-S International Microwave Symposium*, 2014.
16. Y. Wang, et al., "An Advanced Calibration Method for Probe Leakage Correction in On-Wafer Test Systems," *IEEE Transactions on Microwave Theory and Techniques*, Vol. 71, No. 2, 2023, pp. 682–690.

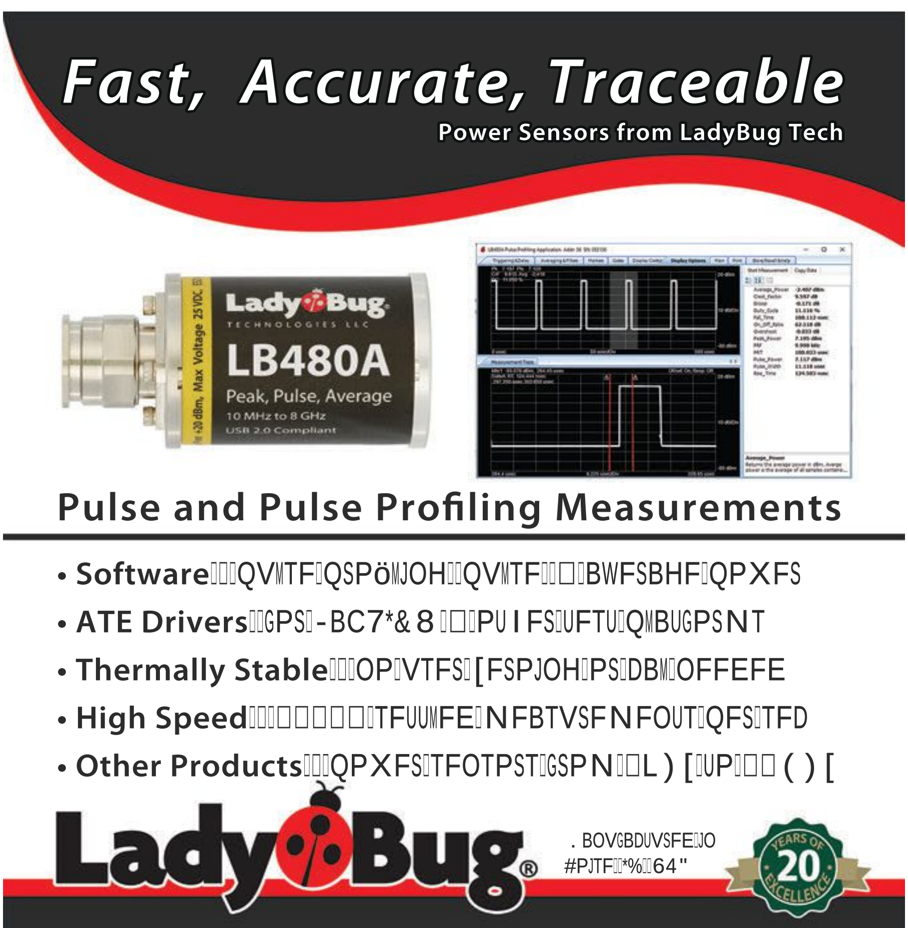

MiniRF
Tiny
4x4 mm
Package
MRFCP5753
5-1225 MHz, 12 dB, 75Ω Coupler
Delivers High Performance for
Broadband and CATV Applications
Passives with a
Passion for Performance
Couplers
Splitters
Transformers
RF Chokes
MRFCP6762
MiniRF is a proven, preferred leader in passive component supply for Broadband/CATV and Wireless Communications, with 1+ billion components shipped. MiniRF passives enable DOCSIS 4.0 & FDX system requirements, max RF output power, and have excellent repeatability and reliability with 100% RF testing. The USA-based design center supports standard and custom components, while multiple low-cost overseas manufacturing operations with no tariffs deliver competitive pricing.
RFMW®
Contact our team of experts for information,
samples and sales: sales@rfmw.com | rfmw.com

INVITED PAPER

Enabling Applications with High-Power Semiconductor Terahertz Sources

Tim Bernstein
yet2, Waltham, Mass.

In the constantly evolving technology landscape, the demand for innovative solutions that address modern challenges in security, communication and imaging has reached unprecedented levels. As industries look to solutions that improve efficiency, safety and scalability, the terahertz (THz) band has emerged as a viable option. Positioned between the microwave and infrared spectra, the THz frequency band possesses properties that enable advancements across multiple domains. ***Figure 1*** shows the THz frequency band and where it resides in the electromagnetic spectrum, along with some popular applications.

THz waves, characterized by their ability to penetrate a variety of materials, non-ionizing nature and high-resolution imaging capabilities, present an opportunity to transform how industries address solutions to complex problems. The application of THz technology spans a wide array of fields, from real-time security screening to next-generation wireless communication and advanced medical diagnostics. This article explores THz light source technology developed by Canon, along with the applications and the broader implications of the adoption of this fundamental technology across industries. It will also highlight the challenges and opportunities associated with commercializing THz technology, offering insights into its future trajectory and impact. The technology is available for licensing or acquisition to enable broader commercial applications and Canon is partnering with yet2, a global technology scouting and innovation firm, to commercialize this technology.

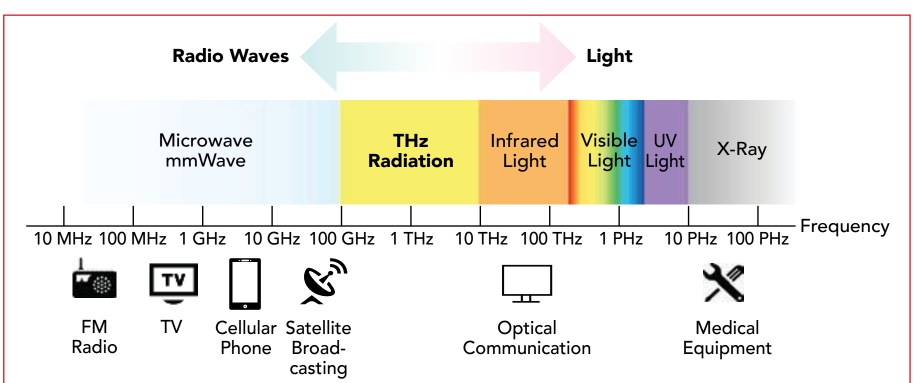

Fig. 1 The electromagnetic spectrum. *Source*: Canon.

THE SCIENCE OF THZ WAVES

THz radiation spans frequencies between 0.1 and 10 THz in the electromagnetic spectrum. This range bridges the gap between the microwave and infrared regions. This frequency band is attracting substantial development attention and activity because it offers properties that are advantageous for a multitude of applications.

Key Characteristics of THz Waves

Non-Ionizing Nature: Unlike X-rays, THz radiation is non-ionizing, meaning it does not have enough energy to remove tightly bound electrons from atoms. This makes THz waves inherently safer for applications involving human interaction, such as medical imaging and security scanning.

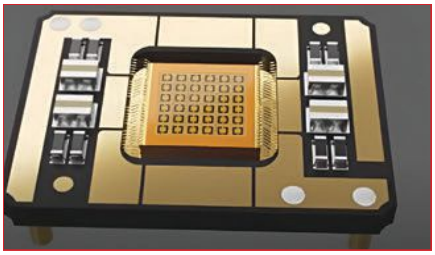

Fig. 2 Canon THz light source. *Source*: Canon.

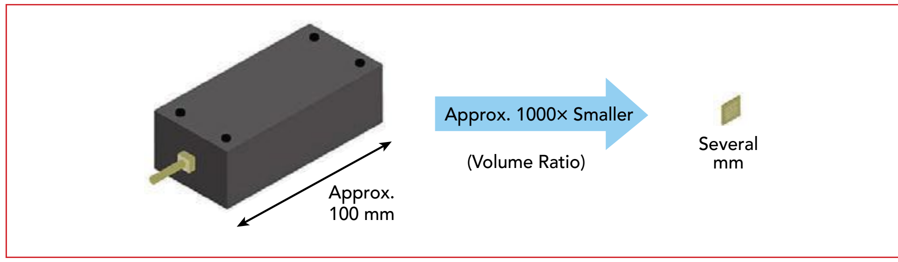

Fig. 3 Size reduction of integrated light source. *Source*: Canon.

Material Penetration: THz waves can penetrate materials like fabric, paper and certain plastics. This capability is an important differentiator in applications such as security screening, where non-invasive detection of concealed items is crucial. Additionally, THz waves are absorbed by water and other liquids, enabling precise identification of substances.

Spectral Fingerprinting: The interaction of THz waves with materials produces unique absorption and reflection patterns, known as spectral fingerprints. These patterns enable the identification and differentiation of materials at a molecular level, making THz waves invaluable for applications in chemical analysis and quality control.

Wavelength and Resolution: With wavelengths shorter than mmWaves but longer than infrared, THz waves strike a balance that offers higher-resolution imaging capabilities. This property is particularly useful in applications requiring detailed visualization, such as non-destructive testing and medical diagnostics.

The ability of THz waves to interact with a wide range of materials stems from their intermediate position in the electromagnetic spectrum. THz waves are reflected by metallic surfaces, allowing for the identification of metallic objects in security settings. Also helpful in security applications, THz radiation is highly absorbed by water. This enables the detection of liquid substances, which is crucial for identifying hazardous liquids. These high frequency THz waves scatter when interacting with powders, providing a non-invasive means to analyze the composition of granular materials.

When compared to the adjacent mmWave and infrared regions of the spectrum, THz waves offer a unique combination of benefits. Even though mmWave frequencies and equipment are widely used in security scanners, THz frequencies and equipment provide more resolution. Additionally, mmWave frequencies do not have the penetration capabilities of THz wave in certain materials. Infrared radiation provides high-resolution imaging, but it is susceptible to scattering and absorption in specific environments, particularly those with high moisture content. The net result is that THz waves offer greater versatility for these and other applications.

EMERGING SCIENTIFIC RESEARCH

There is a significant amount of ongoing research into the THz spectrum and the possibilities. Scientists are exploring advanced methods to enhance the generation and detection of THz radiation, along with devices. Some of the more prominent areas of exploration include:

Quantum Cascade Lasers: These devices promise efficient and compact THz wave generation for portable applications.

Plasmonics: This field involves generating, detecting and manipulating light at metal/dielectric interfaces at nanoscale dimensions. Leveraging surface plasmon resonances to improve the interaction of THz waves with materials is being investigated to enable higher sensitivity in sensors.

Metamaterials: Metamaterials are being investigated for a variety of applications. In the THz frequency range, engineered structures that manipulate THz waves in novel ways are being developed with the goal of enabling applications like cloaking and ultra-high-resolution imaging.

The science of THz signals and the ongoing research are intertwined. These areas highlight the current capabilities of the technology and underscore the potential for future innovation. As research progresses, the boundaries of what is possible with THz technology will continue to expand, driving advancements across multiple fields.

THZ LIGHT SOURCE DEVELOPMENT

To help crystalize the potential of THz waves into reality, Canon has introduced the semiconductor-based THz light source shown in ***Figure 2***. The THz light source uses a resonant tunnel diode (RTD) manufactured on indium phosphide (InP) in an active array antenna structure. InP is a III-V compound semiconductor material like gallium arsenide (GaAs). While GaAs has been a mainstay technology for mmWave applications, InP has higher electron mobility and a wider bandgap, making this technology increasingly attractive for higher frequency applications. InP is also a direct bandgap material, which allows for more efficient light emission and absorption. The direct bandgap makes the material compatible with optical components and suitable for integration into optical networks.

The InP-based high electron mobility RTD that Canon developed operates at 0.45 THz without requiring frequency multipliers. This eliminates bulky and power-hungry components, reducing the overall size and power consumption of the final assembly. This source delivers 11.8 mW of power at 0.45 THz with a power efficiency that is 1.4x better than conventional RTDs. It has a directivity of 13 degrees and the semiconductor chip has a 3.2 mm^2 footprint. The size reduction afforded by the InP-based light source versus a competitive solution is shown in ***Figure 3***. Canon believes that the performance and size of this semiconductor THz light source make it suitable for integration into a wide range of applications. These applications include enabling handheld near real-time imaging in security systems and supporting terabit per second (Tbps) data rates in 6G communications, with a vast array of additional applications possible.

The introduction of Canon's THz technology bridges the gap between academic research and commercial application. This THz light source addresses existing market needs and paves the way for future innovations in areas like improved security protocols, sustainable manufacturing and communication infrastructure. The compact and cost-effective design of this technology makes it an attractive solution for a variety of industries.

InP RTDs are gaining traction in high frequency applications because of their ultra-fast switching speeds. Benchmark data for RTD devices provides a comparative analysis of key performance parameters such as peak-to-valley current ratio, operational frequency and material efficiency. This benchmarking helps researchers and engineers evaluate design improvements, optimize device performance and identify areas where RTDs can outperform traditional semiconductor components. As the RTD technology advances and evolves, these performance benchmarks will enable future innovations.

The final configuration of the light source leverages the InP RTD device technology and packaging into an active array antenna structure. The design of array configurations is a critical aspect of optimizing performance in modern electronic and communication systems. As highlighted in an IEEE paper,[1] constructing arrays involves balancing multiple factors, including element placement, signal integrity and minimizing interference. Designers must consider trade-offs among size, efficiency and cost while ensuring that the array meets specific application requirements. Advanced simulation techniques and computational models help address these challenges, enabling the development of high performance arrays tailored to industry needs.

The antenna structure consists of a synchronized array of 36 active antennas on a single chip. This architecture achieves approximately 10x the output power and 20x better directivity than existing semiconductor THz sources. These advancements enable THz emission over several meters. The 13-degree directivity represents a significant improvement over the 60-degree emission angle of competing technologies. The emission angle eliminates the need for external lenses or horns.

Developing the semiconductor source is one piece of the puzzle. Ensuring the long-term reliability and maintaining the performance of the semiconductor devices requires high performance, robust packaging solutions that protect components from environmental stressors and thermal degradation. Canon worked with Kyocera to develop the package shown in Figure 2. With the final package containing 36 active antennas, heat dissipation became a primary concern. The concerns about heat dissipation eliminated organic FR-4 materials from consideration. Instead, Kyocera proposed an aluminum nitride (AlN) solution because of the high thermal conductivity of the material and the good match to the InP coefficient of thermal expansion.

Another primary package design consideration was the interconnection scheme for the active antenna array. At these frequencies, the impedance of the interconnects and the inductance are appreciable. The AlN packaging technology that Kyocera proposed offered more design flexibility to minimize any performance degradation caused by the package. The final package mitigated heat dissipation, electrical interference and mechanical stress concerns to provide a high performance, high-reliability solution in a small footprint.

saetta labs

Boulder, Colorado USA

saettalabs.com

- Thermally Stabilized
- Ext Ref Input (PLL)
- Status Display
- Lock Detect

Sapphire Loaded Cavity Oscillators
X-Band

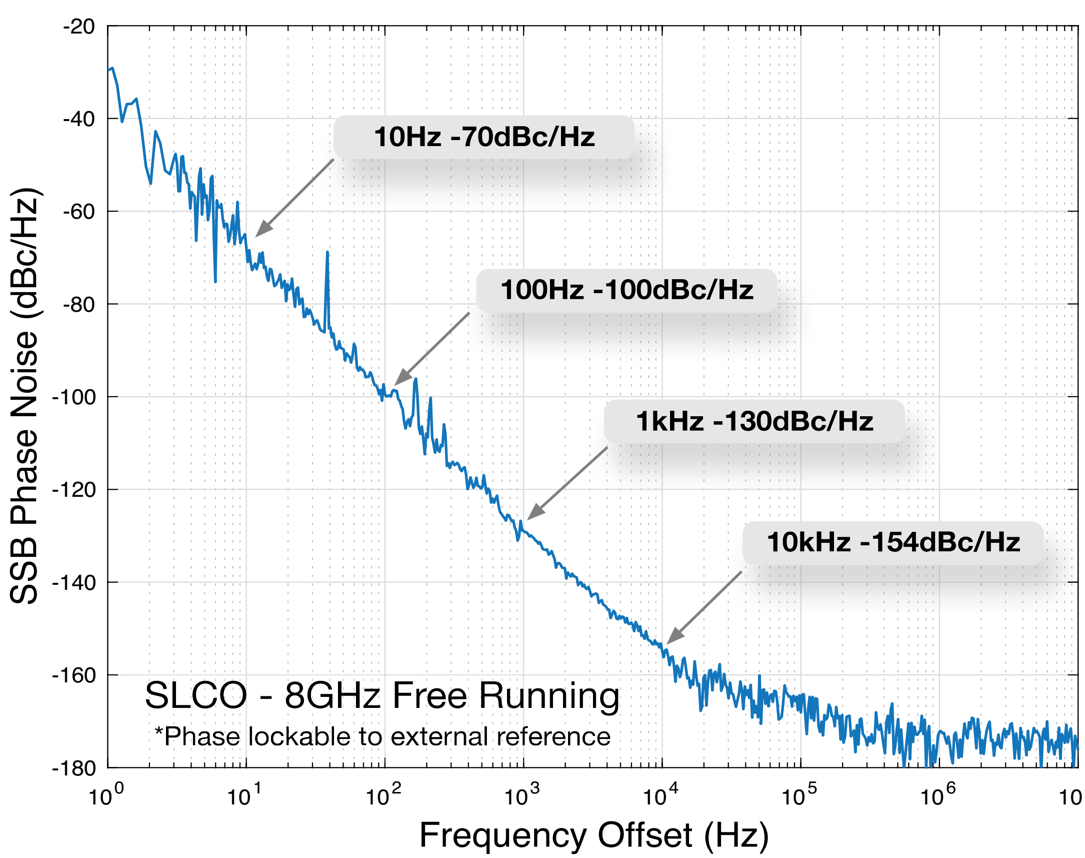

APPLICATIONS AND MARKET NEEDS

Security Screening

Existing mmWave-based security scanners are large and require individuals to remain stationary. This limits system throughput and portability. THz waves offer superior resolution, safety and efficiency, with the potential to:

- Penetrate materials such as fabric, paper and some plastics
- Identify liquids, powders and concealed objects without the radiation risks associated with X-rays
- Enable near real-time imaging in compact devices, potentially reducing security bottlenecks in high-traffic areas like airports and train stations.

Additionally, the ability of THz waves to distinguish between different substances creates the possibility of identifying hazardous liquids without opening containers to add a layer of security and convenience. By reducing the physical footprint of scanning devices, this technology can also be deployed in mobile units. The throughput capacity of the prototype scanner developed by Canon offers significant advantages. The company believes that this scanner is capable of processing approximately 1000 individuals per hour. With this throughput, this system can dramatically improve security operations at venues hosting large-scale events or in transit hubs. ***Figure 4*** shows performance characteristics of body scanners using various technologies, from X-rays through mmWave scanners to an active THz scanner that would incorporate the light source described in this article. ***Figure 5*** shows an artist's concept of what the future of security might look like with THz-enabled scanners.

Body Scanner Canon

Type	THz Active Camera	THz Passive Scanner	MMW Radar Walk-Through	MMW Radar Scanner	X-Ray Scanner
Appearance					
Working Distance	~a Few m	~a Few m	Tens of cm	a Few cm	a Few cm
Resolution	1 mm~	>5 cm	a Few mm	a Few mm	a Few mm
Imaging Method	20k-Pixel Camera (50 fps)	16 ch Sensor at 250 GHz	2D Radar (10-70 GHz)	1D Radar + Scan	Sensor Array
Detection	2D	2D	3D	3D	2D
Throughput	≧1000 People/Hour	~1000 People/Hour	~1000 People/Hour	~100 People/Hour	~100 People/Hour
Size	a Few m^3	a Few m^3	a Few m^3	a Few m^3	a Few m^3
Transparency	O	O	O	O	◎
Cost	TBD	~100k USD	~200k USD	>200k USD	>400k USD
Portability	O	O	Δ	x	x

Fig. 4 Key performance indicators for scanning technologies. *Source*: Canon.

The deployment of THz technology in communication systems could help revolutionize fields like autonomous vehicles, enabling seamless high speed data exchange between devices and supporting large-scale IoT networks. As current 5G systems operate at frequencies up to 60 GHz, leveraging sub-THz and THz bands can provide the leap needed for future communications infrastructure.

Fig. 5 The future of security with THz scanners. *Source*: Canon.

6G Communications and Beyond

Despite the challenges, there is significant interest and development activity in the THz frequencies. The bandwidth available in this band can mitigate spectrum scarcity challenges in next-generation wireless communication. The availability of THz of bandwidth will provide support for Tbps data rates, enabling a broader range of data-intensive applications.

Additional Applications

Security and communications applications seem well-positioned to take advantage of THz technology and systems, but the potential is there for many other applications to benefit. High-resolution inspection of materials and structures without physical contact provides benefits for non-destructive testing. The enhanced precision afforded by THz waves can help speed the evolution of advanced radar applications with further development. High resolution can also aid medical imaging diagnostic applications, enabling early detection of cancers or detailed hydration analysis. THz imaging will also be important in agricultural monitoring. This imaging can assess plant health and detect contaminants to help improve the efficiency of the food chain and food security.

CHALLENGES AND OPPORTUNITIES

The InP-based THz light source described in this article shows exceptional performance and great promise, but additional work is underway to improve the attractiveness of this solution. To improve performance, research and development efforts aim to enhance the resolution of the light source to enable use in a broader range of applications. Efforts are underway to reliably scale

New Bias Tees

We offer a range of in-stock, Bias Tees to address a variety of applications, including test and measurement, research and development, optical communications, satellite communications and more.

In-Stock & Shipped Same-Day

SAME-DAY SHIPPING

CUSTOM CABLES

LIVE TECH SUPPORT

fairviewmicrowave.com
+1 (800) 715-4396

Fairview Microwave®
an INFINITE brand

PRECISION.
PERFORMANCE.

The T32 Series TCXO.

Wide Temp Range
Low Acceleration Sensitivity
High Shock Survivability

- Temp Stability to 1 ppm over -55°C to +125°C
- Shock Survivability to 75,000 g
- Acceleration Stability as low as 0.2 ppb/g
- Frequency: 10-52 MHz
- Rugged 3.2 x 2.5 mm package
- CMOS or Clipped Sine Output
- Supply: +3.0 to +3.6 Vdc
- MIL-PRF-55310, Level B Testing available

Additional Information

GREENRAY
frequency control solutions

TABLE 1
A SAMPLE OF CANON'S THz PATENTS (SOURCE: CANON)

Technology, Market Application	Patent Number	Title	Application Date
RTD for Radar, Communication	WO2023199964A	Antenna apparatus, communication apparatus and image-capturing system	4/13/2023
Sensor/Receiver (Antenna etc.)	US11391625	Element for oscillating or detecting an electromagnetic wave and element manufacturing method	8/23/2019
Sensor/Receiver (Antenna etc.)	US11616918	Element and image-forming device	8/20/2020
Sensor/Receiver (Imaging)	US10897073	Receiver for detecting a terahertz wave and image-forming apparatus	8/20/2019
Sensor/Receiver (Imaging)	US11714000	Detection device and detection system	8/5/2020
Imaging System	US10879281	Image capture device, method of capturing image with the same and irradiation device	5/3/2019

the production of InP-based semiconductors to reduce costs and improve manufacturing yields. To increase the rate of adoption, regulatory requirements for radio wave compliance and international export controls are being addressed.

To deal with these challenges, investments in material science and advanced fabrication techniques are helping to improve device efficiency and scalability. In conjunction, collaboration with academic institutions and industry leaders may accelerate the development of complementary technologies, devices and capabilities like advanced THz detectors and data processing systems. Emerging areas of research include the integration of artificial intelligence to interpret THz imaging data in real-time, enhancing applications in security and medical diagnostics. ***Table 1*** shows a list of Canon patents that the company is using to advance the state of the art in THz technology.

CONCLUSION

Market analysts predict rapid growth for THz technology and systems, driven by demand in telecommunications, medical diagnostics and industrial inspection. Canon's InP-based high-power THz light source that is described in this article represents a significant advancement in the state of the art. Its compact size enables integration into portable devices. The performance allows 1 mm resolution from distances up to 10 m and fabrication on an integrated circuit process shows the roadmap to reduced manufacturing and operational costs as the InP process is scaled.

Canon has developed and tested a prototype THz active camera for body scanning. This system has demonstrated a scanning throughput of approximately 1000 people per hour, which is comparable to mmWave scanners. The design and manufacturing enable superior resolution at a lower cost. The features and advantages of the Canon development enable miniaturized systems that can be integrated into higher volume commercial applications like body cameras for real-time, portable security scanning. To help encourage the vision of a future rich with possibilities for safer, faster and more efficient imaging, communication and security systems, Canon has partnered with yet2 to license and commercialize this technology to make this vision a reality. ■

References

1 Y. Koyama et al., "A High-Power Terahertz Source Over 10 mW at 0.45 THz Using an Active Antenna Array With Integrated Patch Antennas and Resonant-Tunneling Diodes," *IEEE Transactions on Terahertz Science and Technology*, Vol. 12, No. 5, Sept. 2022, pp. 510–519, doi: 10.1109/TTHZ.2022.3180492.

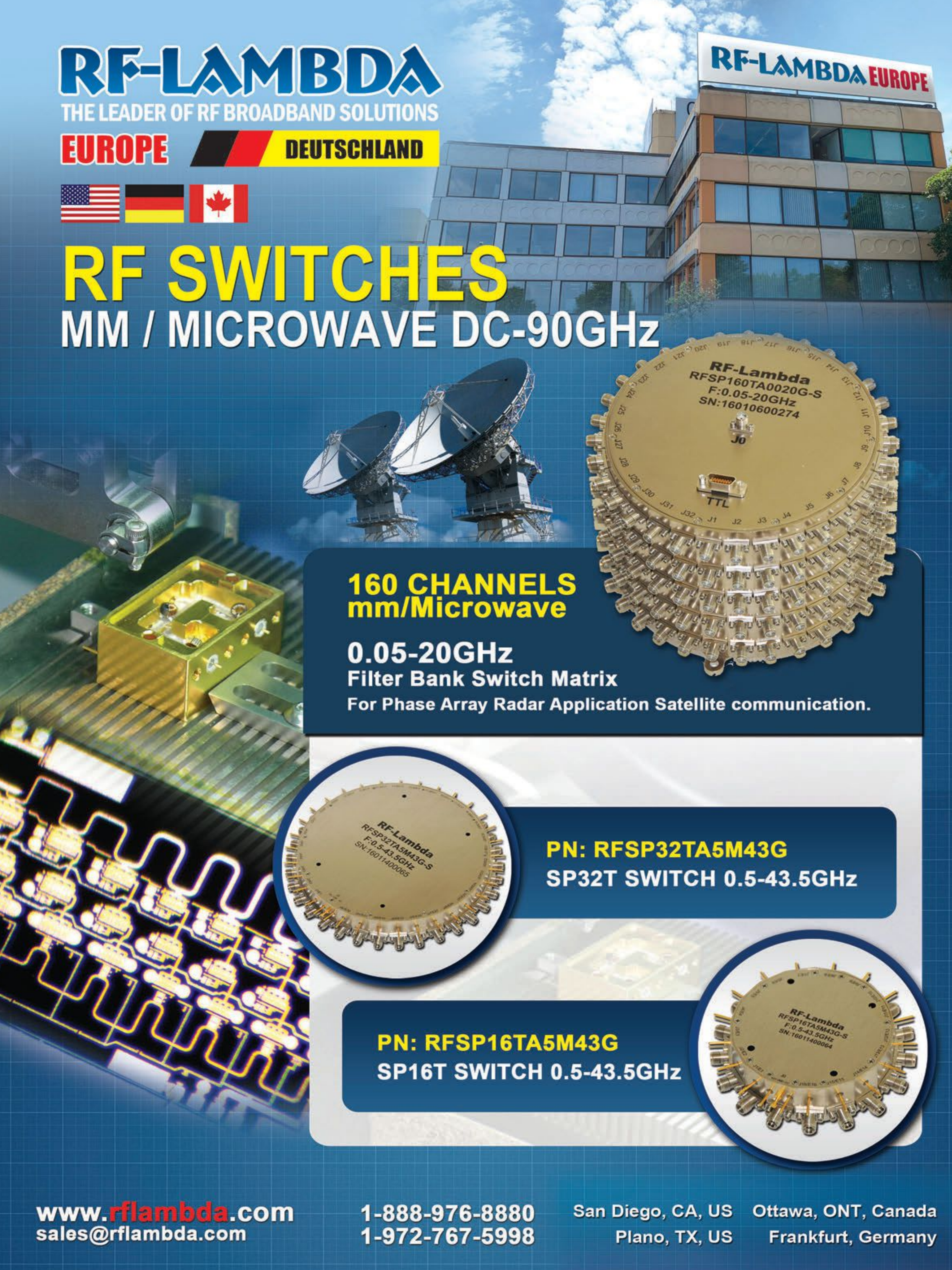

RF-LAMBDA
THE LEADER OF RF BROADBAND SOLUTIONS
EUROPE
DEUTSCHLAND
RF-LAMBDA EUROPE
RF SWITCHES
MM / MICROWAVE DC-90GHz
160 CHANNELS
mm/Microwave
0.05-20GHz
Filter Bank Switch Matrix
For Phase Array Radar Application Satellite communication.
PN: RFSP32TA5M43G
SP32T SWITCH 0.5-43.5GHz
PN: RFSP16TA5M43G
SP16T SWITCH 0.5-43.5GHz
www.rflambda.com
sales@rflambda.com
1-888-976-8880
1-972-767-5998
San Diego, CA, US
Plano, TX, US
Ottawa, ONT, Canada
Frankfurt, Germany

INVITED PAPER

Quartz Crystals in Vibratory Environments

Steve Fry
Greenray Industries, Mechanicsburg, Pa.

Quartz crystal oscillators are commonly used in many electronic systems to provide a very stable frequency source or reference. Crystal oscillators will provide a very clean and relatively noise-free signal when they are in a benign environment and are not experiencing any movement or acceleration forces. However, any change in position or periodic movement, such as vibration, will cause a change in the operating frequency of the oscillator. In many applications, these frequency changes are minimal and may go unnoticed, having no discernible effect on the device's performance. However, for systems that experience a high level of vibration, the output signal may be significantly degraded and may disrupt system operation.

The acceleration sensitivity of a crystal is also commonly referred to as "g-sensitivity." This is usually denoted by Γ. Acceleration forces cause a change in the resonant frequency of all quartz crystals to some degree. This is primarily due to the stress that is applied to the active area of the crystal through the mounting structure. This change is relatively minimal. A typical quartz crystal will measure < 2×10^{-9} per g (0.002 ppm/g or 2 ppb/g). This effect goes unnoticed in many applications but can become very significant in the presence of vibration. The acceleration sensitivity is linearly proportional to applied force up to acceleration levels around 50 g, depending on the crystal mounting structure. One other aspect to be considered is that Γ is a vector quantity and therefore, the frequency shift is highly dependent on the direction of the applied force.

SINUSOIDAL VIBRATIONS

Crystals in many applications experience some level of periodic vibration. The instantaneous frequency of the crystal will shift according to the direction and magnitude of the applied force. During a periodic vibration, the direction of the force is continuously reversed so that the frequency shift goes from positive to negative. This essentially applies frequency modulation (FM) to the RF signal. The magnitude of this frequency shift may, therefore, be determined by measuring the relative level of the vibration-induced sidebands and using FM modulation theory. The acceleration sensitivity or g-sensitivity of the oscillator is then found by using the known peak value of the vibration and normalizing the peak frequency shift to 1 g. ***Figure 1*** shows the instantaneous frequency response of a crystal oscillator to a sinusoidal vibration profile and the frequency shift from positive to negative is evident.

Figure 2 shows the spectrum of a 20 MHz crystal oscillator that is being vibrated at 90 Hz with a 10 g peak magnitude. Standard formulas show the conversion from the side-

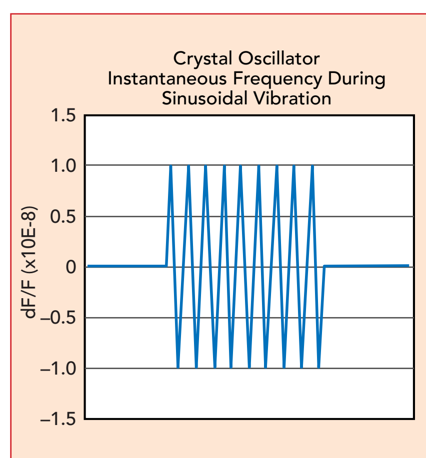

Fig. 1 **Crystal oscillator instantaneous frequency during sinusoidal vibration.**

band level to the acceleration sensitivity or g-sensitivity, defined earlier as Γ. For a single-frequency vibration with the conditions described, Γ = 1.56 ppb/g. The derivation of this value is shown in ***Equation 1***.

$$\vec{\Gamma} = \left(\frac{2 f_v}{\vec{a} \cdot f_{nom}}\right) \cdot 10^{\frac{dBc}{20}} \qquad (1)$$

RANDOM VIBRATION

In most real-world applications, however, the vibration experienced is not a simple periodic force. Systems that operate on mobile platforms will experience random vibrational energy that is spread across the spectrum from less than 10 Hz to 10 kHz or higher. Instead of being defined by a discrete peak vibration level, the random vibration energy is spread over a specific bandwidth and is described by its power spectral density (PSD). The quantity is measured in g^2/Hz, like a noise profile.

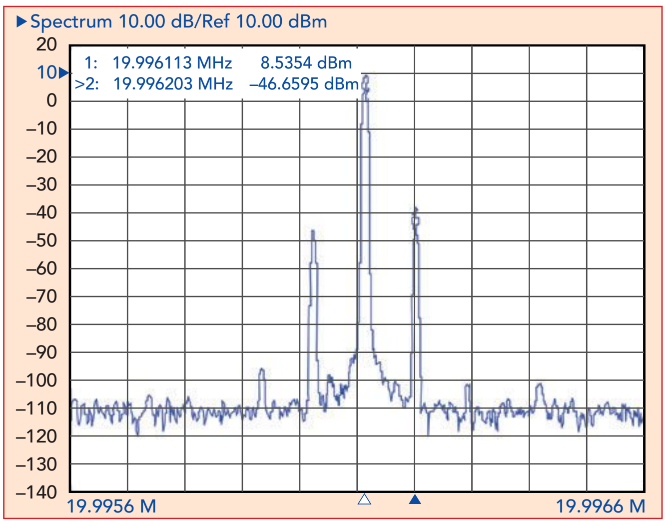

Fig. 2 Sidebands generated in 20 MHz crystal oscillator.

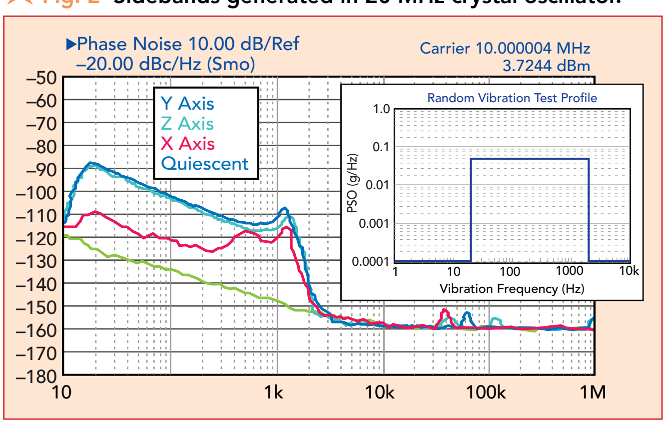

Fig. 3 Phase noise versus frequency for 10 MHz SC-cut OCXO.

Each platform or vehicle will have a unique random vibration signature that will be used during validation and qualification testing. However, it is helpful to characterize oscillators using a flat, random profile over a specific bandwidth and observing the oscillator phase noise response. This can highlight mechanically resonant features in the assembly that may need to be addressed. It is possible to calculate the g-sensitivity from a random profile as well. But instead of using the peak value of vibration, the PSD is used.

Using the random profile approach, the formula in ***Equation 2*** shows the calculation for phase noise using the PSD level at a specific offset or vibration frequency.

Figure 3 shows the phase noise of a very stable 10 MHz ovenized oscillator with an SC-cut crystal during random vibration. This illustrates that even though an oscillator may have a quiet noise profile when at rest, the phase noise is significantly degraded by more than 30 dB with a vibration level of only 0.05 g^2/Hz. Figure 3 shows the results of the phase noise calculations from Equation 1, given the PSD level at a specific offset or vibration frequency when Γ = 0.07 ppb/g. It also points out the vector nature of the quartz, with different results depending on the direction of the applied force.

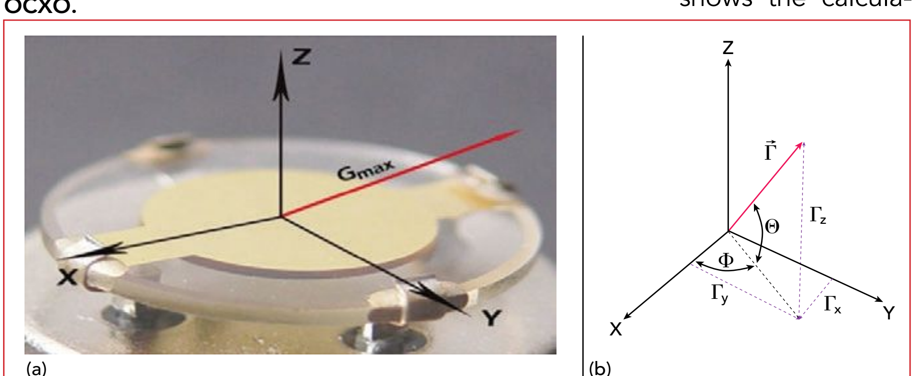

Fig. 4 (a) Quartz crystal oscillator oriented on a coordinate system. (b) Coordinate system and relationships to determine maximum g-sensitivity vector.

VECTOR PROPERTIES

To get a picture of the complete set of 3D characteristics of the crystal, it is necessary to measure the acceleration sensitivity in three orthogonal axes. ***Figure 4a*** shows a quartz crystal oscillator with a set of axes overlaid on the device. ***Figure 4b*** depicts the coordinate system that defines the magnitude and direction of the Γ vector.

The maximum g-sensitivity vector, Γ_{max}, usually does not align precisely with one of the measured axes relative to the crystal package. However, by using trigonometric identities, the magnitude and direction of the Γ_{max} vector can be determined. ***Equations 3*** through ***5*** show the relationships to derive the quantities necessary to determine the maximum g-sensitivity vector in Figure 4b.

$$\pounds(f_v) = 20 \log\left(\frac{\vec{\Gamma} \cdot f_{nom} \cdot \sqrt{2 \cdot PSD}}{2 f_v}\right) \qquad (2)$$

$$|\vec{\Gamma}| = \sqrt{\Gamma_x^2 + \Gamma_y^2 + \Gamma_z^2} \qquad (3)$$

$$\Phi = \cos^{-1}\left(\frac{\Gamma_x}{\sqrt{\Gamma_x^2 + \Gamma_y^2}}\right) \qquad (4)$$

$$\Theta = \sin^{-1}\left(\frac{\Gamma_z}{\vec{\Gamma}}\right) \qquad (5)$$

The effect of changing the direction of the acceleration force is shown in ***Figure 5***. The maximum frequency shift occurs when the acceleration force is in the same direction as the Γ_{max} vector. As illustrated, it decreases as the cosine of α as the direction changes.

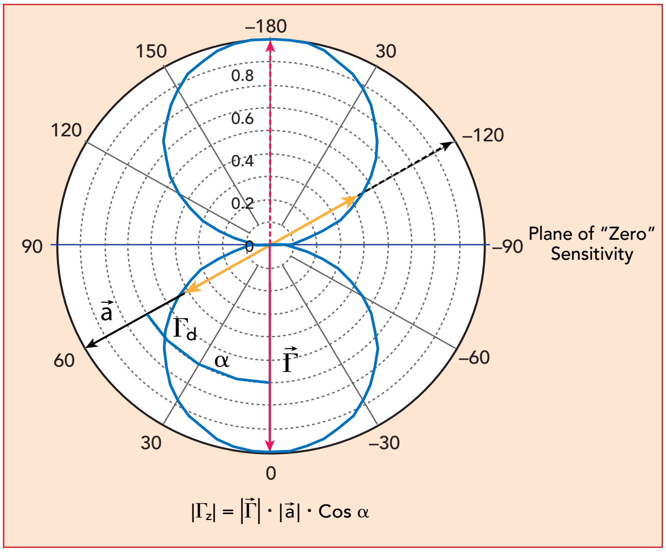

Fig. 5 Acceleration sensitivity versus direction of applied force.

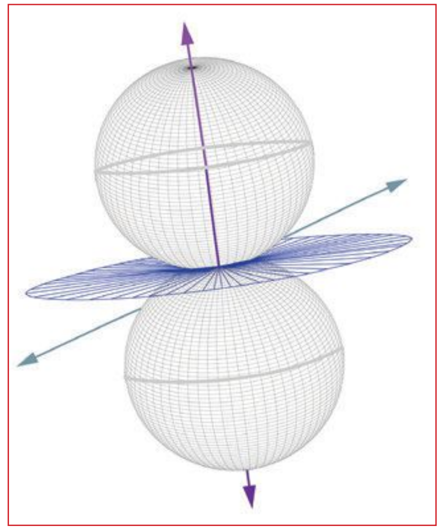

Fig. 6 3D representation of acceleration sensitivity versus direction of applied force.

Figure 5 illustrates the effect in two dimensions, while ***Figure 6*** shows how this also applies in three dimensions. Another potentially useful aspect that can be seen here is the plane of "zero sensitivity" that exists when the acceleration forces are applied in the plane that is perpendicular to the Γ_{max} vector. If a crystal-based device in a particular system experiences vibration forces that are primarily from one direction, orienting the oscillator so that the sensitive axis is perpendicular to the force can result in a substantial reduction of the vibration-induced effects.

MITIGATION METHODS

There are also methods of compensating for the effects of vibration on a crystal oscillator. Active cancellation methods can be used that employ an accelerometer to sense the level of vibration being experienced by the crystal. This signal is then fed back to the oscillator circuit after being scaled and phase shifted properly to cancel the instantaneous frequency shift caused by the vibration.

If the magnitude and direction of the Γ vector are known, it is possible to substantially reduce the effect by using two crystals, which are positioned so that the vectors are anti-parallel, pointing in opposite directions. The two crystals are then connected electrically in ei-

PPI®

HIGH QUALITY
RF/MICROWAVE PASSIVE COMPONENTS

HIGH-Q/ LOW ESR CAPACITORS
TRIMMER CAPACITORS
BROADBAND CAPACITORS
THIN FILM COMPONENTS
RESISTOR PRODUCTS
SINGLE LAYER CAPACITORS
HIGH POWER CUSTOM ASSEMBLIES

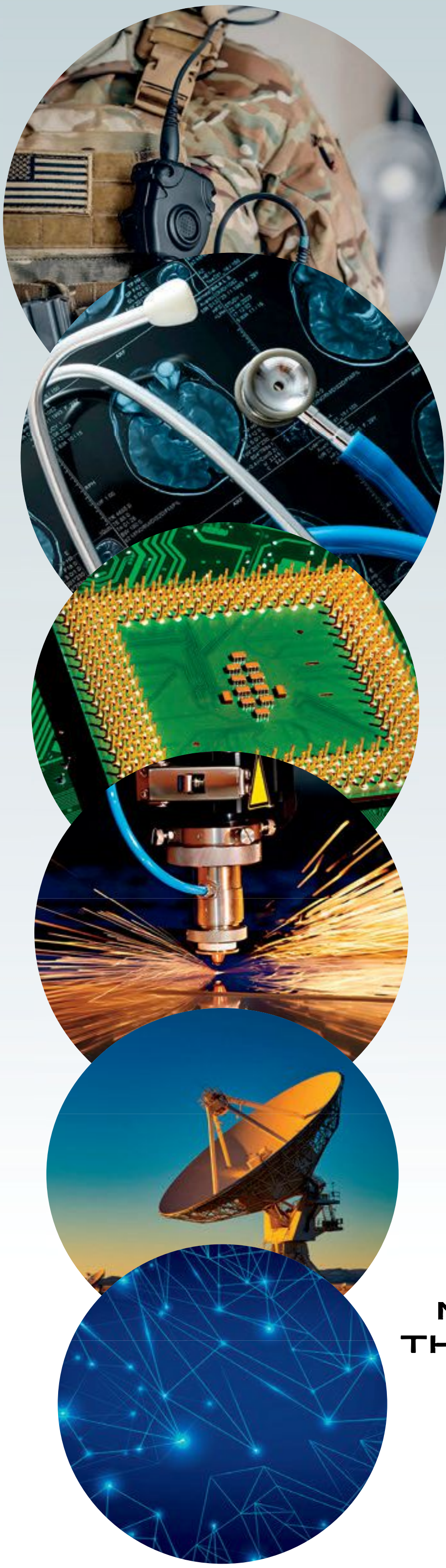

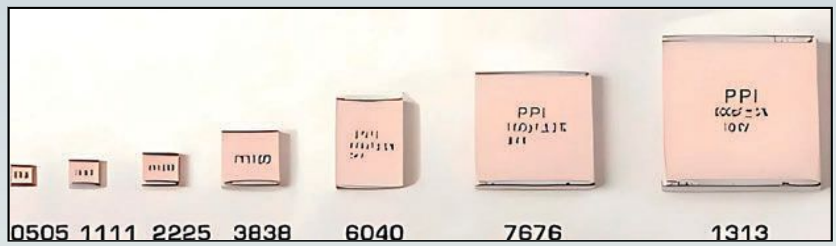

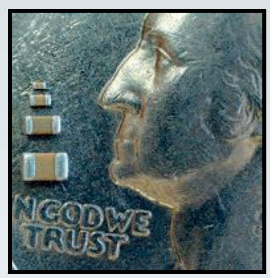

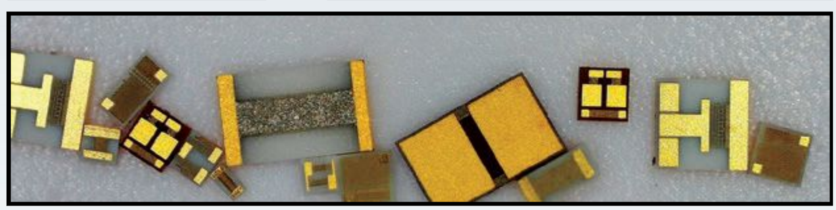

SPECIALIZING IN MAGNETIC & NON-MAGNETIC QUALITY COMPONENTS FOR THE MEDICAL, SEMICONDUCTOR, MILITARY, BROADCAST, INDUSTRIAL LASER, AND TELECOMMUNICATIONS INDUSTRIES

www.passiveplus.com

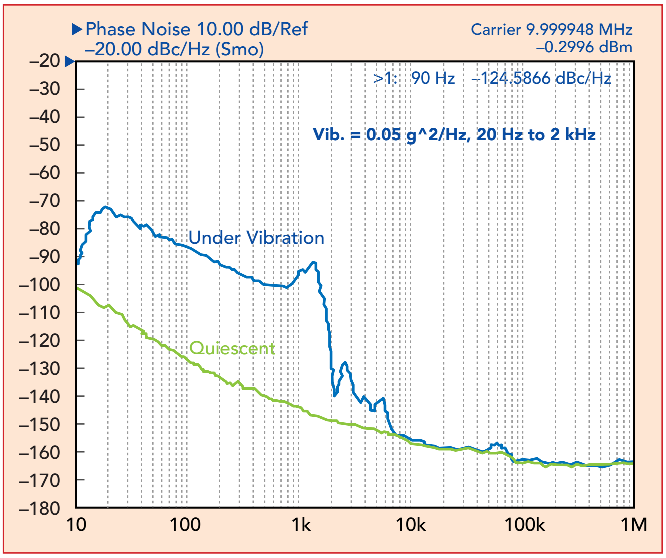

Fig. 7 **Conventional TCXO phase noise response.**

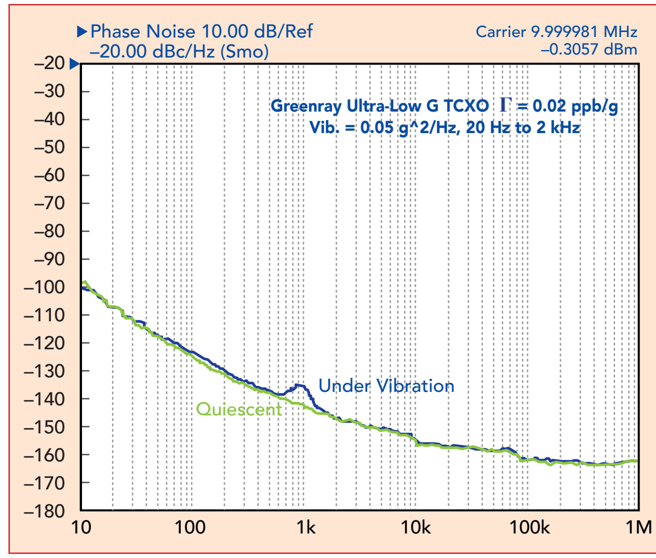

Fig. 8 **Vibration-compensated TCXO phase noise response.**

ther a parallel or series configuration and connected to an oscillator circuit. This type of passive compensation can reduce the effects of vibration on an oscillator substantially. ***Figure 7*** shows the phase noise response of a conventional TCXO that achieves Γ = 2.5 ppg/g. ***Figure 8*** shows the phase noise response of a vibration-compensated TCXO under the same vibration profile as the conventional TCXO in Figure 7. For this case, Γ = 0.02 ppb/g and the graph in Figure 8 shows a phase noise improvement of approximately 40 dB that can be achieved under random vibration conditions using this technique. This passive compensation method is being employed in miniature TCXOs to reduce the effective g-sensitivity to less than 8×10^{-11} per g.

VIBRATION ISOLATION

Another method for reducing the effects of vibration on a system is to use mechanical vibration isola-

DUAL or SINGLE LOOP
SYNTHESIZER & PLO MODULES

Features:

- Proprietary digital Integer and Fractional PLL technology
- Lowest digital noise floor available -237 dBc/Hz figure of merit
- Output frequencies from 100 MHz locked crystal to 30 GHz
- Available with reference clean up dual loop, or single loop for very low noise reference
- Parallel fixed band stepping or SPI interface synthesized up to octave bandwidths
- Reference input range 1 MHz to 1.5 GHz
- Dual RF output or reference sample output available
- +12 dBm standard output power +16 dBm available
- Standard module size 2.25 X 2.25 X 0.5 Inches (LxWxH)
- Standard operating temperature -10 to 60 °C, -40 to +85 °C available

Up to 30 GHz*

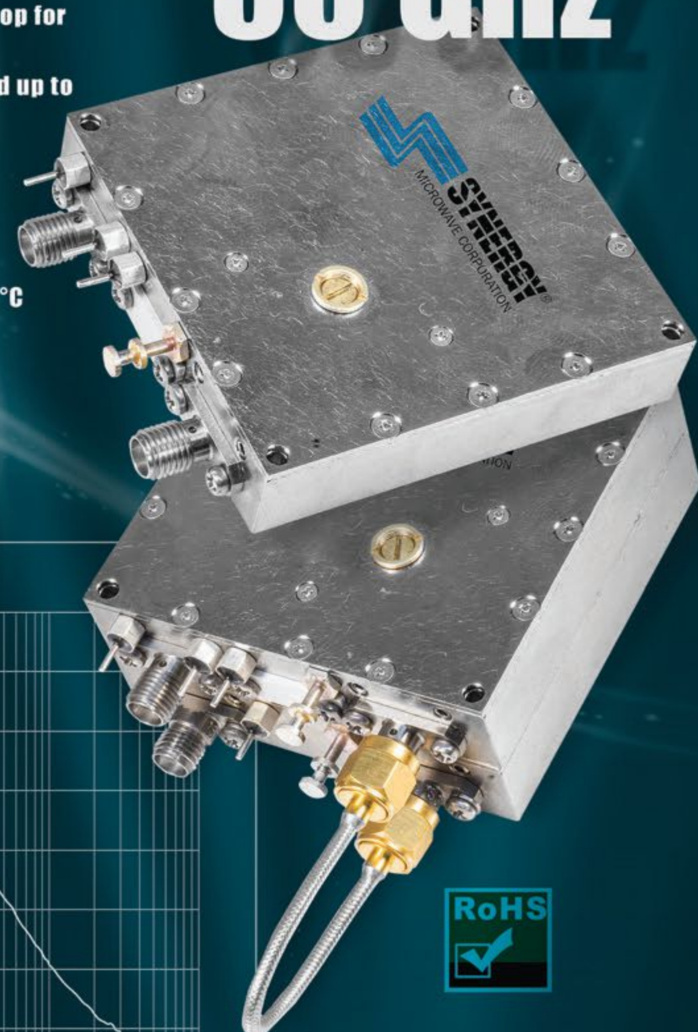

Applications:

- SATCOM, RADAR, MICROWAVE RADIO

* *16 - 30 GHz with added x2 module < 1" in height.*

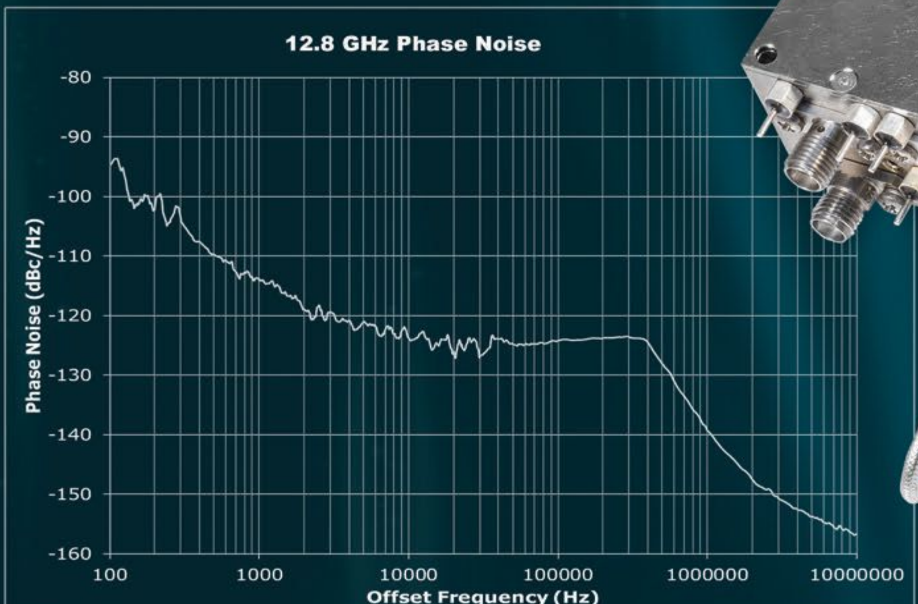

RoHS

Talk To Us About Your Custom Requirements.

SYNERGY®
MICROWAVE CORPORATION

Phone: (973) 881-8800 | Fax: (973) 881-8361
E-mail: sales@synergymwave.com
Web: WWW.SYNERGYMWAVE.COM
Mail: 201 McLean Boulevard, Paterson, NJ 07504

tion. This can be very effective at reducing the high frequency vibrational energy experienced by the component. However, the isolation is only achieved above the natural frequency of the isolator. ***Figure 9*** shows how the effectiveness of the isolation changes relative to the natural frequency of the isolator, placing constraints on the size and weight of the components. ***Figure 10*** shows examples of typical miniature vibration isolators. If isolation at low frequencies is needed, it is usually not practical to use mechanical isolators for components in small assemblies.

CONCLUSION

Quartz crystal oscillators are increasingly important, fundamental building blocks in many electronic systems. Properly designed, they will provide clean, relatively noise-free frequency references in a benign environment without movement or acceleration. However, any change in position or periodic movement will shift the operating frequency of the oscillator. This article has discussed the nature and magnitude of the vibratory environment that a system may encounter. It has also provided some insights into the effects that this vibration will have on the oscillator signal, along with how those effects can be predicted and possibly mitigated to varying degrees.■

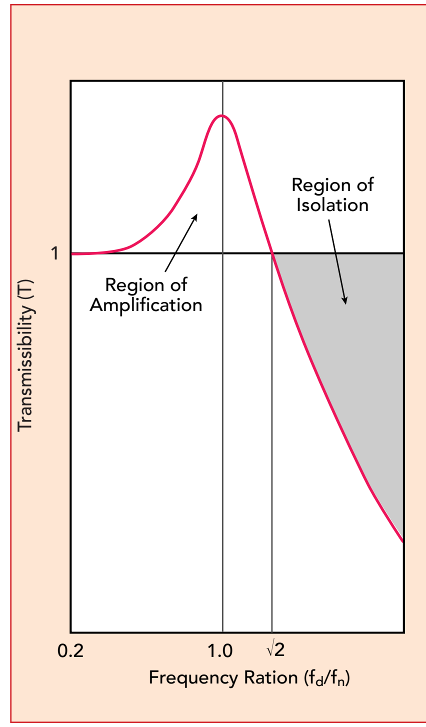

Fig. 9 **Transmissibility versus frequency.**

Fig. 10 **Typical vibration isolators.**

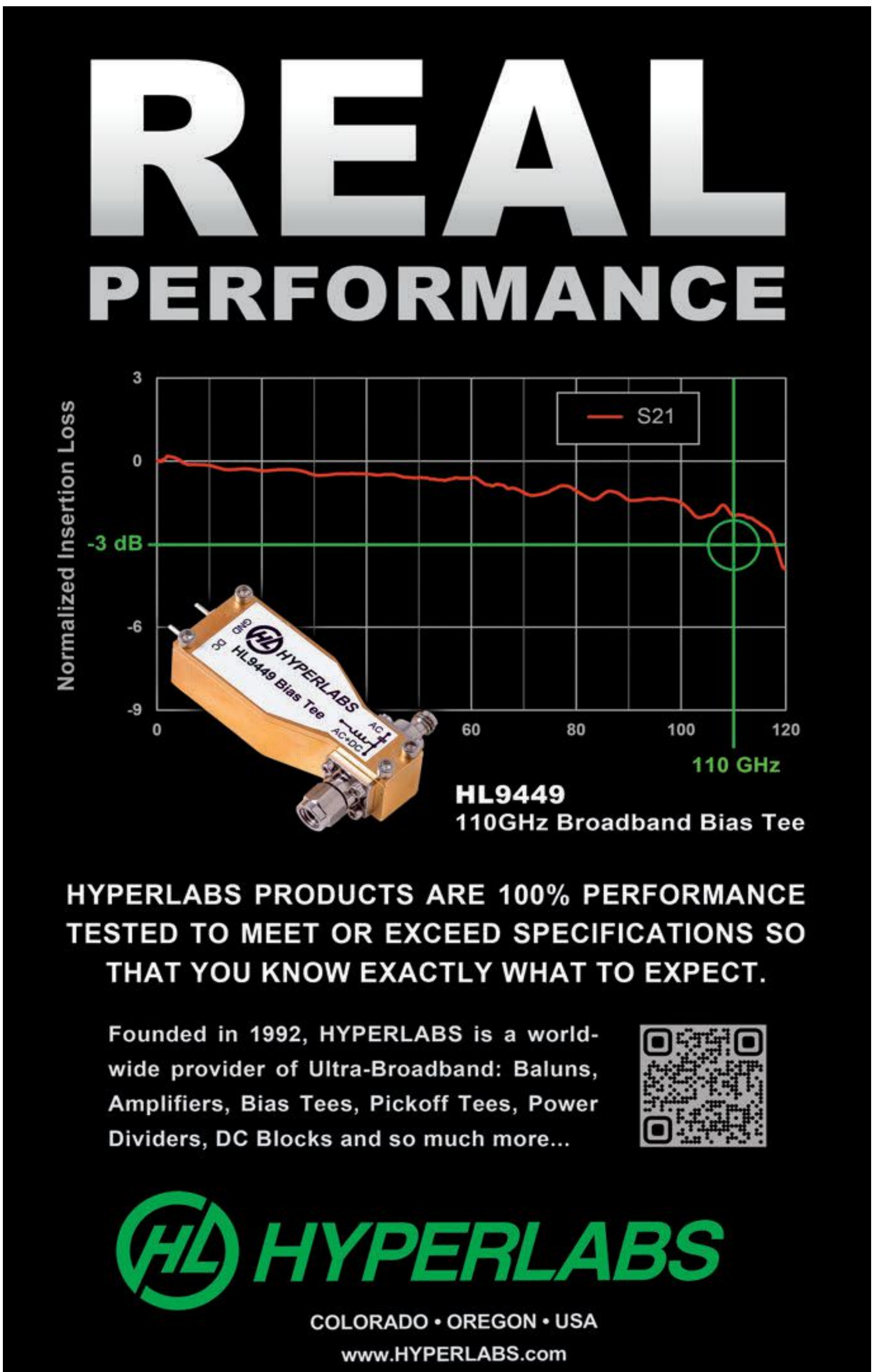

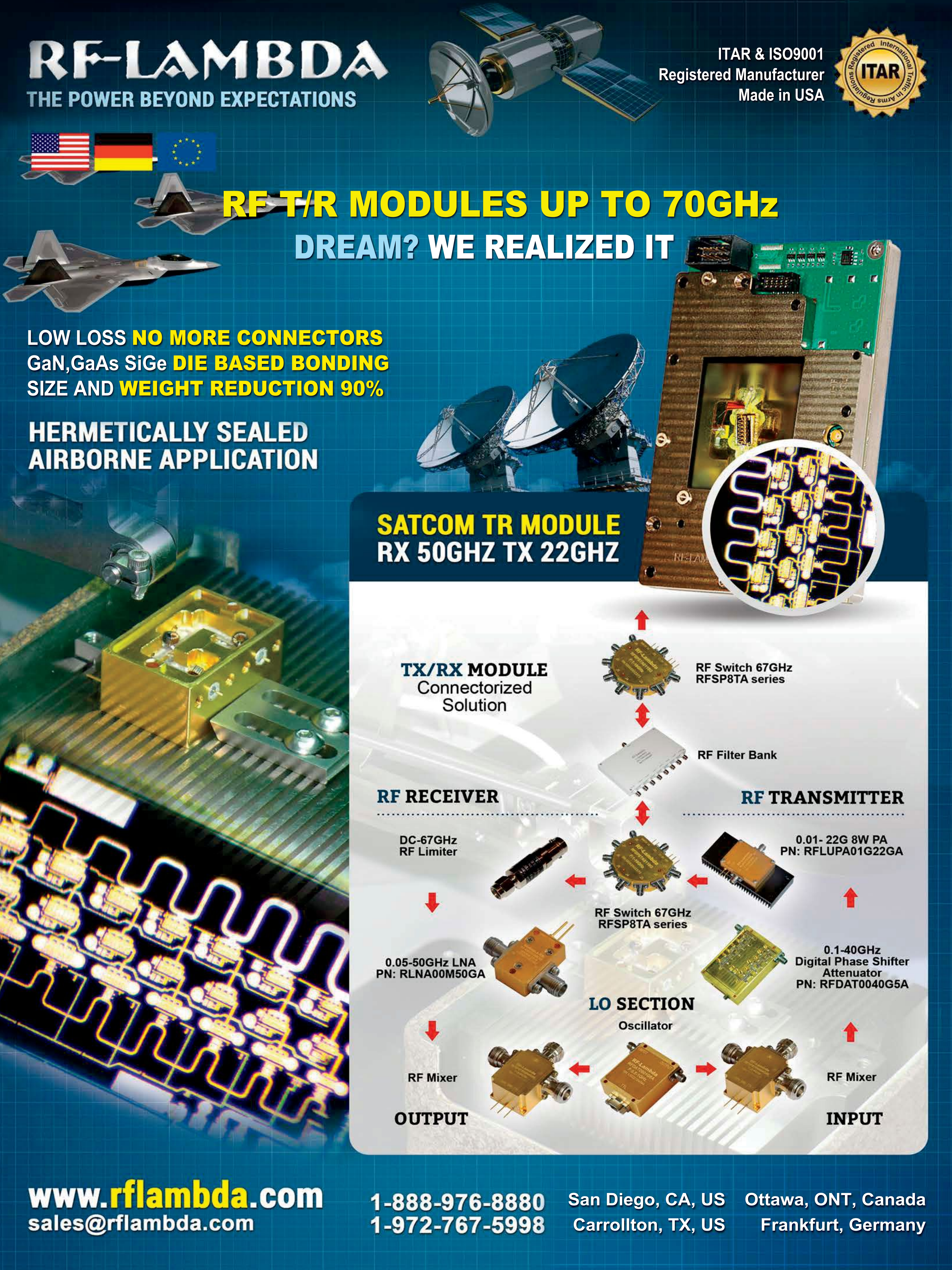

RF-LAMBDA
THE POWER BEYOND EXPECTATIONS
ITAR & ISO9001
Registered Manufacturer
Made in USA
ITAR
RF T/R MODULES UP TO 70GHz
DREAM? WE REALIZED IT
LOW LOSS NO MORE CONNECTORS
GaN,GaAs SiGe DIE BASED BONDING
SIZE AND WEIGHT REDUCTION 90%
HERMETICALLY SEALED
AIRBORNE APPLICATION
SATCOM TR MODULE
RX 50GHZ TX 22GHZ
TX/RX MODULE
Connectorized
Solution
RF Switch 67GHz
RFSP8TA series
RF Filter Bank
RF RECEIVER
RF TRANSMITTER
DC-67GHz
RF Limiter
0.01- 22G 8W PA
PN: RFLUPA01G22GA
RF Switch 67GHz
RFSP8TA series
0.05-50GHz LNA
PN: RLNA00M50GA
0.1-40GHz
Digital Phase Shifter
Attenuator
PN: RFDAT0040G5A
LO SECTION
Oscillator
RF Mixer
RF Mixer
OUTPUT
INPUT
www.rflambda.com
sales@rflambda.com
1-888-976-8880
1-972-767-5998
San Diego, CA, US
Carrollton, TX, US
Ottawa, ONT, Canada
Frankfurt, Germany

Optimizing IoT Device Performance with Front-End Modules

pSemi Corporation
San Diego, Calif.

The proliferation of IoT applications throughout consumer, industrial and commercial markets has pushed the boundaries of wireless communication technology. The ability to maintain stable and efficient connectivity across various environments is paramount. As IoT devices become more complex, designers face a continuous challenge in selecting the best front-end modules (FEMs) that balance power efficiency, RF performance, cost and integration density.

Traditionally, FEMs have relied on specialized IC technologies, such as silicon germanium (SiGe) and gallium arsenide (GaAs), to enhance power amplifier (PA) efficiency. However, as cost pressures increase, the industry is shifting toward highly integrated solutions leveraging RF silicon-on-insulator (RF-SOI) and CMOS technologies. pSemi's propriety RF-SOI technology is disrupting the traditional FEM market through innovative techniques that enable superior PA and receiver sensitivity performance. Additionally, pSemi's RF-SOI technology enables monolithic IoT and Wi-Fi FEMs that provide noise figure and size advantages.

THE EVOLUTION OF IOT DEVICE AMPLIFIER TECHNOLOGIES

Wireless performance in IoT applications depends on the selection of the right FEM technology that balances RF performance, power efficiency, package size and cost. One of the most important choices a FEM designer can make is the amplifier technology. This choice directly influences the link robustness and power consumption of the device. Traditional PA technologies include SiGe, GaAs and bulk CMOS, but pSemi's RF-SOI technology is proving to be an attractive alternative to these traditional solutions.

Standard RF-SOI technology is not typically optimized to support the RF requirements needed for high performance IoT/Wi-Fi FEMs. However, pSemi has optimized its patented UltraCMOS® technology to enable performance that rivals SiGe and GaAs FEMs. UltraCMOS RF-SOI provides an alternative solution by integrating high performance RF components onto a CMOS-based platform. Traditional IoT FEM solutions use a multi-chip solution that combines a SiGe or GaAs IC for power amplification with an RF-SOI IC for

MiCable

New

2~6GHz 100W

GaN Power Amplifier

$21,599 (1-4 pcs)

In Stock

- **High Power** Psat 49/50 dBm
  P1dB 46/47 dBm (Min/Typ.)
- **High OIP3** 50/53 dBm (Min/Typ.)
- **Low Harmonic (2nd/3rd)** -20/-25 dBc (Typ.)
- **Low Spurious** -70 dBc (Typ.)
- **Low VSWR** 1.5:1 (Typ.)
- **High Efficiency** 20% (Typ.)

MPAR-020060S50 is a 2~6GHz 100W GaN amplifier with state-of-the-art GaN design technology. It has higher saturation output power while keeping higher P1dB and better linearity.

The built-in control, monitoring and protection functions are offered. It is designed for high power CW & pulse system applications, such as 5G, LTE, WIFI and other related system module & EMC test.

★ Custom designs are available

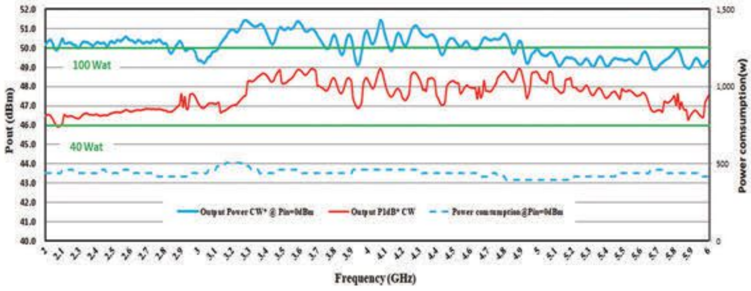

Pout@ Pin=0dBm & P1dB (CW, Load VSWR≤1.2, 25℃)

More Information-
Scan the QR Code

MIcable Inc.

www.micable.cn sales@micable.cn +86-591-87382856

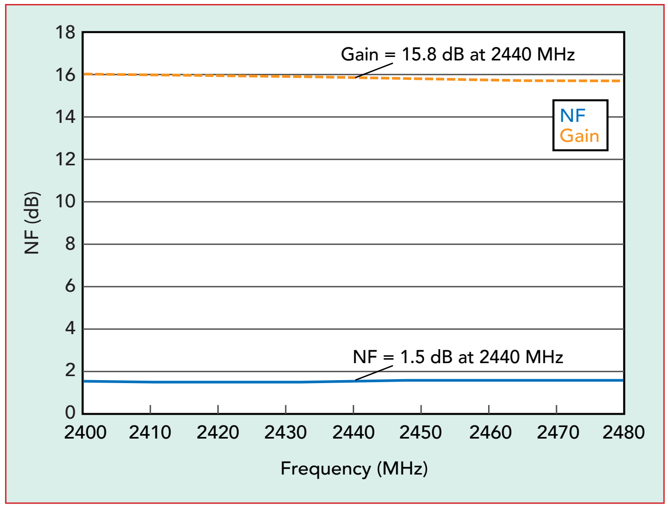

Fig. 1 **PE562212 LNA NF and gain.**

low loss switching and improved receiver sensitivity. pSemi's RF-SOI PA performance exceeds output power requirements while maintaining a competitive power-added efficiency (PAE), boasting best-in-class noise figure performance and meeting customer needs with a cost-effective CMOS-based solution. Using pSemi's RF-SOI technology, the IoT/Wi-Fi FEM PA, LNA and switch are integrated, eliminating the need for multiple chips with different technologies. This integration capability enables pSemi to supply high performance IoT FEMs that are also the smallest on the market. ***Figure 1*** shows the gain and noise figure for the PE562212 FEM over the 2400 to 2480 MHz frequency band.

Incumbent technologies provide solutions that have historically supported the market and are well entrenched, but they have limitations. SiGe-based PAs offer a moderate balance between performance and cost. These amplifiers provide relatively good PAE and they are widely used in low- to mid-tier IoT applications. However, their receive performance is suboptimal, impacting wireless link range and robustness. Additionally, SiGe amplifiers suffer from lower breakdown voltages, which can limit power-handling capabilities.

GaAs PAs have long been the industry standard for high performance RF applications due to their superior linearity and efficiency. GaAs technology offers a high breakdown voltage for higher power handling, better linearity and enhanced capability in high frequency applications. Despite these advantages, GaAs is costly and it presents integration challenges that limit the adoption of this technology in cost-sensitive IoT applications.

Bulk CMOS PAs may be integrated into the system-on-chip (SoC) transceiver of the IoT device. However, these amplifiers do not provide high performance RF capability and are generally optimized for power efficiency only. The output power of these devices is often severely limited by harmonic generation that reaches the limits set by regulatory requirements and certification.

INNOVATIONS IN FEM DESIGN: PSEMI'S ULTRACMOS® SOLUTION

pSemi has pioneered the development of RF-SOI-based FEMs to address the limitations of traditional amplifier technologies. The PE562212, built on pSemi's proprietary UltraCMOS process, represents a significant advancement in IoT FEM product offerings. The PE562212 features monolithic integration incorporating a +21 dBm RF PA, an LNA with a 1.6 dB noise figure, low loss switches, a bypass path with 0.6 dB loss and harmonic/distortion filtering. It is the industry's first multiprotocol FEM supporting Bluetooth®, Bluetooth Low Energy, Zigbee®, Thread and Wi-Fi, making it highly versatile. Transmit digital gain control ensures worldwide operability and application-specific output power requirements through 1 dB gain steps. With a form factor of 1.8 mm x 1.8 mm in a land grid array package, the PE562212 is particularly well-suited for space-constrained IoT applications. Furthermore, its superior link robustness ensures a reliable connection, minimizing excessive packet drops and improving power savings. ***Figure 2***

EUROPE'S PREMIER MICROWAVE, RF, WIRELESS AND RADAR EVENT

EUROPEAN MICROWAVE WEEK
JAARBEURS UTRECHT
THE NETHERLANDS
21-26 SEPTEMBER 2025
www.eumw.eu
WAVES OF INNOVATION

THE EUROPEAN MICROWAVE EXHIBITION

JAARBEURS UTRECHT, THE NETHERLANDS
23 - 25 SEPTEMBER 2025

- 10,000 sqm of gross exhibition space
- Around 5,000 attendees
- 1,700 - 2,000 Conference delegates
- In excess of 300 international exhibitors (including Asia and US as well as Europe)

INTERESTED IN EXHIBITING?

Please contact one of our International Sales Team:

Richard Vaughan,
International Sales Manager
rvaughan@horizonhouse.co.uk

Gaston Traboulsi, France
gtraboulsi@horizonhouse.com

Mike Hallman, USA
mhallman@horizonhouse.com

Victoria and Norbert Hufmann, Germany, Austria & Switzerland
victoria@hufmann.info
norbert@hufmann.info

Katsuhiro Ishii, Japan
amskatsu@dream.com

Jaeho Chinn, Korea
inter11@jesmedia.com

CALL +44(0) 20 7596 8742 OR VISIT WWW.EUMW.EU

CERNEX , Inc.
& CernexWave

RF,MICROWAVE & MILLIMETER-WAVE COMPONENTS AND SUB-SYSTEMS UP TO 500GHz
5G Ready

- AMPLIFIERS UP TO 160GHz
- FREQUENCY MULTIPLIERS/ DIVIDERS UP TO 160GHz
- ANTENNAS UP TO 500GHz

- COUPLERS UP TO 220GHz
- ISOLATORS/CIRCULATORS UP TO 160GHz
- FILTERS/DIPLEXERS/SOURCES UP TO 160GHz
- SWITCHES UP TO 160GHz
- PHASE SHIFTERS UP TO 160GHz
- TRANSITIONS/ADAPTERS UP TO 500GHz
- WAVEGUIDE PRODUCTS UP TO 1THz
- TERMINATIONS/LOADS UP TO 325GHz
- MIXERS UP TO 500GHz

- ATTENUATORS UP TO 160GHz
- POWER COMBINERS/DIVIDERS EQUALIZERS
- CABLE ASSEMBLIES/ CONNECTORS UP TO 110GHz
- SUB-SYSTEMS UP TO 110GHz
- DETECTORS UP TO 500GHz
- UMITERS UP TO 160GHz
- BIAS TEE UP TO 110GHz

Add:1710 Zanker Road Suite 103,San Jose, CA 95112
Tel: (408) 541-9226 Fax:(408) 541-9229
www.cernex.com www.cernexwave.com
E mail: sales@cernex .com

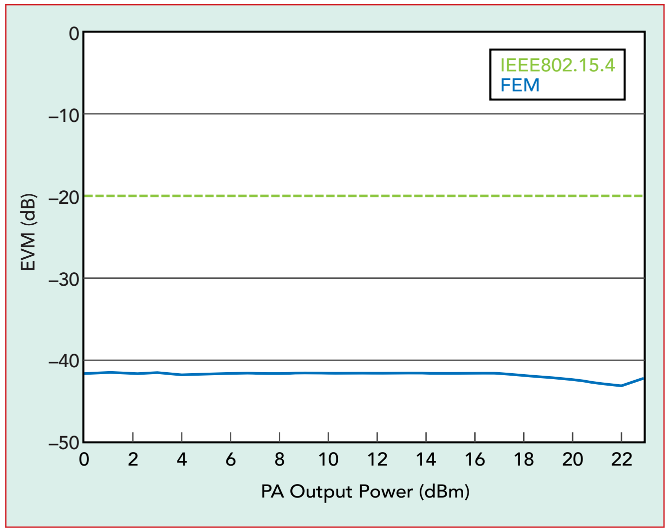

Fig. 2 **PE562212 EVM versus output power.**

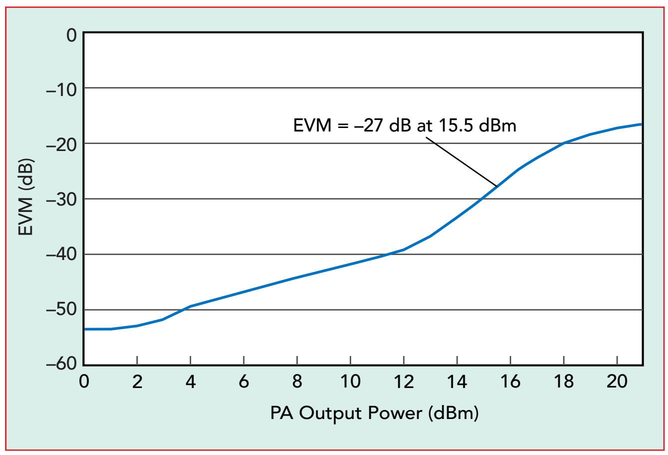

Fig. 3 **PE562212 EVM versus power.**

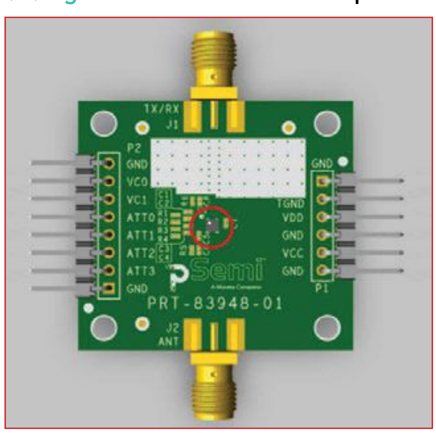

Fig. 4 **PE562212 mounted on EVK.**

shows the EVM performance of the PE562212 at different output power levels and the 802.15.4 specification for a Zigbee Thread application at 2442 MHz.

Unique to the PE562212 is its Wi-Fi capability, enabling low throughput data transfer rates of up to 54 Mbps. Low-power IoT devices benefit from extended operational life and the firmware or software can be updated to add new device features or fix bugs. The PE562212 has been carefully optimized to support protocol versatility with minimal power consumption. ***Figure 3*** shows the EVM performance of the PE562212 over a range of output powers. The measurements in Figure 3 are in accordance with IEEE 802.11n MCS7 Wi-Fi waveform requirements at 2442 MHz.

Figure 4 shows the PE562212 FEM on an evaluation kit (EVK). By leveraging their RF-SOI technology, pSemi has achieved a breakthrough in cost-performance optimization. This makes the PE562212 ideal for next-generation IoT applications.

PROVEN RF-SOI LEADERSHIP

pSemi's proprietary RF-SOI technology is disrupting the existing FEM market. With over 1.5 billion FEM units shipped, pSemi has established itself as a serious contender in the IoT/Wi-Fi FEM market. For cost-effective next-generation FEM applications that require high performance, small form factor and high reliability, consider the pSemi solutions.

pSemi Corporation
San Diego, Calif.
psemi.com

For more information: psemi.com/products/front-end-modules/2-4-ghz-iot-fems/pe562212/

2025 IEEE International Conference on

Artificial Intelligence & Data Analytics

JUNE 24, 2025

The Joyce Cummings Center
Tufts University Medford Massachusetts

Explore new research & break-throughs in AI; gain valuable insights; network; and get inspired by the brightest minds working in this multi-faceted field!

Space is limited! Sponsorships available!

ICAD 2025

KEYNOTE SPEAKERS

Matthias Scheutz

Professor, Tufts University School of Engineering

Sadid Hasan

AI Lead at Microsoft

Mark Maybury

VP Commercialization, Technology & Strategic Innovation at Lockheed Martin

REGISTER HERE:

IEEE-ICAD.ORG

Vibration-Isolated OCXO Module

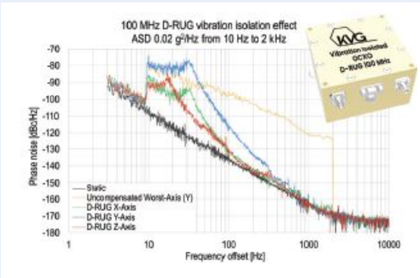

KVG is a German company with a 75+ year history focusing on the development and production of high-end frequency control products. Increasing demand for high performance crystal oscillators in mobile applications where vibrations impact performance, led to the development of our vibration-isolated OCXO D-RUG module. It is designed to avoid the phase noise deterioration of crystal oscillators in these applications.

This module uses an ultra-low g-sensitivity OCXO encapsulated in a specially developed mechanical vibration damping system. The 80 x 80 x 50 mm package weighs less than 600 g. The damping system resonant frequency is below 40 Hz. It has excellent dynamic phase noise performance at a frequency offset of 100 Hz and beyond. The effective g-sensitivity can be improved by a factor of 10 at 100 Hz and by a factor of 100 at 1 kHz. It guarantees reliable performance under harsh temperature, altitude, vibration and shock conditions, specified by MIL-STD-810G Change Notice 1 and RTCA DO-160G. This module is ideally suited for civil and military airborne applications.

It exhibits outstanding dynamic phase noise under harsh vibration conditions. With random vibration from 10 Hz to 2 kHz and acceleration spectral density of 0.02 g^2/Hz, the D-RUG 100 MHz module improves dynamic phase noise at frequency offset of 100 Hz and beyond significantly, compared to an uncompensated OCXO. The dynamic phase noise from 1 kHz is as good as the static phase noise.

Key features:

- Ruggedized package 80 x 80 x 50 mm
- Frequency options 80, 100, 120, 240 MHz
- Dual-output option
- Resonance frequency < 40 Hz
- Significant improvement of effective g-sensitivity from frequency offset of 100 Hz
- Outstanding dynamic phase noise performance
- Customized dynamic phase noise test
- Customized military-grade qualification and screening tests.

KVG Quartz Crystal Technology GmbH
Neckarbischofsheim, Germany
kvg-gmbh.de

IMPI

59TH ANNUAL MICROWAVE POWER SYMPOSIUM

Hosted by the International Microwave Power Institute

June 24-26, 2025

Westin Edmonton Hotel
Edmonton, Alberta, Canada

Join the **International Microwave Power Institute (IMPI)** as they host the highly anticipated **IMPI 59 Symposium**! This premier event is set to gather **researchers, technologists, engineers, and industry leaders from around the world** to explore the latest technological advancements in **microwave and radio frequency power applications**.

Key topic areas:

- Solid State Applications
- Hydrogen Production
- Modeling and Simulation
- Food Processing Technologies
- Microwave and Plasma Chemistry
- RF Applications
- IEEE Microwave Theory and Technology Society (MTT-S) Special Session
- Lunar Construction Innovations
- Advanced Materials
- Industrial Processing & Mining Solutions

Discover cutting-edge research, network with global professionals, and shape the future of microwave power technologies!

Scan to register or visit impi.org/events/symposium/ for more information.

Software Optimizes Antenna Design and Integration

Antenna integration requires an understanding of the complex interplay of factors that include antenna selection, placement on the PCB and spacing and orientation with other antennas. Taoglas recently introduced AntennaXpert, a suite of user-friendly digital tools to streamline, simplify and customize antenna design and integration. Available on the Taoglas website, the toolset includes the Taoglas Antenna Integrator, Antenna Builder and Cable Builder.

The newest tool in the suite, the Taoglas Antenna Integrator, enables users to preview their embedded antennas, including the performance of multiple or MIMO antenna systems in the concept phase of a project. This accelerates time to market and helps to avoid potential issues with component placement. The Antenna Integrator empowers design engineers to do much of the groundwork and reduce design time. It helps users optimize RF performance, component placement and PCB size while simplifying mechanical integration and reducing development time. Users input a custom PCB size and then select and place multiple Taoglas antennas on the digital board. Once configured, the design is submitted to Taoglas and users receive a technical report that includes detailed antenna performance parameters, including return loss and efficiency, within 24 hours.

Antenna Builder empowers design engineers to configure cable lengths and connectors for external and embedded antenna applications. In the tool, users select their preferred antenna from Taoglas' portfolio of off-the-shelf antennas and customize the connector type and cable length to fit their requirements. Cable Builder allows users to customize RF cable assemblies precisely for their specifications. Users select the cable type, cable length and type of connectors on each side. Customized antennas and cable assemblies are built and shipped in as little as 24 hours from one of Taoglas' global facilities.

Taoglas
San Diego, Calif.
taoglas.com
For inquiries:
mediarelations@taoglas.com

Abstract Submission Deadline: **May 5, 2025**
Submission Website Opens: **March 2025**

For details and a complete list of paper topics visit
2025.amta.org

47th Annual Meeting and Symposium of the Antenna Measurement Techniques Association

Raytheon and the U.S. Army Electronic Proving Ground are proud to host the 47th Annual Meeting and Symposium of the Antenna Measurement Techniques Association (AMTA) in Tucson, Arizona, USA from November 2-7, 2025. Raytheon and the U.S. Army Electronic Proving Ground cordially invite you to attend and participate in this annual event.

To learn more about AMTA, visit **www.amta.org.**

Symposium Highlights

- High-quality technical papers presented on a continuous basis over four days – no parallel sessions
- Technical Tours, Social Events, and Daytime Companion Tours
- Exhibits showcasing the latest innovations in antenna, RCS, and 5G OTA/MIMO measurements
- Networking opportunities with industry experts
- In-depth Short Course as well as a practical Boot Camp will be offered

Hosted by Raytheon An RTX Business

Get Customized Phase-Locked Oscillators in 48 Hours

Z-COMM's new SFSLX product line is a novel phase-locked product platform providing RF and microwave engineers with accelerated product development. This first-of-its-kind program allows a quick and easy way for engineers to configure a phase-locked oscillator to specific frequency specifications. Through an easy online ordering system, the engineer selects any output frequency from 50 MHz through 22.5 GHz with resolution steps of 0.1 Hz and specifies the reference frequency input from 5 to 200 MHz. Within 24 to 48 hours, the custom phase-locked oscillator will be on the way, ready to be used. The SFSLX performance characteristics are shown in ***Table 1***.

The SFSLX series are housed in a surface-mount package measuring 0.6 x 0.6 x 0.20 in. (15.25 x 15.25 x 5 mm). They are available on tape and reel for production quantities. For ease of testing, the SFSLX-EVL companion evaluation board is available. The SFSLX-EVL, measuring 1.75 x 1.75 in. (44.45 x 44.45 mm) without the SMA protrusion, provides SMA connections for reference in, power in, RF out, lock detect, Sync and RF mute. The RF mute connection also has a momentary push-to-mute button.

Accelerate your R&D by ordering your custom phase-locked oscillator today.

Z-Communications, Inc.
applications@zcomm.com
store.zcomm.com

TABLE 1
PERFORMANCE CHARACTERISTICS

Product Feature	Value	Notes
Frequency (GHz)	.05 to 22.5	
Resolution (Hz)	0.1	
Reference (MHz)	5 to 200	Customer provided 3.6 Vpp max.
Power	3.3 Vdc	@520 mA (typ.)
Phase noise (dBc/Hz typ.) 1 KHz 100 KHz 10 MHz	-107 -116 -148	@6 GHz
RF Output (dBm)	3 to 8	High to low frequency
Mute (V)	3.3	
Sync (V)	3.3	
Lock Detect (V)	3.3	

Microwave Journal
Frequency Matters.
Catch up on the latest industry news with the bi-weekly video update
Frequency Matters from Microwave Journal @ www.microwavejournal.com/frequencymatters

High Isolation Baluns Operate to 67 GHz

HYPERLABS INC. has expanded its industry-leading balun product line with the introduction of a series of high isolation baluns that cover frequencies up to 67 GHz. The newly released HL9607 isolation balun operates over a broadband frequency range of 150 kHz to 67 GHz. The HL960X series also includes models that operate to 26.5, 40 and 50 GHz.

The HL960X series isolation baluns provide 18 dB of port-to-port isolation, while the designs are also optimized for phase and amplitude balance across their specified frequency bands. These aspects make the isolation baluns an excellent choice for use in high speed analog-to-digital conversion, balanced receivers, baseband digital modulation and signal integrity enhancement. Furthermore, the isolation baluns are also ideal for testing poorly matched or non-50 Ω devices as well as for enabling differential measurements with single-ended, two-port VNAs.

The miniaturized form factor of the HL960X series isolation balun has housing dimensions of 2.40 x 1.25 x 0.40 in. while offering industry-leading performance. The high performance compact designs are space savers for benchtop test setups as well as within integrated systems applications. The broadband HL960X series isolation baluns are meticulously built and tested at the HYPERLABS Colorado manufacturing facility by a skilled team of hybrid assemblers. The HL960X series S-parameter data files are available upon request, as well as demonstration units for performance evaluations. Contact HYPERLABS or your local sales representative for more information.

Founded in 1992, HYPERLABS is a worldwide provider of broadband and ultra-broadband components that cover frequencies up to 110 GHz and beyond. Components products include baluns, amplifiers, power dividers, bias tees, pickoff tees, DC blocks, transition time convertors, samplers, harmonic mixers and more.

HYPERLABS
Louisville, Colo.
HYPERLABS.com

Disruptive Technology, Transformative Solutions

Accelerate design cycles, reduce costs and future-proof designs with Apollo MxFE™.

Analog Devices Inc.

https://players.brightcove.net/706011717001/VwMdg0a0kC_default/index.html?videoId=6328949464112

IR HiRel's Decades-Long Space Heritage Poster

Register to receive a free poster (24 x 36 in.) and celebrate half a century of IR HiRel space heritage.

IR HiRel

https://bit.ly/4gWEjv2

Ask Microwave Journal

Try our AI-powered search tool that makes it easy to find exactly what you need. Type your question or topic in natural language into the search bar and get reliable, relevant results from our technical database.

Microwave Journal

www.microwavejournal.com/ask-microwave-journal

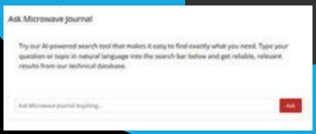

RF-Lambda Electromagnetic Compatibility (EMC) Division

Check out this video highlighting RF Lambda's electromagnetic compatibility (EMC) division.

RF Lambda

www.youtube.com/watch?v=7qU0g7LWWj4html?videoId=6328949464112

Getting Started with the FSW - ACLR Measurements

This video provides step-by-step instructions on how to measure adjacent channel leakage ratio using a Rohde & Schwarz FSW series signal and spectrum analyzer.

Rohde & Schwarz

www.youtube.com/watch?v=vr_4dKYmF1g

Signal Hound's PN400: Next-Gen Phase Noise and VCO Testing

Signal Hound's PN400 harnesses the power of two SM series spectrum analyzers, offering RF engineering professionals an unrivaled value in comprehensive signal analysis.

Signal Hound

www.youtube.com/watch?v=QeT09_UAcd4

NEW PRODUCTS

FOR MORE NEW PRODUCTS, VISIT WWW.MWJOURNAL.COM/BUYERSGUIDE
FEATURING VENDORVIEW STOREFRONTS

DEVICES/ COMPONENTS/MODULES

Reduction in Ceramic Filter Size

VENDORVIEW

3H 6DR750-X30-4SS/W reduced size filters from the 300 to 1500 MHz range in SMT format with no reduction in electrical performance. Reduced from 1.0 × 0.70 × 0.32 in. to 1.0 × 0.38 × 0.32 in. Fo is 750 MHz, passband is 735 to 765 MHz, passband insertion loss is 2.65 dB, rejection is 50 dB at DC to 675 MHz and 50 dB at 850 to 1500 MHz. Input power is 5 W and meets MIL-STD-202 conditions.

3H Communication Systems
www.3hcomm.com

WR-12 Receiver Module

VENDORVIEW

Combining a low noise input amplifier, LO frequency multiplier and a balanced mixer, model SSR-7931535010-12-SR1 is an integrated receiver module covering frequencies from 71 to 86 GHz. With a typical noise figure of 5 dB and conversion gain of 10 dB, the receiver accepts LO signals from 11.5 to 14.7 GHz.

Eravant
www.eravant.com

V-Band WR19 Diplexer

VENDORVIEW

Exceed Microwave has developed a V-Band WR19 waveguide diplexer with steep rejection on both bands, rejecting 50.2 to 50.4 GHz, the space research frequency band. Return loss on both channels is 15 dB minimum with insertion loss of 0.6 dB at the center of the band. The housing of the diplexer is made with invar to provide stable performance over temperature. Exceed Microwave, an AS9100D/ISO9001:2015 ITAR registered company, provides custom designed passive components.

Exceed Microwave
www.exceedmicrowave.com

0.5-1 GHz High Power Drop-in 90° Hybrid

VENDORVIEW

MIcable's Q8T050100 has low insertion loss (0.25 dB maximum), excellent VSWR (1.25:1 maximum), extremely good amplitude unbalance (± 0.55 dB maximum) and phase unbalance (+ 5 degrees maximum), high isolation (20 dB minimum) and 400 W power handling capability with excellent stability and heat dissipation ability in a small package. It is suitable for power amplifier, power combining network, antenna feed network, modulator and phase shifter applications.

MIcable
www.micable.cn

Mounted Rotary Step Attenuators

These Telonic Berkeley step attenuators are available in nine different models with attenuation ranges from 1 to 100 dB, in steps of 1 to 10 dB. There are two basic case designs, both 1.31 in. diameter with lengths of 1.50 in. (subminiature) and 2.29 in. (miniature). This mechanical configuration reduces panel mounting space to a minimum and permits incorporation of these attenuators into many existing designs.

Telonic Berkeley
www.telonicberkeley.com

Ceramic Chip Capacitors

Vishay Intertechnology Inc. introduced a new series of surface-mount multilayer ceramic chip capacitors (MLCCs) for high voltage commercial applications. Offered in seven case sizes ranging from 1206 to 2225, VJ....W1HV High Voltage MLCC Commercial Series devices extend the capacitance values of the company's existing high voltage MLCCs with the ultra stable C0G (NP0) dielectric and are also available with the X7R dielectric for even higher capacitance.

Vishay Intertechnology Inc
www.vishay.com

NewProducts

CABLES & CONNECTORS

Flexible Micro-Miniature Coaxial Cables

Amphenol RF announced the expansion of their BNC product portfolio with additional options featuring flexible micro-miniature coaxial cables. Offering engineers more design possibilities without sacrificing performance, these configurations have frequency ranges of up to 9 GHz and support Wi-Fi 7. A bayonetted interface gives BNC connectors a reliable and secure connection while also allowing for easy mating and unmating. The high performance reliability of BNC connectors makes them ideal for testing and measurements, telecommunications and industrial applications. Featuring a corrosion-resistant nickel-plated brass body and ferrule, BNC connectors are engineered to endure the harshest environments.

Amphenol RF
www.amphenolrf.com

MICRO-ADS

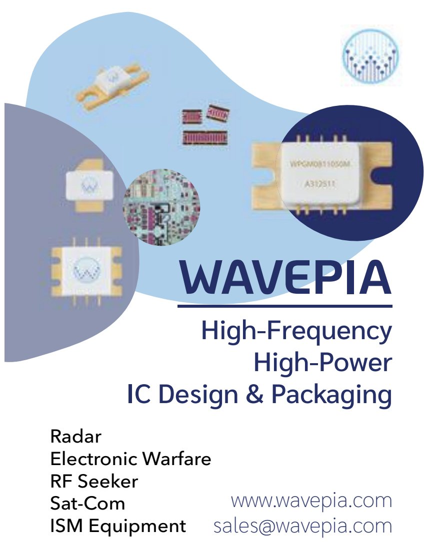

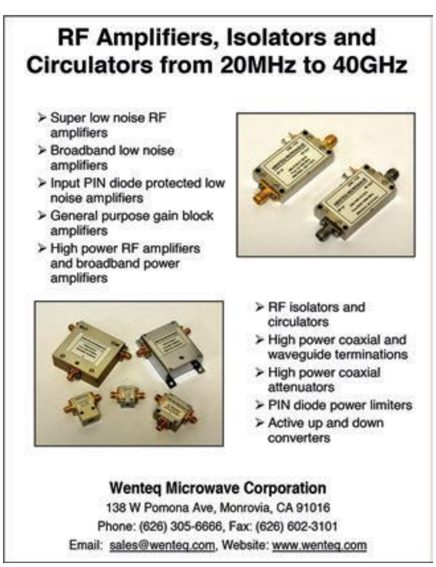

TCOM Cable Assemblies

VENDORVIEW

Fairview Microwave has launched a line of TCOM cable assemblies. They are designed to deliver outstanding RF performance with options tailored for either low loss or low-PIM configurations, depending on the connector type. The TCOM cable assemblies feature a robust design with two shields, ensuring enhanced signal integrity and minimized interference. With performance guaranteed across a wide frequency range from DC to 10 GHz, they provide reliable connectivity for demanding RF applications.

Fairview Microwave
www.fairviewmicrowave.com

40 GHz and 18 GHz Right-Angle Adapters

VENDORVIEW

Pasternack has announced the launch of its new 40 GHz 2.92 mm, 18 GHz TNC and type N radius right-angle adapters. These high performance adapters deliver signal transmission across a wide frequency range, offering VSWR ratings as low as 1.2 and 1.3 maximum for reliable, optimized RF performance. Designed with a unique radius right-angle body geometry, these adapters ensure precise in-series connections while minimizing signal loss.

Pasternack
www.pasternack.com

ARINC Blindmate Microwave Contacts

The Phoenix Company of Chicago's new size 5, 8, 12 and 16 ARINC PkZ®contacts offer a multitude of benefits that make them an ideal solution for in-flight entertainment systems, including routers, modems and modem managers, in both commercial and business aircraft. These benefits stem from their superior electrical performance, robust design and flexibility, addressing key requirements for reliable and high-quality in-flight connectivity and entertainment experiences. All contacts feature a constant impedance over an axial mating tolerance of .110 in. with performance options to 18 GHz and 50 GHz.

The Phoenix Company of Chicago, Inc.
www.phoenixofchicago.com

Quad Small Form-Factor Pluggable (QSFP) Connector

Withwave's QSFP28 connector is designed with 38 pins in 0.8 mm pitch and is based on differential pair 100 Ohm. With four data channels in one connector, data can be transferred at up to 28 Gbps/channel. This interface can replace four standard SFP+ with one, saving space and cost.

withwave co., ltd
www.with-wave.com

AMPLIFIERS

Exodus AMP20081, 80–1000 MHz, 500 W, 400 W P1

VENDORVIEW

Exodus Advanced Communications model AMP20081 operates 80 to 1000 MHz > 500 W. The unit produces > 600 W nominal power with typically > 500 W P1dB. The minimum gain is 56 dB with excellent flatness. Included are amplifier monitoring parameters for forward/reflected power, VSWR, as well as voltage, current and temperature sensing for optimum reliability and ruggedness. Nominal weight is < 40 kg and dimensions are 19 (W) x 27 (L) × 8.75 (H) in.

Exodus Advanced Communications
www.exoduscomm.com

Tiny LNA with Big Gain for Tight SWaP-C Requirements

VENDORVIEW

Mini-Circuits has further miniaturized its MMIC product line by shoehorning a high gain, wideband MMIC LNA into a 1.5 × 1.5 mm QFN-style package to address more demanding SWAP-C requirements. The amplifier provides an outstanding combination of ultrawide bandwidth from 0.05 to 10 GHz, 22 dB gain, 1.1 dB NF and +21.5 dBm P1dB to meet the RF requirements of modern-day systems as well as their ever-tightening mechanical constraints.

Mini-Circuits
www.minicircuits.com

Logarithmic Video Amplifier

VENDORVIEW

Quantic PMI Model SDLVA-18G40G-CD-1 is a successive detection logarithmic video amplifier (SDLVA) designed to operate over the 18 to 40 GHz frequency range with a dynamic range of -70 to +5 dBm; TSS of -70 dBm typical, -68 dBm maximum; log linearity of ±2.5 dB (-40°C to +85°C) and VSWR of 2.5:1. This model is designed for high speed applications while maintaining flatness and accuracy. Package size is 3.2 × 1.8 × 0.4 in. with 2.92 mm (RF) and SMA (video) female connectors.

Quantic PMI
www.quanticpmi.com

New**Products**

GaN-on-SiC Bare Die Power Amplifier

VENDOR**VIEW**

Now available at RFMW, the GRF0020D is one of the first of a new class of GaN-on-SiC bare die power amplifiers from Guerrilla RF. Offering up to 30 W of saturated power when using 50 V supply rails and 19 W with 28 V rails, the GRF0020D is engineered for high performance applications, supporting frequencies up to 7 GHz and delivering a gain range from 13.8 dB to 24.3 dB.

RFMW
www.RFMW.com

2-6 GHz, 300 W RF Module

Stellant PST's latest development expands on its proven innovative integrated RF GaN power amplifier designs by further increasing the RF power density, while improving overall operating efficiency. These highly integrated designs are ideal for use in communication, electronic warfare and radar transmitter systems where space, cooling and power are limited. Applications include ground, ship and airborne platforms.

Stellant Systems
www.stellantsystems.com

SYSTEMS

Modular Power System

Highland Technology's P940 is a modular power system that allows you to mix-and-match DC and three-phase AC supplies, loads and more in a single 3U chassis. Featuring USB and Ethernet control, including SCPI and fast UDP monitoring, front panel GUI and waveform monitor outputs, synchronized multi-module control and provision for up to 8 plug-in modules in a 3U rackmount enclosure.

Highland Technology
www.highlandtechnology.com

SOURCES

Temperature Compensated Crystal Oscillator

Greenray Industries, Inc. has announced the availability of the T32 Series temperature compensated crystal oscillator. The T32 TCXO is available from 10 to 52 MHz and offers tight frequency stability as low as ±1 ppm over -55°C to +125°C, a rugged, 3.2 × 2.5 mm package and shock survivability to 75,000 g. Long-term aging is < 4 ppm over 10 years and acceleration sensitivity is as low as 0.5 ppb/g. Output is CMOS or clipped sine. Additional features include +3.3 VDC supply, low power consumption and testing per MIL-PRF-55310 level B is available. The T32 TCXO is well-suited to a wide variety of systems applications including high shock electronics, mobile radio, mobile instrumentation, airborne and wireless communications and microwave receivers.

Greenray Industries, Inc.
www.greenrayindustries.com

Phase Locked Dielectric Resonator Oscillators

VENDOR**VIEW**

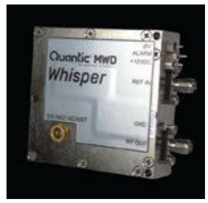

The Whisper Series Phase Locked Dielectric Resonator Oscillators (PLDROS) are the premier choice for mission-critical frequency control and timing applications. Designed to meet and exceed stringent system requirements, Whisper Series PLDROs deliver exceptional frequency stability and low phase noise performance, even in the harshest environmental conditions. Available in X-Band and Ku-Band frequencies ranging from 8 to 18 GHz, these oscillators can be fully customized with phase locked loops and tuning for enhanced performance.

Quantic MWD
www.quanticmwd.com

Satcom Ultra-Low Noise DRO

The GSDRO1200-8XT is offered in Synergy's "GOLD Standard" series, surface-mount dielectric resonator oscillators (DROs) combining ultra-low phase noise with extended temperature range. This product is ideally suited for free running and phase locked applications in high performance satcom LNB converters, data rate clocking converters, radar, military communications and test instrumentation. It operates at 12 GHz with typical phase noise of -123 dBc/Hz at 10 KHz offset. The operating temperature range is from -40°C to +85°C.

Synergy
www.synergymwave.com

TEST & MEASUREMENT

VNA

VENDOR**VIEW**

Rohde & Schwarz has expanded its vector network analyzer (VNA) portfolio with the R&S ZNB3000, which offers best-in-class RF performance. It combines high measurement accuracy with exceptional speed. With its high throughput rate, the new VNA is especially suitable for high volume production and short ramp-up time environments such as large-scale production of RF components. Innovative PCB-based frontends offer higher stability and minimize thermal drift allowing reliable measurements over several days without recalibration.

Rohde & Schwarz
www.rohde-schwarz.com

ZERO BIAS SCHOTTKY DETECTORS

For 0.01 - 50 GHz

Many Models Available in Stock

> Single unit covers 0.01 - 50 GHz
> Matched input for low VSWR
> Flat frequency response
> High sensitivity (0.5 mV/µW up to 50 GHz)
> Optional output connectors (SMA, BNC, SMC)
> Great for instrumentation and laboratory use

MODEL	FREQ. RANGE	MAX. VSWR	MAXIMUM FLATNESS (± dB)	LOW LEVEL SENSITIVITY (mV / µW)
DZR50024A	10 MHz-50 GHz	1.3:1 (to 18 GHz) 1.6:1 (to 26 GHz): 1.8:1 (to 40 GHz) 2 :1 (to 50 GHz)	± 0.3 (to 18 GHz) ± 0.6 (to 26 GHz) ± 0.8 (to 40 GHz) ± 1.0 (to 50 GHz)	0.5
DZR50024B	10 MHz-50 GHz			0.5
DZR50024C	10 MHz-50 GHz			0.5

*All models have 2.4 mm (M) input connector
*Standard output polarity is negative.
Add letter "P" to end of model number for positive output.

Custom Designs - Write / Call for Quote

Other Products:
Amplifiers, Comb Generators, Limiters, Switches, Integrated Subsystems

Herotek

155 BAYTECH DRIVE, SAN JOSE, CA. 95134--2303
PH: 408-941-8399 . FAX: 408-941-8388
E-Mail: Info@Herotek.com
Web Site: http.//www.herotek.com
Visa/MasterCard Accepted

Reviewed by: Reena Dahle

Bookend

EW 105: Space Electronic Warfare

By: David L. Adamy

This book by David Adamy is the fifth and final book in the electronic warfare (EW) series focuses. It focuses on how EW impacts satellites. The book contains ten chapters and three appendices:

Chapters

1. Introduction
2. Spherical Trigonometry
3. Orbit Mechanics
4. Radio Propagation
5. Radio Propagation in Space
6. Satellite Links
7. Link Vulnerability to EW
8. Duration and Frequency of Observations
9. Intercept From Space
10. Jamming From Space

Appendices

11. Formulas From Signal Intelligence and EW
12. Important Numbers for Space EW
13. Decibel Math

In these chapters and appendices, the author starts off by first providing the reader with an understanding of the history of the intelligence of satellite programs, orbit mechanics and the fundamentals of radio propagation before diving into satellite link vulnerability and jamming scenarios from space. This is a very good resource for someone who works in the anti-jamming electronics field looking to broaden the applications of their product to space applications.

ISBN: 9781630818340
Pages: 230
To order this book, contact:
Artech House (2021)
us.artechhouse.com

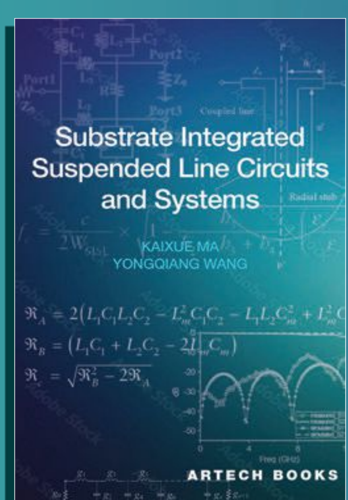

Substrate Integrated Suspended Line Circuits and Systems

Author: Kaixue Ma, Yongqiang Wang

ISBN 13: 978-1-68569-029-8

ePub: 978-1-68569-030-4

Publication Date: March 2024

Subject Area: Microwave

Binding/pp: Hardcover/296

Price: $124/ £94

Substrate Integrated Suspended Line Circuits and Systems is a comprehensive guide to a cutting-edge transmission line technology known as the substrate-integrated suspension line (SISL).

- Explores the fundamentals and practical applications of SISL, outlining its structure, passive and active circuit variations, and front-end sub-systems.
- Emphasizes the advantages of substrate-integrated suspension line, explaining its ability to retain the strengths of suspended lines while addressing the limitations of conventional waveguide suspended line circuits.
- Discusses high-performance RF, microwave, and mm-wave circuits and systems.
- Presents in-depth insights into the innovative SISL technology and its applications within the realm of high-frequency circuits and systems.

This book serves as an excellent reference book for those who are working on RF and microwave engineering and would like to develop high performance RF and microwave circuits.

ARTECH HOUSE
BOSTON | LONDON

To learn more, please visit:
https://us.artechhouse.com/
https://uk.artechhouse.com/

Featuring 2 Days of Keynotes • Technical Sessions • Workshops

EDI CON Online brings much needed technical training and information directly to engineers' desktops and mobile devices. Free, real-time training with easy registration and access.

EDI CON ONLINE
EDUCATIONAL DAYS

4 Focused Tracks with Free Seminars On:

APRIL 23
5G/6G, IoT, Radar/Automotive/SATCOM

OCTOBER 22
SI/PI/PCB/Interconnect/EMI

Live attendees can participate in Q&A sessions & earn IEEE CEU's

EDICONONLINE.COM

Organized by horizon house

Official Publications Microwave Journal Signal Integrity Journal
Signal Integrity • Power Integrity • EMC/EMI

Advertising**Index**

Sales Representatives

Eastern and Central Time Zones
Carl Sheffres
Group Director
(New England, New York, Eastern Canada)
Tel: (781) 619-1949
csheffres@mwjournal.com

Michael Hallman
Associate Publisher
(NJ, Mid-Atlantic, Southeast, Midwest, TX)
Tel: (301) 371-8830
Cell: (781) 363-0338
mhallman@mwjournal.com

Pacific and Mountain Time Zones
Brian Landy
Western Reg. Sales Mgr.
(CA, AZ, OR, WA, ID, NV, UT, NM, CO, WY, MT, ND, SD, NE & Western Canada)
Tel: (831) 426-4143
Cell: (831) 713-9085
blandy@mwjournal.com

International Sales
Michael O'Kane
Tel: +44 (0) 1875 825 700
Cell: +44 (0) 7961 038 245
mokane@impressmedia.com

Germany, Austria, and Switzerland (German-speaking)
Victoria and Norbert Hufmann
victoria@hufmann.info
norbert@hufmann.info

France
Gaston Traboulsi
Tel: +44 207 596 8742
gtraboulsi@horizonhouse.com

Korea
Jaeho Chinn
JES MEDIA, INC.
Tel: +82 2 481-3411
corres1@jesmedia.com

China
Shanghai
Linda Li
ACT International
Tel: +86 136 7154 0807
lindal@actintl.com.hk

Wuhan
Phoebe Yin
ACT International
Tel: +86 134 7707 0600
phoebey@actintl.com.hk

Shenzhen
Annie Liu
ACT International
Tel: +135 9024 6961
anniel@actintl.com.hk

Beijing
Cecily Bian
ACT International
Tel: +86 135 5262 1310
cecilyb@actintl.com.hk

Hong Kong
Floyd Chun
ACT International
Tel: +852 28386298
floydc@actintl.com.hk

Taiwan, Singapore
Simon Lee
ACT International
Tel: +852 2838 6298
simonlee@actintl.com.hk

Japan
Katsuhiro Ishii
Ace Media Service Inc.
Tel: +81 3 5691 3335
amskatsu@dream.com

Submitting ad material?
Visit: www.adshuttle.com/mwj
(866) 774-5784
outside the U.S. call
+1-414-566-6940

Ed Kiessling
(781) 619-1963
ekiessling@mwjournal.com

Corporate Headquarters: 685 Canton Street, Norwood, MA 02062 • Tel: (781) 769-9750

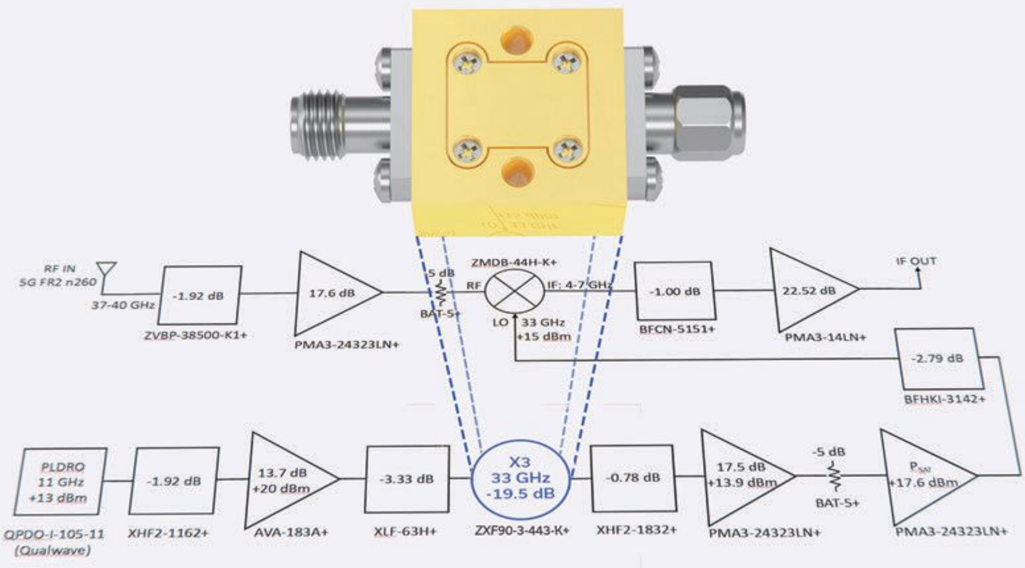

9 TO 72 GHz

Coaxial Frequency Multipliers

For High-Frequency LO Chains,
Upconverters & More

xN

LEARN MORE

High-frequency multipliers cover 9 to 72 GHz with +12 to +20 dBm input in compact, coaxial housings.

Model Name	Description	F Low	F High
ZXF90-3-223-K+	X3 Frequency Multiplier, SMA-F to 2.92 mm-M, 50Ω	10 GHz	22 GHz
ZXF90-3-443-K+	X3 Frequency Multiplier, SMA-F to 2.92 mm-M, 50Ω	20 GHz	43.5 GHz
ZXF90-3-453-V+	X3 Frequency Multiplier, SMA-F to 1.85 mm-M, 50Ω	20 GHz	45 GHz
ZXF90-3-64-E+	X3 Frequency Multiplier, 2.92 mm-F to 1.85 mm-M, 50Ω	30 GHz	60 GHz
ZXF90-3-723-E+	X3 Frequency Multiplier, 2.92 mm-F to 1.85 mm-M, 50Ω	40 GHz	72 GHz
ZXF90-2-44-K+	X2 Frequency Multiplier, 2.92 mm-F to 2.92 mm-F, 50Ω	12.4 GHz	40 GHz
ZXF90-2-153-K+	X2 Frequency Multiplier, 2.92 mm-F to 2.92 mm-F, 50Ω	9 GHz	15 GHz

Mini-Circuits®

FABS and LABS

Virginia Diodes, Inc.: Making THz Spectrum Useful

Virginia Diodes, Inc. (VDI) was founded in 1996 by the current CEO, Dr. Thomas W. Crowe. Dr. Crowe earned his M.S.E.E. and Ph.D. from the University of Virginia (UVa), slightly more than a mile from the current VDI facility in Charlottesville, Va. While at UVa, his research centered on developing Schottky diode technology tailored for terahertz (THz) applications. In 1996, VDI was launched as a spin-off from the Terahertz Research Program at UVa.

VDI was formed to bring high frequency component innovations to a broader market and support further research in the area. From its inception in 1996 to 2001, VDI sold Schottky diodes for scientific applications, including radio astronomy and high frequency radar. By the early 2000s, VDI had expanded its product line to include mixers, detectors, multipliers and sources operating into the THz frequency range. By 2004, the company was selling transmitter and receiver modules for THz sub-systems. During this period, VDI moved into the current Charlottesville facility and developed capabilities to replace the UVa facilities.

Market applications are creating the need for products and systems at higher mmWave and THz frequency ranges. In response, VDI's product portfolio has expanded dramatically. The company still offers W-Band (75 to 110 GHz) and G-Band (110 to 300 GHz) diodes and a range of single-function components that include detectors, mixers, waveguide amplifiers and frequency multipliers. These component families now include banded offerings from 50 GHz to beyond the THz range. VDI is also integrating these functional capabilities into higher-level receiver and transmitter assemblies and modules that cover frequency bands from 50 GHz to approximately 3 THz. The company rounds out its high frequency portfolio with a family of passive components that include bandpass filters, waveguide sections, tapers, horn antennas and directional couplers that operate in millimeter and THz waveguide bands.

As frequencies increase, so do testing challenges. A standard solution is to add frequency extenders to lower frequency test equipment. These frequency extenders up-convert and down-convert signals to the appropriate frequencies for test. VDI is the gold standard for test and measurement capabilities at millimeter and THz frequency bands with a broad range of frequency extenders that operate from 26 GHz to 1.5 THz for VNAs and spectrum analyzers. The company also makes extension modules for signal generation, noise testing and portable spectrum analyzer applications. Depending on the applications, these extenders operate in bands from 50 GHz to the THz frequency range. In addition to its test and measurement portfolio, VDI has power meters, noise source modules and compact converters that operate in standard waveguide bands up to 500 GHz, with the power meter capable of measuring applications above 3 THz.

The addressable market applications have grown along with the product portfolio. VDI's earliest customers were in radio astronomy, atmospheric science and plasma diagnostics. Now, VDI low noise receivers operating to 900 GHz have flown on CubeSat platforms to study ice clouds and tropical storm evolution. VDI is developing high-power solid-state sources that use dynamic nuclear polarization to produce hundreds of milliwatts at 300 GHz and beyond for magnetic resonance signal applications. They are also involved in 6G and next-generation communications and automotive radar applications. VDI continues to support these and many other fields of research with targeted research and development to improve the sensitivity and power at frequencies up to 5 THz. What started as a university activity has grown into 30,000 sq. ft. across two locations that employs approximately 120 people who are all focused on making the THz spectrum useful.

www.vadiodes.com

SPECTRAN® V6
BEYOND REALTIME

Setting the Mobile Benchmark

The **ULTIMATE** Real-Time Spectrum Analyzer Tablet

8 | 18 | 55 | 140 GHz 2x 490 MHz RTBW

HIGH-END SPECTRUM ANALYZER:

- 9 kHz up to 140 GHz
- Optional Tx (Generator)
- 2x 490 MHz Bandwidth
- 3 THz/s Sweep Speed
- 16-Bit ADC
- -170dBm/Hz | 4dB NF
- IQ Recording & Playpack
- 8h Continuous Runtime
- Temp. Range -40° to +60°
- GPS & Time Server
- Opt. Handle & Stand
- Incl. RTSA-Software

RUGGED PREMIUM PC POWER:

- 15.6″ 1500nit FullHD Touchscreen
- AMD 8-Core 8845HS CPU
- 64 GB LPDDR5 RAM
- Up to 64 TB Highspeed SSD
- 2x M.2 2280 & 3x M.2 2242
- Many I/Os incl. USB4, SD & HDMI
- SIM slot, opt. WiFi, Bluetooth, 5G
- SFP+ 10G Ethernet, SATA, RS232
- Rugged Aluminum Casing
- Hot-Swap Batteries
- Front & Rear Cameras, Smart Pen
- Windows or Linux

MADE IN GERMANY

www.aaroniausa.com
ubuy@aaroniausa.com
+1 (214) 935-9800

www.aaronia.com
mail@aaronia.de
+49 6556 900 310

AARONIA AG®
WWW.AARONIA.COM


WERLATONE
A STEP AHEAD
SOLUTIONS FOR EVERY MILITARY PLATFORM
COMMUNICATIONS | EW | RADAR
DC TO X-BAND
INTEGRATED SUB-ASSEMBLIES
BEAMFORMERS
WAVEGUIDE SOLUTIONS
E-PLANE COMBINERS
FIXED | AIRBORNE | GROUND MOBILE | SHIPBOARD
WE OFFER A VARIETY OF POWER LEVELS RANGING FROM 10 W CW TO 20 KW CW
WERLATONE'S HIGH POWER, MISMATCH TOLERANT® SOLUTIONS
ARE DESIGNED TO OPERATE IN EXTREME LOAD MISMATCH CONDITIONS.
BRING US YOUR CHALLENGE | WWW.WERLATONE.COM
WERLATONE
LEARN MORE

eXclusive Digital Content ›››

REVIEW BOARD MWJ APPROVED

Hemicyl-Shaped Circularly-Polarized Wideband DRA

Sumer Singh Singhwal and Ladislau Matekovits
Department of Electronics and Telecommunications, Politecnico di Torino, Turin, Italy

This article describes a novel circularly-polarized hemicyl-shaped dielectric resonator antenna (DRA) that is excited with orthogonal feeds. It has a wide impedance bandwidth of 3.5 to 5.1 GHz, as well as a circular polarization bandwidth of 3.55 to 5 GHz. The antenna's average gain is 5.5 dBi. Because it operates in the sub-6 GHz band, it can be used for a variety of wireless applications, including 5G.

For wireless communication, a DRA is preferred for a variety of reasons, including its characteristic small size, wide impedance bandwidth, low loss due to its dielectric body, flexible excitation schemes due to its 3D geometry and more design parameters (degrees of freedom). Long et al.[1,2] suggested cylindrical and hemispherical DRAs in 1983. Various forms and feed mechanisms were subsequently explained.[3-6]

A variety of DRA shapes have been proposed. These include trapezoidal,[7] triangular,[8,9] hexagonal,[10] V-shaped,[11] ring,[12] hemispherical[2,13] and half-split cylindrical.[14] DRAs are used in different novel applications, such as sensing,[15] cognitive radio,[16] implantable devices[17] and MIMO.[18]

Pan et al.[19] analyzed the performance of low-permittivity (ε_r = 5) and high-permittivity DRAs (ε_r = 10). Sun and Leung[20] proposed a dual-band dual-polarization cylindrical DRA (CDRA) using K9-glass with a low permittivity (ε_r = 6.85). DRA radiation fields can be improved by using materials with lower dielectric constants ($5 \le \varepsilon_r \le 20$) and using the proper cylinder size.[1] It is not easy to build an efficient DRA out of low dielectric material. Because it does not require the use of magnetic walls, a hemispherical DRA (HDRA) is favored due to the ease of theoretical analysis and its simple geometry.[21, 22] Its shape also creates a straightforward interface to free space.

This article investigates the hemicyl-shaped DRA, a new variant. It is a combination of a CDRA and an HDRA. Orthogonal feeds are used to obtain wideband circular polarization. Antenna designers prefer circular polarization in antennas due to minimal polarization losses and the ability to counteract multipath interference and fading. It operates in the sub-6 GHz band, which has a wide range of wireless communication applications. The antenna has a 34.5 percent impedance bandwidth and a 33 percent circular polarization bandwidth that roughly overlaps the impedance bandwidth. Its gain is 5.5 dB in the proposed application band.

DESIGN AND OPERATING PRINCIPLE

Design Methodology

The hemicyl-shaped DRA is shown in ***Figure 1*** and its design parameters are listed in ***Table 1***. To capture the advantages of low ε_r material, the DRA is fabricated with a material having ε_r = 4.5. The design relation for medium permittivity material with $\varepsilon_r \geq 10$ is given in ***Equation 1*** for the $HE_{11\delta}$ mode.[3-6] This cannot be directly applied to a low dielectric constant DRA, therefore, Equation 1 is taken as a starting point and is tuned by rigorous parametric analysis performed using the electromagnetic simulator HFSS.

$$f_0 = \frac{c \times 6.324}{2\pi a\sqrt{\varepsilon_{rDRA} + 2}} \left(0.27 + 0.36\frac{a}{2H} + 0.02\left(\frac{a}{2H}\right)^2\right) \quad (1)$$

Where:
α = radius of the CDRA
H = height of the CDRA
ε_{rDRA} = dielectric constant of the DRA material
c = velocity of light in a vacuum.

RT/duroid 5870, which has ε_r = 2.33, with dimensions of 72 mm × 72 mm and a thickness of 0.8 mm, is used as the antenna's substrate. The microstrip feed line has a width of 2.4 mm. A perpendicular feed configuration excites the DRA orthogonally. Two conformal 2 mm diameter probes excite orthogonal modes to produce circular polarization.

The design approach consists of two steps. In step 1, a CDRA is built with a height of an HDRA and a diameter of d1. In step 2, an HDRA with a radius of r2 is placed on top of the CDRA to improve its performance. ***Figure 2*** compares the performance of steps 1 and 2 with respect to impedance bandwidth, axial ratio (AR) bandwidth and gain. The CDRA excites the HDRA, which efficiently enhances CDRA height and improves performance characteristics like impedance bandwidth, gain and axial ratio bandwidth (ARBW).

Various strategies for feeding a DRA have been addressed.[3-6] Both microstrip and probe feed lines are employed to excite the DRA. The L-shaped feed structure shown in Figure 1 comprises two conformal probes carved on the DRA and positioned orthogonally to one another. By adjusting the corresponding probe lengths, phase quadrature is achieved between two hybrid modes ($HE^x_{11\delta}$ and $HE^y_{11\delta}$), resulting in a wide circular polarization bandwidth.

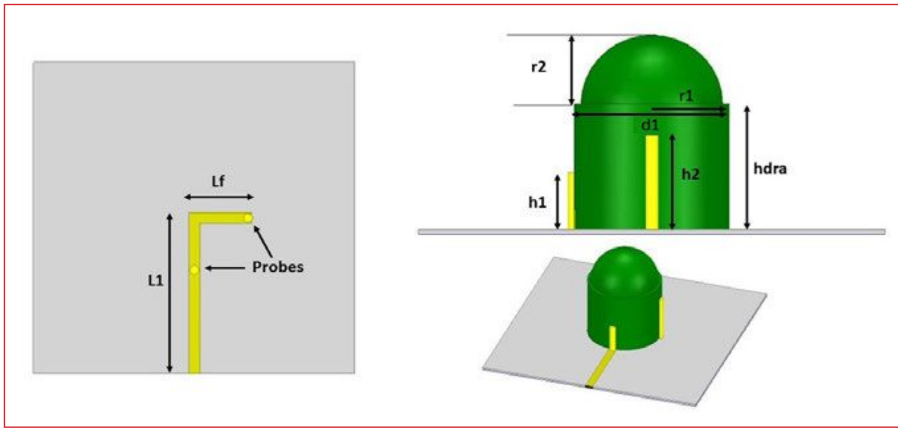

Fig. 1 **DRA design layout.**

TABLE 1						
DESIGN PARAMETERS						
hdra	L1 (mm)	h1 (mm)	h2 (mm)	Lf (mm)	r2 (mm)	d1 (mm)
20	37.2	9	15	14	11	24

Operating Principle

The operating principle of the hemicyl DRA is divided into three parts: excitation by Probe 1, resulting in the DRA $HE^x_{11\delta}$ mode, excitation by Probe 2, resulting in the DRA $HE^y_{11\delta}$ mode and excitation by Probes 1 and 2, resulting in circular polarization. The probe heights are optimized by parametric analysis using HFSS.

There are two slight troughs at 3.75 GHz and 4.65 GHz in the AR plot shown in Figure 2. This corroborates the $HE^x_{11\delta}$ and $HE^y_{11\delta}$ modes. ***Figure 3*** shows the impedance bandwidths for each of

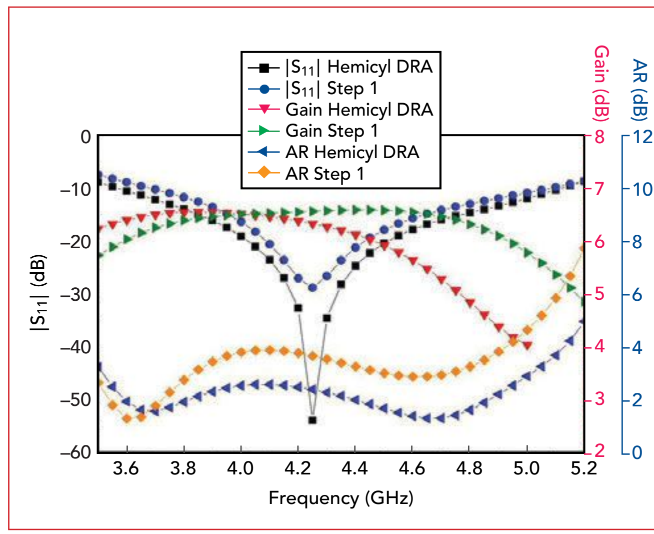

Fig. 2 **Performance comparison of design steps 1 and 2.**

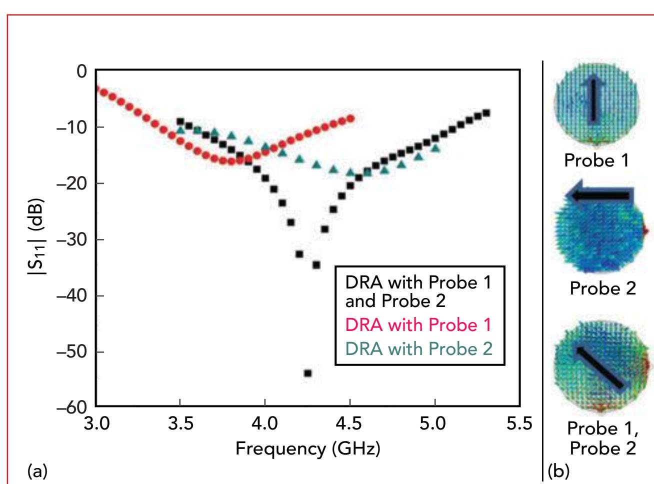

Fig. 3 **Comparison of DRA $|S_{11}|$ (a) and electric fields (b) for different probe configurations.**

the three cases, along with their corresponding electric fields.

PARAMETRIC ANALYSIS

Parametric analysis studies the effect of a single parameter on performance while keeping all other design parameters constant. Exhaustive parametric analysis is necessary to achieve an optimized design. Three main parameters are studied in detail: the CDRA and HDRA radii, the heights of Probes 1, 2 and 3 and the effect of ε_r. Although other parameters, such as feed position, feed width and the size of the ground plane, are also important, these parameters have been left out of the results for brevity.

CDRA and HDRA Radii

Figure 4 shows the responses from the parametric variation of CDRA and HDRA radii for 10, 11, 12 and 13 mm values. It is observed that the impedance bandwidth widens and the resonant frequency shifts downward with increasing r1. Note that the resonant frequency is inversely proportional to the radius in Equation 1. Gain varies between 3.5 and 6.5 dB for all r1 values, while the ARBW widens as r1 increases. It is also observed that ARBW improves as r2 increases. Therefore, the hemisphere radius controls cir-

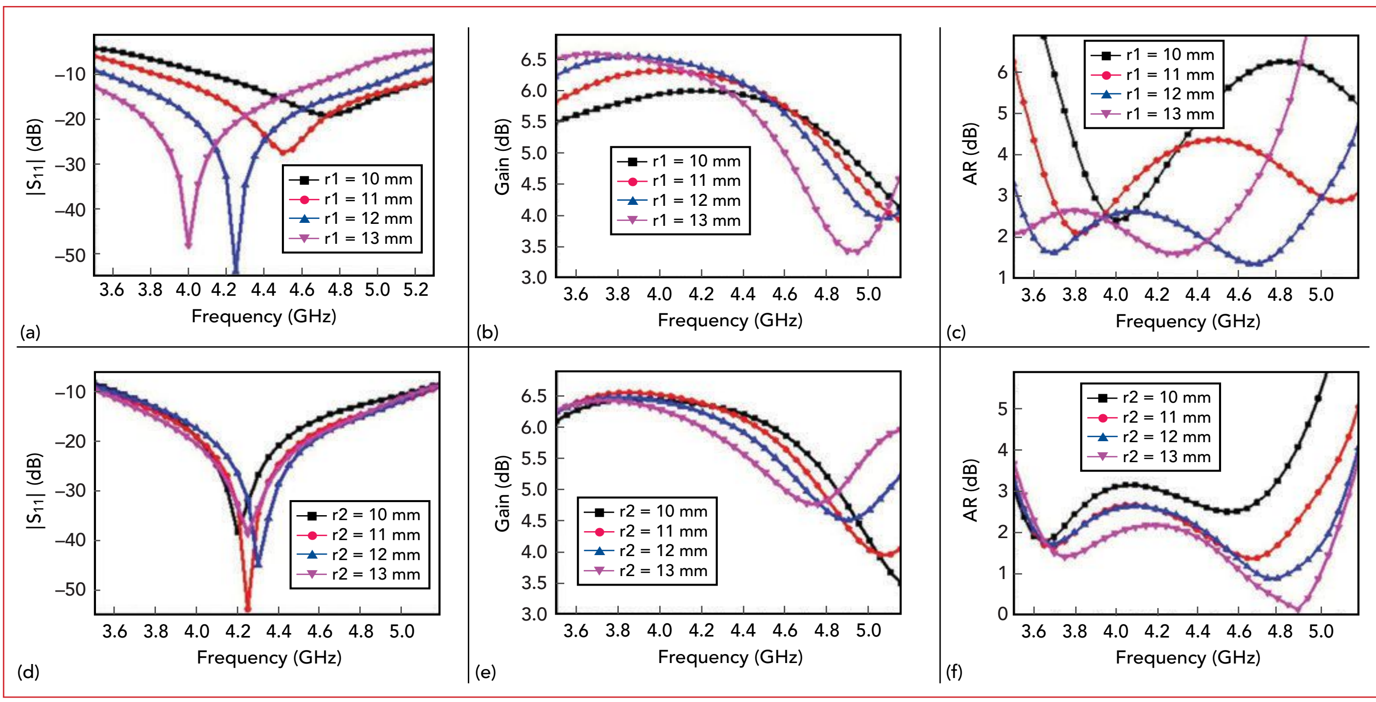

Fig. 4 **Parametric variation of $|S_{11}|$, gain and AR for r1 (a, b, c) and r2 (d, e, f).**

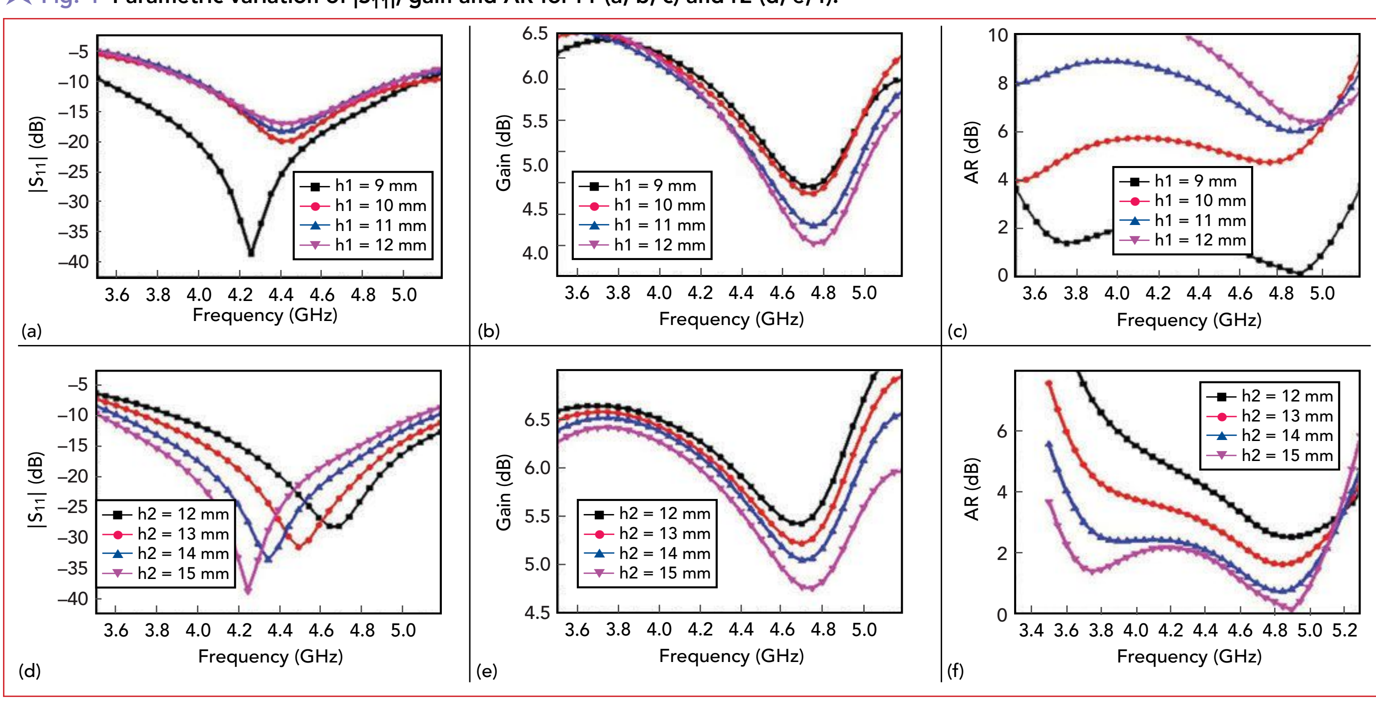

Fig. 5 **Parametric variation of $|S_{11}|$, gain and AR for h1 (a, b, c) and h2 (d, e, f).**

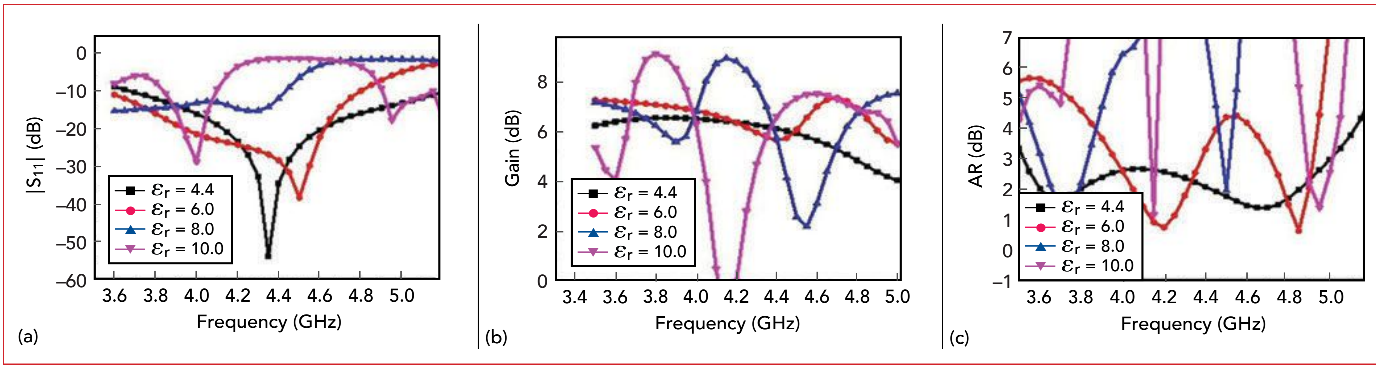

Fig. 6 **Parametric variation of $|S_{11}|$ (a), gain (b) and AR (c) for different dielectric constants.**

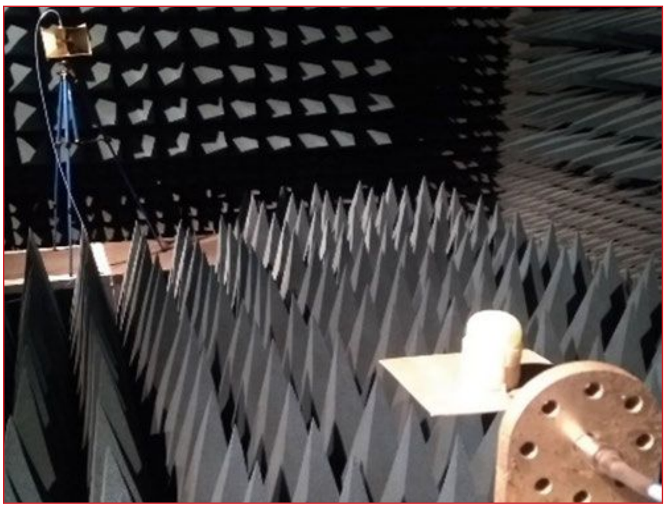

Fig. 7 **DRA measurement setup.**

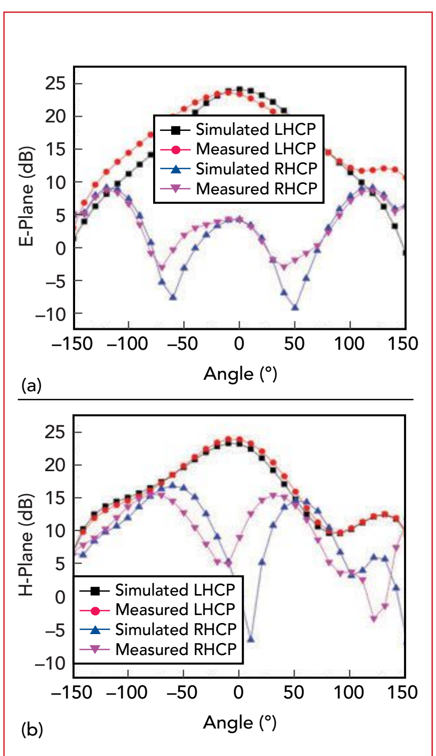

Fig. 8 **Antenna patterns at 4.3 GHz: E-plane (a) and H-plane (b).**

cular polarization in the DRA without impacting impedance bandwidth, providing an additional degree of freedom.

Probe Height

The parametric variation of h1 has been studied for 1 to 20 mm probe lengths. For brevity, responses are shown for 9, 10, 11 and 12 mm lengths in ***Figure 5***. It is observed that gain and impedance bandwidth decrease as h1 increases and the AR decreases as h1 decreases. Note that h1 at 9 mm is approximately equal to 0.26 λ_{eff}, where $\lambda_{eff} = \lambda_0/\sqrt{\varepsilon_{rDRA}}$.

The parametric variation of h2 has been studied for 1 to 20 mm probe lengths. For brevity, responses are shown for 12, 13, 14 and 15 mm lengths. It is observed that the resonant frequency shifts downward and impedance bandwidth and gain decrease as h2 increases, and the ARBW increases as h2 increases. Note that h2 at 15 mm is approximately a half wavelength (0.45 λ_{eff}) at the resonant frequency.

Parametric responses are shown for dielectric constants of 4.4, 6, 8 and 10. From ***Figure 6***, it is observed that that low dielectric material DRA exhibits the widest bandwidth.[1,15]

PROTOTYPE DRA MEASURED RESULTS AND DISCUSSION

A photograph of the prototype undergoing measurement in an anechoic chamber is shown in ***Figure 7***. Simulated and measured radiation patterns at 4.3 GHz in the E- and H-planes are shown in ***Figure 8***. LHCP gain dominates RHCP in the broadside direction. RHCP-dominant radiation in the broadside direction can be achieved by repositioning Probe 2 on the opposite side of the cylinder along with the microstrip feed line.

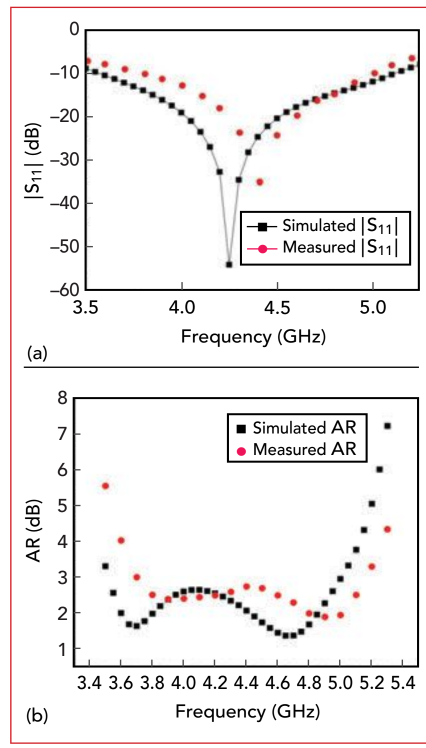

Fig. 9 **Simulated and measured impedance bandwidth (a) and axial ratio (b).**

Measured results agree closely with the simulation, exhibiting some variations due to fabrication tolerances. Radiation efficiency varies between 92 and 96 percent, peaking at 96 percent at the center of the operating frequency band. The impedance bandwidth is broad, ranging from 3.5 to 5.1 GHz, with a 4.3 GHz center frequency, as shown in ***Figure 9a***. The ARBW covers practically the entire operational band from 3.55 to 5 GHz, as shown in ***Figure 9b***. The peak gain in the broadside direction is 6.5 dBi.

CONCLUSION

A hemicyl-shaped DRA exhibits a wide impedance bandwidth of 34.5 percent, an overlapping ARBW of 33 percent and an average gain of 5.5 dBi in its operating band. With operation in the sub-6 GHz band, this design approach is applicable in numerous applications. In addition to excellent performance with wide impedance and ARBWs, this antenna has a simple structure, without cuts, slits or slots that make other antenna designs complex and difficult to fabricate. ■

ACKNOWLEDGEMENT

This Project is part of the Project no: E13C24002390006 with SOE2024-35 under Ministero dell'Universita e della ` Ricerca Italia. Reference: PNRR M4C2 Bando Giovani Ricercatori, Investimento 1.2 - Avviso N. 201 del 03/07/2024-SOE2024-35.

References

1. S. A. Long, M. McAllister and L. Shen, "The Resonant Cylindrical Dielectric Cavity Antenna," *IEEE Transactions on Antennas and Propagation*, Vol. 31, No. 3, May 1983, pp. 406–412.
2. M. W. McAllister and S. A. Long, "Resonant Hemispherical Dielectric Antenna," *Electronics Letters*, Vol. 20, No. 16, August 1984, pp. 657–659.
3. K. M. Luk and K. W. Leung, Eds., *Dielectric Resonator Antennas*, Baldock, U.K.: Research Studies Press, 2003.
4. A. Petosa, *Dielectric Resonator Antenna Handbook*, Artech Publication House, Norwood, Mass., U.S., 2007.
5. A. Petosa and A. Ittipiboon, "Dielectric Resonator Antennas: A Historical Review and the Current State of the Art," *IEEE Antennas and Propagation Magazine*, Vol. 52, No. 5, October 2010, pp. 91–116.
6. R. K. Mongia and P. Bhartia, "Dielectric Resonator Antennas—A Review and General Design Relations for Resonant Frequency and Bandwidth," *International Journal of Microwave and Millimeter-Wave Computer-Aided Engineering*, Vol. 4, No. 3, July 1994, pp. 230–247.
7. Y. Pan and K. W. Leung, "Wideband Circularly Polarized Trapezoidal Dielectric Resonator Antenna," *IEEE Antennas and Wireless Propagation Letters*, Vol. 9, June 2010, pp. 588–591.
8. S. Maity, M. Gangopadhyaya and B. Gupta, "45°– 45°– 90° Triangular Dielectric Resonator Antenna with Broadside Radiation Patterns," *AEU International Journal of Electronics and Communication*, Vol. 94, September 2018, pp. 51–54.
9. S. Fakhte, S. S. Singhwal, L. Matekovits and B. K. Kanaujia, "Manipulating the Radiation Pattern of Equilateral Triangular Dielectric Resonator Antenna Using Asymmetric Grooves," *AEU – International Jou*mal of Electronics and Communications, Vol. 145, February 2022.
10. V Hamsakutty, A. V. P. Kumar, J. Yohannan and K. T. Mathew, "Coaxial Fed Hexagonal Dielectric Resonator Antenna for Circular Polarization," *Microwave and Optical Technology Letters*, Vol. 48, No. 3, January 2006, pp. 581–582.
11. S. S. Singhwal, B. K. Kanaujia, A. Singh and J. Kishor, "Circularly Polarized V-Shaped Dielectric Resonator Antenna," *International Journal of RF and Microwave Computer-Aided Engineering*, Vol. 29, No. 9, May 2019.
12. R. K. Mongia, A. Ittipiboon, M. Cuhaci and D. Roscoe, "Circularly Polarized Dielectric Resonator Antenna," *Electronics Letters*, Vol. 30, No. 17, 1994, pp. 1361–1362.
13. B. Mukherjee, P. Patel and J. Mukherjee, "A Novel Cup-Shaped Inverted Hemispherical Dielectric Resonator Antenna for Wideband Applications," *IEEE Antennas and Wireless Propagation Letters*, Vol. 12, September 2013, pp. 1240–1243.
14. P. Ranjan and R. K. Gangwar, "Probe Feed Half Split Cylindrical Dielectric Resonator Antenna for Wideband Application," *AEU-International Journal of Electronics and Communications*, Vol. 69, No. 11, November 2015, pp. 1709–1714.
15. S. S. Singhwal, B. K. Kanaujia, A. Singh and J. Kishor, "Novel Circularly Polarized Dielectric Resonator Antenna for Microwave Image Sensing Application," *Microwave and Optical Technology Letters*, Vol. 61, No. 7, July 2019, pp. 1821–1827.
16. S. Pahadsingh and S. Sahu, "Planar UWB Integrated with Multi Narrowband Cylindrical Dielectric Resonator Antenna for Cognitive Radio Application," *AEU-International Journal of Electronics and Communications*, Vol. 74, April 2017, pp. 150–157.
17. S. S. Singhwal, L. Matekovits, I. Peter and B. K. Kanaujia, "A Study on Application of Dielectric Resonator Antenna in Implantable Medical Devices," *IEEE Access*, Vol. 10, January 2022, pp. 11846-11857.
18. S. S. Singhwal, B. K. Kanaujia, A. Singh and J. Kishor, "Dual-Port MIMO Dielectric Resonator Antenna for WLAN Applications," *International Journal of RF and Microwave Computer-Aided Engineering*, Vol. 30, No. 6, December 2019.
19. Y. -M. Pan, K. W. Leung and K. -M. Luk, "Design of the Millimeter-Wave Rectangular Dielectric Resonator Antenna Using a Higher-Order Mode," *IEEE Transactions on Antennas and Propagation*, Vol. 59, No. 8, August 2011, pp. 2780–2788.
20. Y. X. Sun and K. W. Leung, "Dual-Band and Wideband Dual-Polarized Cylindrical Dielectric Resonator Antennas," *IEEE Antennas and Wireless Propagation Letters*, Vol. 12, March 2013, pp. 384–387.
21. A. A. Kishk, G. Zhou and A. W. Glisson, "Analysis of Dielectric-Resonator Antennas with Emphasis on Hemispherical Structures," *IEEE Antennas and Propagation Magazine*, Vol. 36, No. 2, April 1994, pp. 20–31.
22. K. W. Leung, K. M. Luk, K. Y. A. Lai and D. Lin, "Theory and Experiment of a Coaxial Probe Fed Hemispherical Dielectric Resonator Antenna," *IEEE Transactions on Antennas and Propagation*, Vol. 41, No. 10, October 1993, pp. 1390—1398.

REVIEW BOARD MWJ APPROVED

Novel mmWave Antenna Arrays with Improved Radiation Characteristics for 5G Applications Based on a Super Wideband Unequal Feed Network

Abolfazl Azari
Ecole Polytechnique Fédérale de Lausanne, Switzerland
K. N. Toosi University of Technology, Iran

Anja Skrivervik
Ecole Polytechnique Fédérale de Lausanne, Switzerland

Hadi Aliakbarian
K. N. Toosi University of Technology, Iran

A super wideband unequal 1 × 8 power divider is developed for 5G mmWave antenna arrays. The power divider is connected to Vivaldi antenna elements and dual-polarized aperture-coupled antenna elements. The Vivaldi array operates from 20 to 45 GHz with a 77 percent bandwidth, an average gain of 12 dBi and a maximum sidelobe level (SLL) less than -17 dB. The aperture-coupled array exhibits a 50 percent bandwidth from 24 to 40 GHz, an average gain of 12 dBi, and a maximum SLL of less than -15 dB for both horizontal and vertical polarizations. The performance of these arrays is compared with other recent 5G mmWave antenna arrays in terms of bandwidth, gain and SLL. The potential of 5G in terms of bandwidth and data rate is enabled at mmWave frequencies. The 5G mmWave bands defined by 3GPP are n257 (26.5 to 29.5 GHz), n258 (24.25 to 27.5 GHz), n259 (39.5 to 43.5 GHz), n260 (37 to 40 GHz) and n261 (27.5 to 28.35 GHz).[1,2] The proposed antenna arrays are suitable candidates for massive MIMO systems in these 5G frequency bands.

An antenna array is essential at 5G mmWave frequencies to overcome high propagation loss and improve performance. The divider/splitter plays a very important role in the antenna array. The main drawback, however, of power dividers is limited operational bandwidth.[3]

A non-uniform amplitude taper can be applied to the phased array power divider to reduce SLLs at the expense of gain reduction and an increase in main lobe beamwidth.[4] The most common amplitude tapering methods are binomial, Taylor and Chebyshev. Binomial tapering can eliminate the sidelobes but with a high variation and is difficult to implement. Taylor tapering maintains the sidelobes at a constant level, while Chebyshev provides optimum beamwidth for a given SLL. Amplitude tapering via unequal power distribution is usually implemented by adjusting transmission line widths used for quarter wavelength transformers.[5]

A Taylor feed network using an unequal power divider was described by Hill and Kelly[6] for 5G phased array antennas with the goal of reducing the SLL. The achieved SLL was -15 dB but in a limited operational bandwidth of 27.5 to 28.65 GHz. A planar 1 × 8 array antenna using a substrate-integrated cavity as a power divider was proposed by Mao et al.[7] for 26 GHz 5G applications. The array had an impedance bandwidth from 24 to 29.5 GHz with a gain of over 10 dBi from 24.8 to 27.7 GHz and SLL less than -15 dB. A 1 × 8 Vivaldi array with an equal power divider was introduced by Zhu et al.[8] for 5G mmWave applications. The operational band was 24.65 to 28.5 GHz, with a gain between 6.96 and 11.32 dB. The SLL, however, was poor. As a series–fed array antenna, a non-uniform eight-angled dipole array antenna was described by Wang et al.[9] for a wide bandwidth of 22 to 44 GHz. The gain variation was between 7.6 and 10.9 dBi with a SLL of -17 dB.

Most of these array antennas were single-polarized and did not employ very large bandwidth power dividers. A dual-polarized 1 × 8 array antenna was proposed by Parchin et al.[10] for 5G mmWave applications. However, its bandwidth was only 40 percent from 26.5 to 39.5 GHz with an unexceptional SLL.

This article describes a super wideband, high gain and low SLL array antenna for 5G mmWave applications. First, a super wideband, unequal power divider is developed to operate from 24 to 40 GHz. Then, it is integrated with an end-fire single-polarization Vivaldi element and a broadside dual-polarized aperture-coupled antenna element. The measured performance of each is compared with that of other recently published works.

POWER DIVIDER DESIGN

The T-junction power divider as a basic three-port network is considered for the design of the feed network, as seen in ***Figure 1***. The input and output impedance of the T-junction power divider is set to a characteristic impedance Z_0 = 50 Ω. The impedance at α is shown in ***Equation 1***:[11]

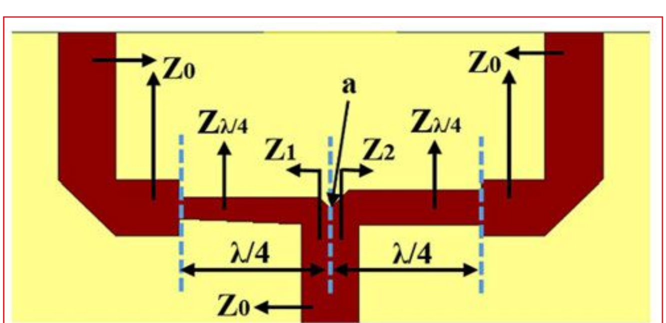

Fig. 1 Unequal 1 to 2 T-junction power divider.

$$Z_a = Z_1 \,||\, Z_2 \quad (1)$$

If a λ/4 transformer is used, then the impedance of the transformer is given by ***Equation 2***:[11]

$$Z_{\lambda/4} = \sqrt{Z_a Z_0} \quad (2)$$

When designing a wideband T-junction power divider, the transformer length should be selected for an acceptable impedance match across the entire bandwidth.

The radiation characteristics and SLL can be improved by altering the amplitude distribution of the array.[5] To implement a non-uniform amplitude distribution in a T-junction power divider, the width of the two sides can produce unequal power weightings. The relation of power and impedance is expressed as ***Equation 3***:[11]

$$p = \frac{v^2}{2Z} \quad (3)$$

The microstrip impedance according to the microstrip width to substrate height W/h is shown in ***Equation 4***:[5]

$$Z = \begin{cases} \dfrac{60}{\sqrt{\varepsilon_{eff}}} \ln\left[\dfrac{8h}{W} + \dfrac{W}{4h}\right] & \dfrac{W}{h} \le 1 \\ \dfrac{120\pi}{\sqrt{\varepsilon_{eff}}\left[\dfrac{W}{h} + 1.393 + \dfrac{2}{3}\ln\left(\dfrac{W}{h} + 1.444\right)\right]} & \dfrac{W}{h} > 1 \end{cases} \quad (4)$$

The relation between the power weighting and microstrip width can be extracted in ***Equation 5*** as:

$$\frac{P_1}{P_2} = \frac{Z_2}{Z_1} = \frac{\frac{W_1}{h} + 1.393 + \frac{2}{3}\ln\left(\frac{W_1}{h} + 1.444\right)}{\frac{W_2}{h} + 1.393 + \frac{2}{3}\ln\left(\frac{W_2}{h} + 1.444\right)} = \frac{\ln\left(1 + 4\left(\frac{h}{W_2}\right)\right)}{\ln\left(1 + 4\left(\frac{h}{W_1}\right)\right)} \quad (5)$$

Different microstrip widths lead to different microstrip impedances and subsequently, different transformer lengths. Therefore, altering the width of T-junction sides for a target power weighting is associated with the appropriate transformer length.

In this design, the target frequency band is from 24 to 40 GHz. The coincident conditions that should be met by unequal power distribution are maximum possible gain and SLL improvement, as well as impedance matching for a bandwidth of 50 percent. With this goal, an initial 1 × 8 power divider is designed and modeled. Modeling, simulation and optimization are performed using Ansys HFSS.

1 × 8 ARRAY ANTENNA DESIGN

To function effectively in the designed array, the antenna element must be wideband, operating from 24 to 40 GHz, compact and high gain. Two types of antenna elements are considered: end-fire and broadside. A novel Vivaldi antenna introduced by Azari et al.[12] is selected for the end-fire element shown in ***Figure 2***. It

Fig. 2 **Vivaldi antenna structure (a) and fabricated element (b).**

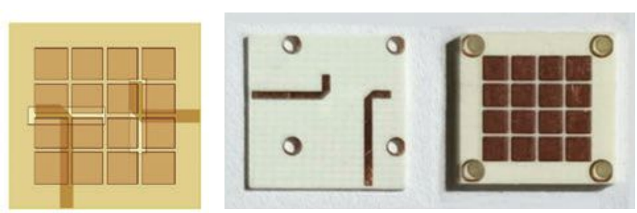

Fig. 3 **Aperture antenna structure (a) and fabricated element (b).**

TABLE 1

1 X 8 POWER DIVIDER AMPLITUDE WEIGHTS

Array Port	1 & 8	2 & 7	3 & 6	4 & 5
Initial Amplitude Weighting	0.67	0.77	0.91	1
Optimized Amplitude Weighting	0.66	0.75	0.92	1

is fabricated on a Rogers 4350B substrate with ε_r = 48, a thickness of 0.254 mm and an element spacing of 5.5 mm. It integrates easily into the feed network, can be implemented in a dual-polarization configuration, operates over 23 to 45 GHz bandwidth and provides uniform end-fire radiation patterns across the entire bandwidth with a measured gain greater than 5 dBi.

For the broadside element, a super wideband dual-polarized aperture-coupled antenna introduced by Azari et al.[13] is selected. It is fabricated on two layers of Rogers 4350B substrate, again with ε_r = 3.48, a thickness of 0.254 mm for the feed layer and 0.762 mm for the radiating patch layer, as shown in ***Figure 3***. It has a wide bandwidth of 24 to 44 GHz, compact size, high gain, high isolation and high polarization discrimination.

The well-known Chebyshev tapering as a power weighting can be exploited to reduce the SLL to a specific value. In this work, an amplitude distribution based on a MATLAB code is considered to enhance the SLL, while the 3 dB beamwidth remains almost constant for the maximum possible gain.[14] The achieved SLL is -17 dB and the initial amplitude weights are listed in ***Table 1***.

The designed power divider with initial parameters is attached to the antenna elements shaping the antenna array. The parameters of the power divider are optimized for impedance match, maximum gain and SLL in the target band of 24 to 40 GHz. The resultant optimized amplitude weights are also summarized in Table I. Rogers 4350B material with ε_r = 3.48 and a thickness of 0.254 mm is used as the substrate. The final power divider structure is shown in ***Figure 4***, with its parameters shown in ***Table 2***.

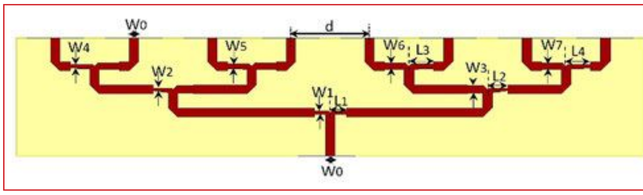

Fig. 4 **1 x 8 unequal power divider structure.**

TABLE 2

1 X 8 UNEQUAL POWER DIVIDER PARAMETERS

Parameter	W_0	W_1	W_2	W_3	W_4	W_5
Size (mm)	0.65	0.28	0.175	0.508	0.24	0.32
Parameter	W_6	W_7	L_1	L_2	L_3	L_4
Size (mm)	0.42	0.4	1.13	1.33	1.66	1.66

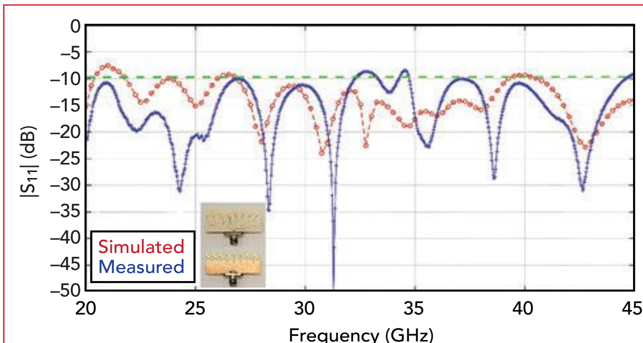

Fig. 5 **Simulated and measured $|S_{11}|$ of the 1 x 8 Vivaldi antenna array.**

1 × 8 VIVALDI ARRAY ANTENNA

Figure 5 shows the simulated and measured $|S_{11}|$ of the 1 × 8 Vivaldi array from 20 to 45 GHz. The results demonstrate a good impedance match, with greater than 10 dB return loss for 5G mmWave frequencies from 24 to 44 GHz. An exception to this return loss value occurs in a region between 33.5 and 35 GHz outside the 5G bands.

Figures 6 and ***7*** show the simulated and measured radiation patterns in the E- and H-planes for both co- and cross-polarizations at selected frequencies across the band. Both the SLL and cross-polarization are better than -17 dB. The average antenna gain is approximately 12 dBi over the 24 to 40 GHz band, as shown in ***Figure 8***.

1 × 8 APERTURE-COUPLED ARRAY ANTENNA

Two unequal power dividers are also connected to a novel dual-polarized aperture-coupled antenna, as shown in ***Figure 9***. The two layers are fabricated separately, aligned and bonded. Commercial 2.92 mm female connectors are edge-mounted for connection to the array. S-parameters results plotted in ***Figure 10*** show -10

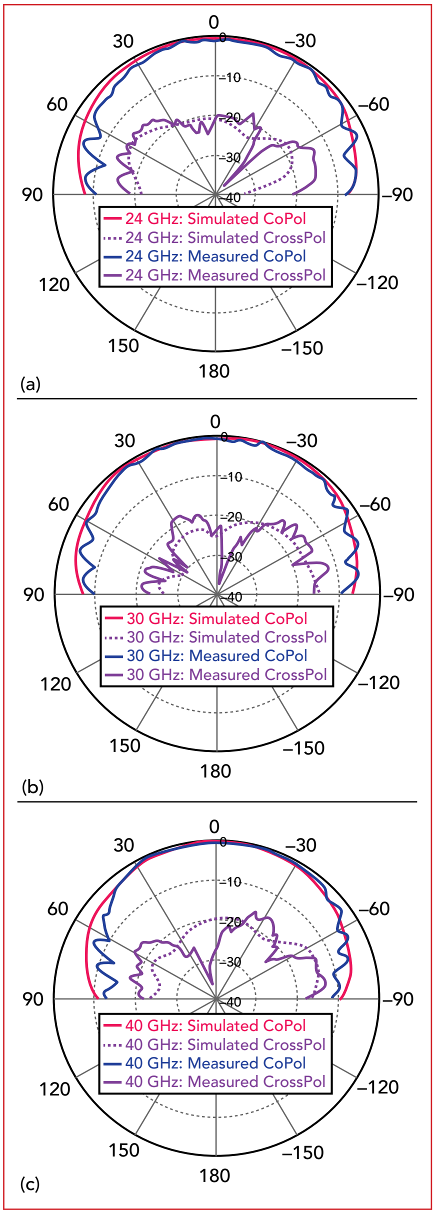

Fig. 6 **Vivaldi array simulated and measured E-plane radiation patterns: 24 (a), 30 (b) and 40 (c) GHz.**

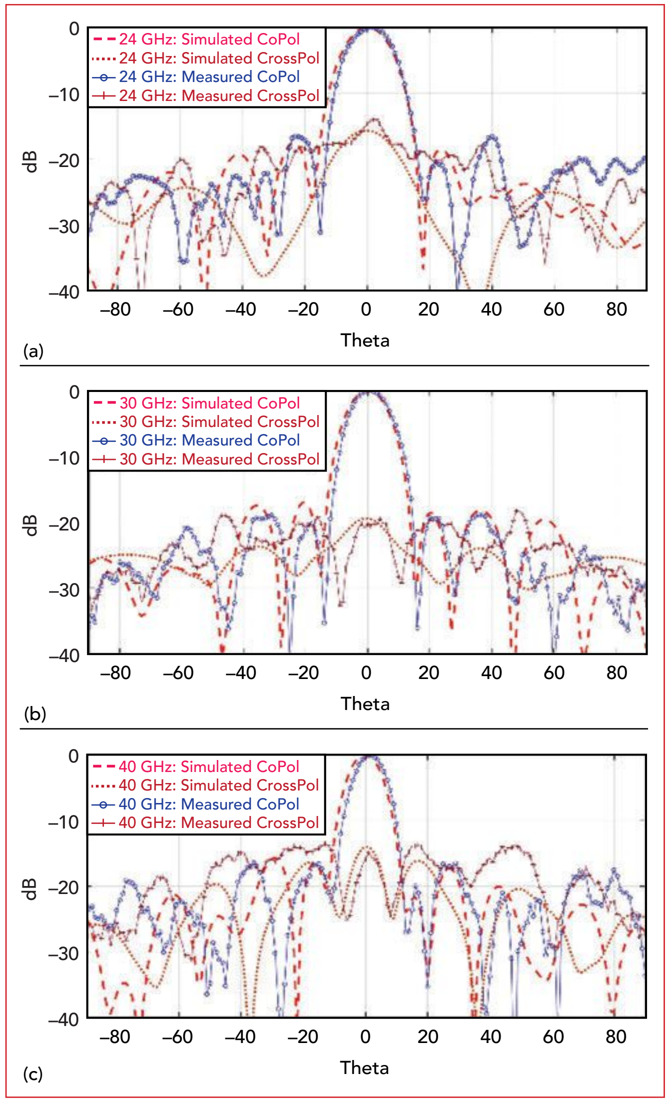

Fig. 7 **Vivaldi array simulated and measured H-plane radiation patterns: 24 (a), 30 (b) and 40 (c) GHz.**

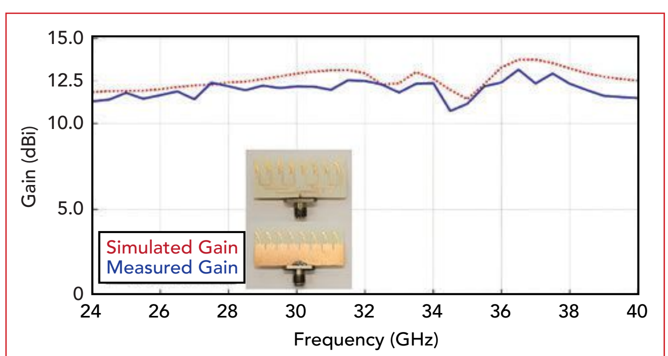

Fig. 8 **Vivaldi array simulated and measured gain.**

dB impedance matching and -30 dB mutual coupling from 24 to 40 GHz.

Horizontally-polarized E- and H-plane radiation patterns for both co- and cross-polarizations are plotted at selected frequencies across the band in ***Figure 11*** and ***Figure 12***, respectively. Vertically-polarized radiation patterns are plotted in ***Figure 13*** and ***Figure 14***. Simulated and measured gains for both polarizations are shown in ***Figure 15***. The unused port is terminated by a dummy load in the measurement process.[15]

The average gain is approximately 12 dBi with the SLL less than -15 dB and cross-polarization isolation greater than 20 dB. Minor discrepancies with the simulated radiation patterns and degradation in measured gain compared to simulation are attributed to imperfect alignment of the radiating and feeding substrate.

PERFORMANCE COMPARISON

Table 3 summarizes a comparison with recently published 1 × 8 array antennas for 5G mmWave applications. This array exhibits greater bandwidth with superior gain and SLL performance. The single-polarized Vivaldi array and unequal power divider have 77 percent bandwidth, from 20 to 45 GHz, with an average 12 dBi gain and SLL less than -17 dB. The dual-polarized aperture-coupled array with unequal power dividers has a 50 percent bandwidth, an average gain of 12 dBi and an SLL of less than -15 dB.

CONCLUSION

An unequal 1 × 8 super wideband power divider is designed with improved amplitude weighting for maximum gain and low SLL when used as an antenna array feed. With this divider, a single-polarized Vivaldi 1 × 8 antenna array and a dual-polarized aperture-coupled 1 × 8 antenna array are developed for super wideband 5G systems. Super wideband performance is demonstrated with appropriate radiation patterns, high average gain and low SLL. These antenna arrays are promising candidates for 5G systems, massive MIMO and other mmWave applications. ■

References

1. A. Azari and H. Aliakbarian, "Requirements for 5G Applications; A Strategic Approach," *Microwave Journal*, September 2022, Web: https://www.microwavejournal.com/articles/38759-requirements-for-5g-applications-a-strategic-approach.
2. A. Azari, A. K. Skrivervik and H. Aliakbarian, "Design Methodology for Wideband Bowtie Patch Antenna for 5G mmWave Applications," *17th European Conference on Antennas and Propagation*, March 2023.
3. F. A. Shaikh, S. Khan, A. Z. Alam, M. H. Habaebi, O. O. Khalifa and T. A. Khan, "Design and Analysis of 1-to-4 Wilkinson Power Divider for Antenna Array Feeding Network," *IEEE International Conference on Innovative Research and Development*, May 2018.
4. R. C. Hansen, *Phased Array Antennas*, Vol. 14, Wiley Interscience, New York, N.Y., 1998.
5. C. A. Balanis, *Antenna Theory Analysis and Design*, John Wiley & Sons, Inc., Hoboken, N.J., 2016.
6. T. A. Hill and J. R. Kelly, "28 GHz Taylor Feed Network for Sidelobe Level Reduction in 5G Phased Array Antennas," *Microwave and Optical Technology Letters*, Vol. 61, No. 1, January 2019, pp. 37–43.
7. C. -X. Mao, M. Khalily, P. Xiao, T. W. C. Brown and S. Gao, "Planar Sub-Millimeter-Wave Array Antenna with Enhanced Gain and Reduced Sidelobes for 5G Broadcast Applications," *IEEE Transactions on Antennas and Propagation*, Vol. 67, No. 1, January 2019, pp. 160–168.
8. S. Zhu, H. Liu, Z. Chen and P. Wen, "A Compact Gain-Enhanced Vivaldi Antenna Array with Suppressed Mutual Coupling for 5G mmWave Application," *IEEE Antennas and Wireless Propagation Letters*, Vol. 17, No. 5, May 2018, pp. 776–779.
9. H. Wang, K. E. Kedze and I. Park, "A High-Gain and Wideband Series-Fed Angled Printed Dipole Array Antenna," *IEEE Transactions on Antennas and Propagation*, Vol. 68, No. 7, July 2020, pp. 5708–5713.
10. N. O. Parchin, J. Zhang, R. A. Abd-Alhameed, G. F. Pedersen and S. Zhang, "A Planar Dual-Polarized Phased Array With Broad Bandwidth and Quasi-Endfire Radiation for 5G Mobile Handsets," *IEEE Transactions on Antennas and Propagation*, Vol. 69, No. 10, October 2021, pp. 6410–6419.
11. D. M. Pozar, *Microwave Engineering*, 4th Edition, John Wiley & Sons, Inc., Hoboken, N.J., 2012.
12. A. Azari, A. Skrivervik, H. Aliakbarian and R. A. Sadeghzadeh, "A Super Wideband Dual-Polarized Vivaldi Antenna for 5G mmWave Applications," *IEEE Access*, Vol. 11, July 2023, pp. 80761–80768.
13. A. Azari, A. K. Skrivervik and H. Aliakbarian, "A mmWave Low Complexity and Low-Cost Super Wideband Dual Polarized Aperture Coupled Antenna for 5G Applications" *IEEE Access*, Vol. 12, June 2024, pp. 85601– 85607.
14. A. Azari, A. Skrivervik and H. Aliakbarian, "Design of a Novel Wide-Angle Rotman Lens Beamformer for 5G mmWave Applications," *Scientific Reports*, Vol. 14, No. 1245, January 2024.
15. A. Azari, A. K. Skrivervik, H. Aliakbarian, "Design Methodology for High Performance Low- Cost Microstrip Termination Load for mmWave Applications," *Electronics Letters*, Vol. 59, No. 22, November 2023.

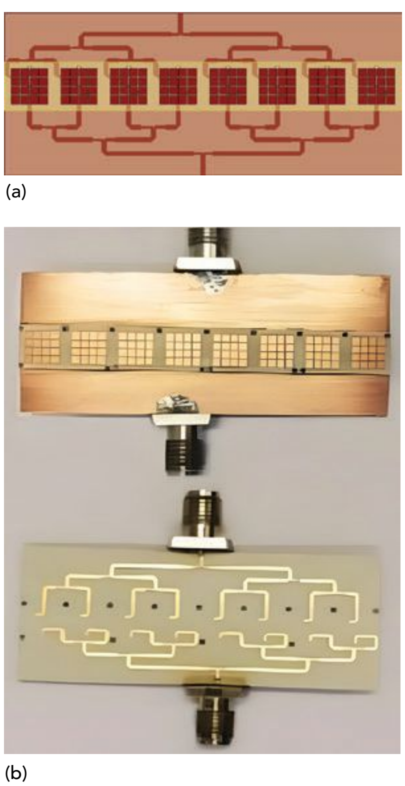

Fig. 9 1 x 8 dual-polarized aperture-coupled antenna: assembled (a), top and bottom layers (b).

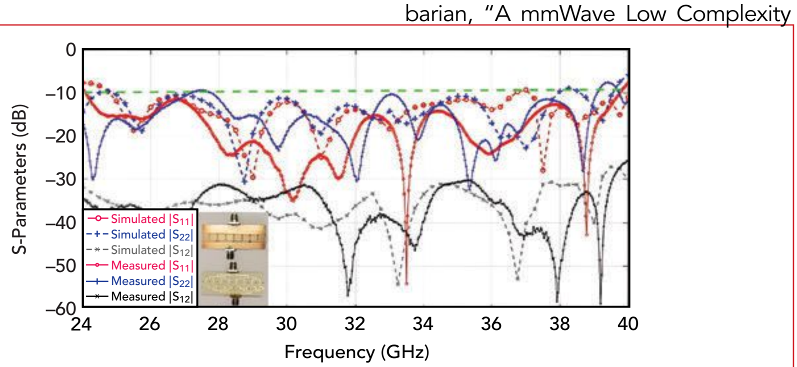

Fig. 10 1 x 8 dual-polarized aperture antenna simulated and measured S-parameters.

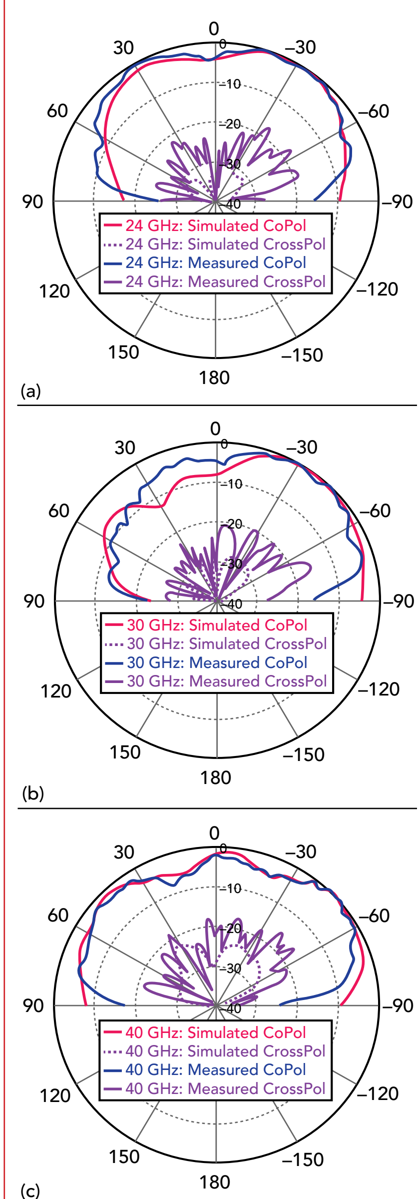

Fig. 11 Horizontally-polarized aperture-coupled array simulated and measured E-plane radiation patterns: 24 (a), 30 (b) and 40 (c) GHz.

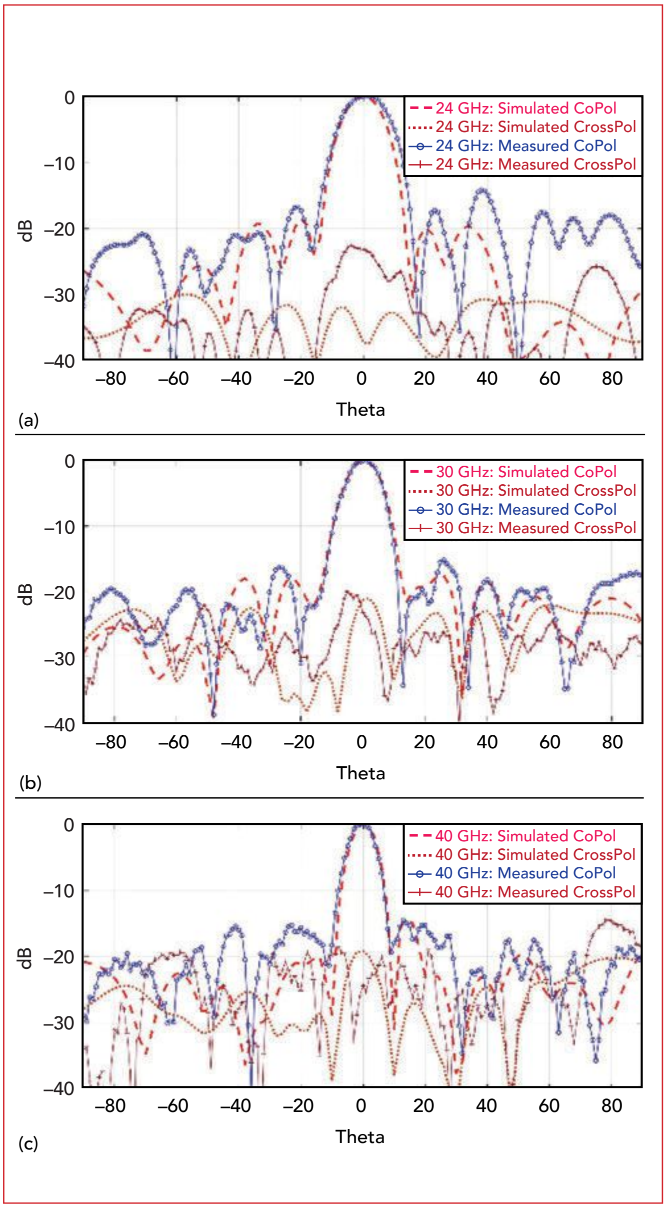

Fig. 12 Horizontally-polarized aperture-coupled array simulated and measured H-plane radiation patterns: 24 (a), 30 (b) and 40 (c) GHz.

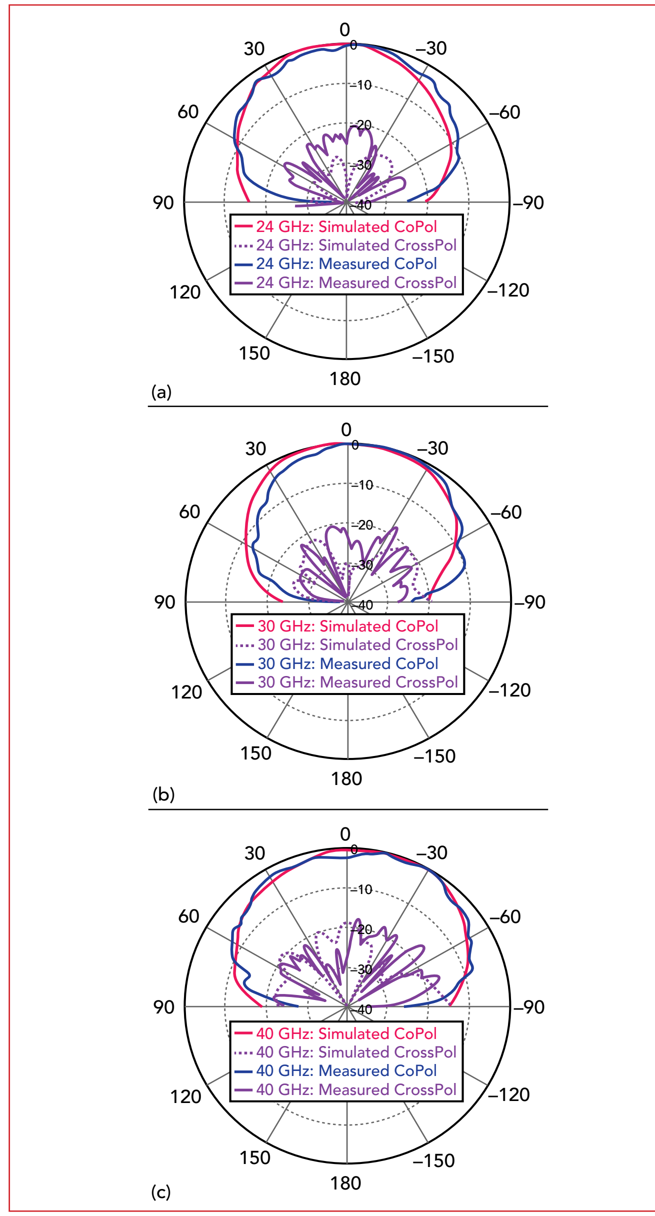

Fig. 13 Vertically-polarized aperture-coupled array simulated and measured E-plane radiation patterns: 24 (a), 30 (b) and 40 (c) GHz.

TABLE 3

COMPARISON WITH OTHER WORK

Reference	Array	Polarization	Frequency Band (GHz)	Average Gain (dBi)	SLL (dB)
6	1 x 8	Single	27.5 to 28.65	-	-15
7	1 x 8	Single	24.8 to 27.7	11	-15
8	1 x 8	Single	24.65 to 28.5	9.14	-9
9	1 x 8	Single	22 to 24	9.2	-17
10	1 x 8	Dual	26.5 to 39.5	10.2	-13
Vivaldi Array	1 x 8	Single	20 to 45	12	-17
Aperture-Coupled Array	1 x 8	Dual	24 to 40	12	-15

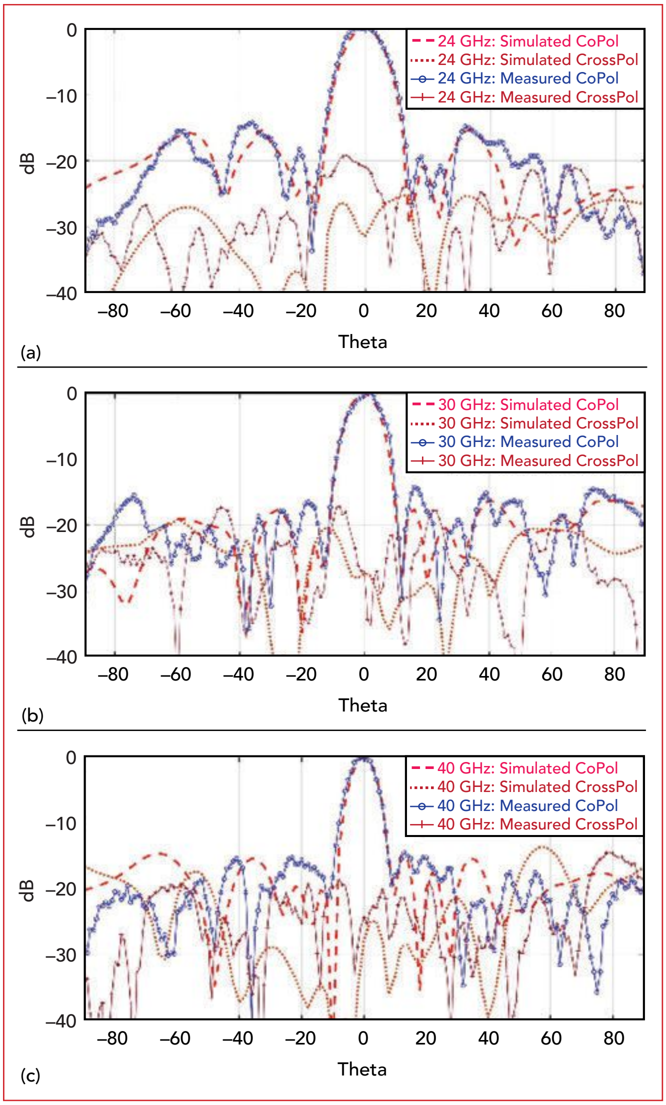

Fig. 14 Vertically-polarized aperture-coupled array simulated and measured H-plane radiation patterns: 24 (a), 30 (b) and 40 (c) GHz.

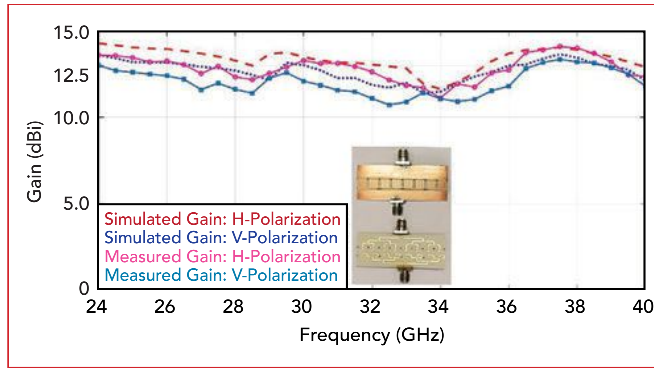

Fig. 15 1 x 8 dual-polarized aperture-coupled array antenna simulated and measured gain.